Global modelling of ice-nucleating particles and impacts on mixed-phase clouds

by:

Jesús Vergara Temprado

Submitted in accordance with the requirements for the degree of Doctor of Philosophy

University of Leeds

School of Earth and Environment

December 2017

Declaration of Authorship

The candidate confirms that the work submitted is his own, except where work which has formed part of jointly-authored publications has been included. The contribution of the candidate and the other authors to this work has been explicitly indicated below. The candidate confirms that appropriate credit has been given within the thesis where reference has been made to work of others.

The first chapter will consist on the following paper, which is already published in the journal Atmospheric Chemistry and Physics:

Jesús Vergara-Temprado, Benjamin J. Murray, Theodore W. Wilson, Daniel O'Sullivan, Jo Browse, Kirsty J. Pringle, Karin Ardon-Dryer, Allan K. Bertram, Susannah M. Burrows, Darius Ceburnis, Paul J. DeMott, Ryan H. Mason, Colin D. O'Dowd, Matteo Rinaldi, and Ken S. Carslaw Contribution of feldspar and marine organic aerosols to global ice nucleating particle concentrations. *Atmos. Chem. Phys.* **17,** 3637–3658 (2017).

In this paper, the candidate prepared and ran the simulations in which the results are based, analysed them and evaluated the modelled ice-nucleating particle distributions. The candidate also wrote and lead the process of submitting the paper with help and support from KSC and BJM. TWW, DOS, JB and KJP helped on him interpretation and technical details of the analysis. The other authors contributed with data and comments to the paper.

The second chapter will consist on an already submitted paper to 'Journal of Geophysical Research: Atmospheres':

Jesús Vergara-Temprado, Mark A. Holden, Thomas R. Orton, Daniel O'Sullivan, Nsikanabasi S. Umo, Jo Browse, Carly Reddington, María Teresa Baeza-Romero, Jenny M. Jones, Amanda Lea-Langton, Alan Williams, Ken S. Carslaw and Benjamin J. Murray. Is Black Carbon an unimportant ice-nucleating particle in mixed-phase clouds? Submitted to Journal of Geophysical Research: Atmospheres

In the modelling section the candidate ran the model used in this study, analysed the results and evaluated it against several BC campaigns. On the experimental section the candidate calculated the INP values obtained from the freezing experiments and parameterized the upper limit. The candidate also lead together with MAH and BJM the writing of the paper. MAH, TRO, DOS, NSU, MTBR, JMJ, ALL and AW prepared the experimental setup and did the experiments for the experimental section. JB, CR and KSC supported the candidate with the modelling section and writing of the paper. This paper already has received positive comments from the three reviewers. The editor of the journal has recommended to address the comments before accepting the paper.

The third chapter will consist on the manuscript:

Jesús Vergara-Temprado, Annette Miltenberger, Kalli Furtado, Daniel Grosvenor, Ben J. Shipway, Adrian A. Hill, Jonathan M. Wilkinson, Paul R. Field, Benjamin J. Murray and Ken S. Carslaw. Strong control of Southern Ocean cloud reflectivity by ice-nucleating particles.

This manuscript has been submitted to Proceedings of the National Academy of Science (PNAS). The candidate prepared, ran, analysed the simulations and evaluated them against satellite. AM and KF helped the candidate with the configuration of the runs. DG helped the candidate with the satellite data. AAH, BJS, JMW, PRF developed large parts of the microphysical scheme used. BJM and KSC helped the candidate with the interpretation and writing of the paper.

Acknowledgments

First of all, I want to sincerely thank my two supervisors, Ken Carslaw and Benjamin Murray who have supported me through this PhD, showing me the way to do research, asking me questions to improve my ability to think critically about my own research and helping me to grow as a scientist. I am especially thankful to both of them for the time spent in meetings with me whenever I had something to discuss, their willingness to support me in any moment I needed and the trust they have placed on me to produce scientific results from the very first moments of my PhD.

I want to acknowledge the researchers from the University of Leeds with whom I have been working and collaborating from the ice-nucleation group, the aerosol modellers group and the cloud modelling group. Special thanks are due to Annette Miltenberger who has always been willing to help me whenever I had any problem with a model or needed to discuss anything related to cloud physics and to Daniel O'Sullivan for his interest and effort on discussing various topics related to ice nucleation that helped me to increase my knowledge in this field from the very beginning. I am grateful to Theodore Wilson, Daniel Grosvenor, Kirsty Pringle, Thomas Whale, Leighton Regayre, Daniel McCoy, Mark Holden, Hamish Gordon, Robin Stevens, Alberto Sanchez-Marroquin, Douglas Hamilton, Susannah Burrows among several other scientists with whom I have had interesting and constructive discussions along these years. I want to thank the BACCHUS project for providing the funding needed for this project and to the MetOffice of the UK for allowing me to use their resources to produce several of the results shown in this thesis. Thanks to Paul Field for supervising and supporting this collaboration with the MetOffice.

I am especially grateful to all the friends I have had in Leeds all these years who have accompanied me in this journey, certainly making the time spent in this city very memorable and pleasant.

Finally, I want to thank my mother Concepción, my father José María and my brother José Alberto who have been supporting me during my childhood and my youth, a support without which this thesis would not have been possible.

"Finalmente, quiero dar las gracias a mi madre Concepción, a mi padre José María, y a mi hermano José Alberto, quienes me han estado apoyando durante mi niñez y mi juventud, un apoyo sin el que esta tesis no habría sido posible."

Abstract

The process of cloud glaciation strongly alters the properties of mixed-phase clouds. Between 0^{o}C to about -37^{o}C, cloud liquid droplets can either exist in the liquid phase in metastable state known as supercooling, or they can be composed of solid ice crystals. For a liquid droplet to freeze at these temperatures, the action of an external agent, known as ice-nucleating particle (INP) is needed. The atmospheric distribution of ice-nucleating particles was simulated in past studies as a function of the aerosol concentration, however, new experimental information about the ice-nucleating ability of different aerosol species and several new atmospheric measurements of INP are now available to be used in models.

In this thesis, I use this new information to develop a global atmospheric model of the distribution of ice-nucleating particles to assess the relative importance of mineral dust, marine organic aerosols and black carbon for contributing to atmospheric concentrations of INPs. The model is evaluated against several datasets of INP concentrations measured in the atmosphere to test its realism and locate regions of the world where additional currently missing sources of INP could be important. The results show that feldspar aerosols dominate the atmospheric INP concentration for most parts of the globe, whereas marine organic aerosols are more relevant in the remote Southern Ocean. Black carbon particles, in contrast, seem not to play a substantial role when new estimates of its ice-nucleating ability are used.

With the information obtained by this model, I explore whether the representation of ice-nucleating particles in climate models plays a role in the Southern Ocean radiative bias. This bias is related to modelled clouds reflecting too-little solar radiation, causing large errors in sea-surface temperatures and atmospheric circulations. I combine cloud-resolving simulations over regions of 1000 km with the new estimates of the INP concentration in remote regions to show that the simulated clouds reflect much more solar radiation than predicted by a global climate model, agreeing much better with satellite observations in both magnitude and frequency.

Overall, these results will improve our understanding of the role, distribution and importance of ice-nucleating particles in the atmosphere and provide the scientific community new points of view to understand model biases.

Table of Contents

List of figures

Chapter 1:

Chapter 2:

Chapter 3:

Chapter 4:

Appendix A:

Supplementary information for Chapter 3:

List of Tables:

Abbreviations

BC Black Carbon

CCN Cloud condensation nuclei

CDNC Cloud droplet number concentration

CFDC Continuous flow diffusion chambers

CNT Classical nucleation theory

CTT Cirrus clouds thinning

DM10 DeMott et al. 2010

DM15 DeMott et al. 2015

ECMWF European Centre for Medium-Range Weather Forecasts

H-M Hallet-Mossop process

INP Ice-nucleating particle

IPCC Intergovernmental Panel on Climate Change

LW Longwave

LWP Liquid water path

M92 Meyers et al. 1992

n_s Density of active sites

OMF Organic mass fraction

SP2 Single Particle Soot Photometer

SS Sea-salt

SW Shortwave

U10M Wind speed at 10m over the surface

VT17 Vergara-Temprado et al. 2017

WIOM Water insoluble organic mass

WSOM Water-soluble organic material

Chapter 1 Introduction

1. Clouds

Clouds have large climatic impacts in the Earth system. Made of suspended droplets of water in a solid or liquid state, they are one of the principal components of the water cycle producing precipitation and redistributing water and energy across the planet. They also play a principal role in the radiative balance of the Earth by reflecting and absorbing both solar (shortwave) and infrared (longwave) radiation. Individual clouds can cool or warm the surface of the planet depending on their height. Low clouds, have temperatures at their top similar to the surface of the planet, which means they emit similar amounts of longwave radiation back to space while reflecting large proportions of the incoming solar radiation. This causes overall a net cooling effect at the surface and top of the atmosphere. High clouds on the other hand, absorb much more terrestrial longwave radiation than they emit, causing a net warming of the surface. Globally, it is estimated that clouds reflect about 46 W/m^2 of shortwave radiation and emit to Earth about 28 W/m^2 longwave radiation [*Ramanathan et al.*, 1989; *Zelinka et al.*, 2017].This causes in total a cooling effect of around 18 W/m^2. This natural cloud forcing is about six times larger than the present-day radiative forcing caused by changes in anthropogenic emissions of greenhouse gases estimated in the latest IPCC report (~2.8W/m^2 [*Myhre et al.*, 2013a]). Given the magnitude of the natural cloud radiative forcing, any human or natural-induced change in the properties of the clouds can potentially have large effects on climate. Moreover, as the atmosphere warms in the coming century clouds will respond, changing their properties and feeding back on climate. Most climate models predict that these cloud feedbacks will have an overall warming effect on climate [*Zelinka et al.*, 2017], however, the magnitude of these cloud feedbacks is currently one of the largest uncertainties for future climate projections.

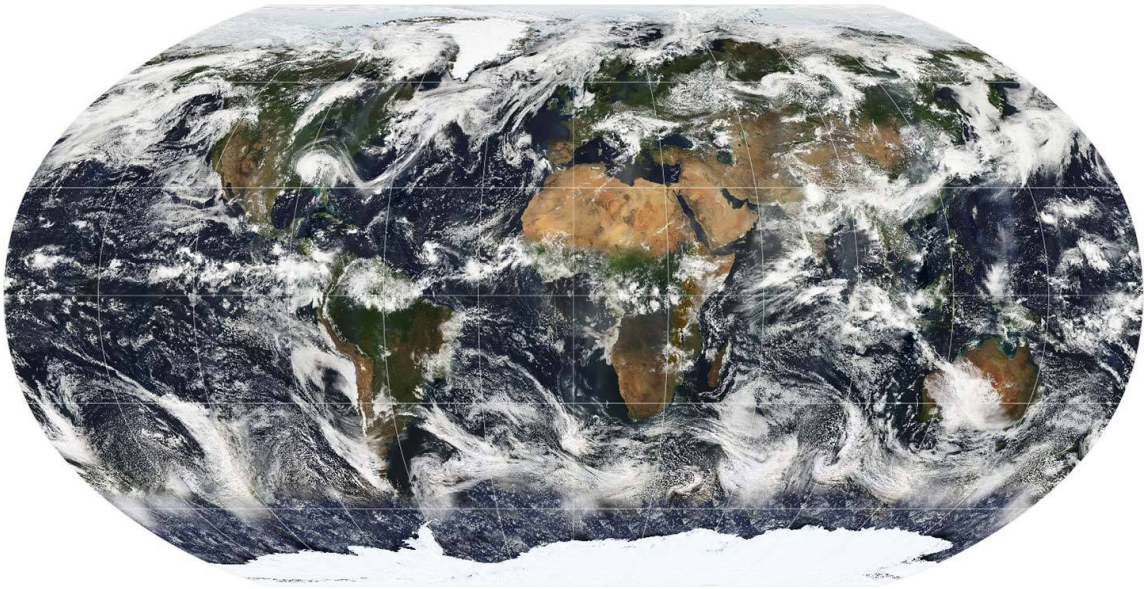

Figure 1 Example distribution of clouds in the atmosphere. The image is based largely on cloud cover observations from the moderate-resolution imaging spectroradiometer (MODIS) on the 11th of July 2005. Credits to NASA Earth.

1.1. Aerosol impacts on liquid clouds

Aerosols particles are small pieces of matter (liquid, solid or mixture) suspended in the atmosphere. Their sizes can vary from a few nanometres to a few micrometres. Larger particles than a few tens of microns have fall speeds large enough so they do not persist in the atmosphere long enough to be transported large distances or influence atmospheric properties strongly. Typically, aerosol particles are distributed across different size ranges forming lognormal modes. Depending of their size, each mode its assigned a different name. The 'nucleation mode' is composed of the smaller particles up to about 10 nm. Larger particles (from about 10 nm to 100 nm) form what is called the 'Aitken mode'. The next mode (between 100nm to 1μm) is called the 'accumulation mode' and for sizes larger than 1μm, the particles are included in what is known as the 'coarse mode'. Aerosol particles are essential for cloud formation as supersaturated water condenses onto aerosols to form cloud droplets creating a cloud. In the last century, large anthropogenic increases in the emissions of aerosol particles have affected climate in several ways [*Boucher et al.*, 2013]. First by absorbing and reflecting sunlight back into space, in what is called the aerosol direct effect [*Myhre et al.*, 2013b], and then by affecting

cloud radiative properties [*Twomey*, 1974]. These aerosol-cloud interactions are commonly referred as aerosol indirect effects.

For the same amount of condensed liquid, a larger concentration of aerosols in the atmosphere will produce more and smaller cloud droplets, which will make the clouds reflect more sunlight in what is called the first indirect effect of aerosol in clouds [*Twomey*, 1974; *Boucher et al.*, 2013; *Carslaw et al.*, 2013] .An additional effect is that the collision-coalescence of droplets becomes less efficient with increased droplet concentration, which makes them less likely to become rain droplets, hence increasing the lifetime of the clouds [*Albrecht, 1989; Lohmann*, 2006].

Aerosols can also influence the formation and development of clouds in what is called the semi-direct effect in which the reflection and absorption of radiation by aerosol particles can produce changes in the atmospheric thermal profile [*Ackerman*, 2000]. The magnitude of all these aerosol cloud interactions has remained one of the largest uncertainties in anthropogenic radiative forcing for several IPCC reports, despite large efforts in the atmospheric science community to reduce it [*Boucher et al.*, 2013].

Although it is clear that humans have affected the concentration of aerosol particles able to modify the atmosphere's radiative properties and to act as cloud condensation nuclei in clouds, it is still unknown how human-induced changes may modify the concentration of aerosols with the ability to nucleate ice. A major issue that the scientific community face at this point is the lack of basic understanding of the sources (natural or anthropogenic) of ice-nucleating particles (INPs). Changes in the concentrations of these particles, could change the process of cloud glaciation, which dramatically impacts cloud radiative properties and triggers the cold rain process in which the formation of ice and subsequent grow at the expense of liquid water produces precipitating ice crystals reducing the lifetime of clouds [*Wegener*, 1923]. INPs could also affect the formation pathway of cirrus clouds, modifying the concentration and size of ice crystals which influences its lifetime and radiative properties [*Hoose et al,. 2012*]. Possible anthropogenic effects on the INP distribution could be related to increases in the emissions of dust by human activities, deactivation of ice-nucleating particles due to sulphur coatings on aerosols or emission of black carbon aerosols with the capability to nucleate ice. However, so

far, just a few studies have looked into the magnitude of a possible anthropogenic climate modification due to ice-nucleating particles, and their conclusions are largely dependent on fundamental unresolved questions related to the representation and efficiency of different aerosol species to nucleate ice [*Lohmann*, 2002; *Storelvmo et al.*, 2008; *Girard and Sokhandan Asl*, 2014].

Most climate models currently do not account for the differences in the atmospheric concentration of ice-nucleating particles, mainly because of some of the uncertainties previously mentioned. Attempting to improve the understanding of how ice-nucleating particles are distributed and what effect they have on clouds is currently a major challenge in the atmospheric science community. Improving our understanding on how to better represent the INP concentration globally making use of the most recent laboratory information of the INP ability of different aerosol species and the most up to date dataset of atmospheric INP observations is going to be the main subject of this topic. Then I will attempt to estimate the importance that improving the representation of ice-nucleating particles have for representing cloud microphysics in models.

1.2. Cloud droplet formation

Clouds can be formed when atmospheric relative humidity exceeds 100%. Generally, it occurs when a moist air parcel experiences an adiabatic updraft into higher levels of the atmosphere, which causes its temperature to fall, thereby lowering the saturation vapour pressure needed for water to condense. Moist air can also reach saturation by some other processes such as cooling by the emission of longwave radiation back to space, which is one of the main processes causing fog formation [*Gultepe et al.*, 2007].

When supersaturation is reached, water starts to condense onto aerosol particles following Köhler theory [*Köhler*, 1936]. To derive and explain Köhler theory we need to account for two properties of aerosol particles that affect the saturation vapour pressure of water: the solute effect and the effect of the aerosol particle curved surface.

Aerosol particles are typically a mixture of water and one or more components acting as solutes. The addition of a solute to water results in a decrease in the

saturation vapour pressure of water. This phenomenon is approximated by the Raoult's law:

$$p^r = x \cdot p^* \quad (1)$$

where p^* is the saturation water pressure of pure water over a flat surface, p^r the saturation vapour pressure due to the presence of solutes and x the mole fraction of the solute. For a solution droplet, the ratio p^r/p^* can be expressed as function of the radius of the droplet (r) in the form:

$$\frac{p^r}{p^*} = 1 - \frac{B}{r^3} \quad (2)$$

With B referring to a factor that does not depend on the radius. The second important effect is the change of the saturation vapour pressure over a curved surface, also known as the Kelvin effect. Over curved interfaces, molecules have less adjacent molecules than in flat surfaces, making it easier for them to escape to the gas phase, which increase the saturation vapour pressure of water. This effect is expressed by the Kelvin equation:

$$p^k = p^* \, exp\left(\frac{2\sigma \mathrm{M}}{\rho \, RTr}\right) \quad (3)$$

where p^k is the saturation water pressure due to the Kelvin effect σ is the surface tension of water, M the molar mass, ρ the density of water, R the universal gas constant and T the temperature. The ratio p^k/p^* can then be expressed in a simplified form as:

$$\frac{p^k}{p^*} = \exp\left(\frac{A}{r}\right) \approx 1 + \frac{A}{r} \quad (4)$$

where A is a factor that does not depend on the radius. Combining these two effects we arrive to the Köhler equation that explains the activation of aerosols into cloud droplets in water supersaturated environments. In a simplified form, the saturation water pressure after accounting for these two effects (p) can be written as:

$$p = p^*\left(1 - \frac{B}{r^3}\right)\left(1 + \frac{A}{r}\right) \approx \left(1 + \frac{A}{r} - \frac{B}{r^3}\right) \quad (5)$$

The form of the Köhler equation as function of the radius can be seen in Figure 2.

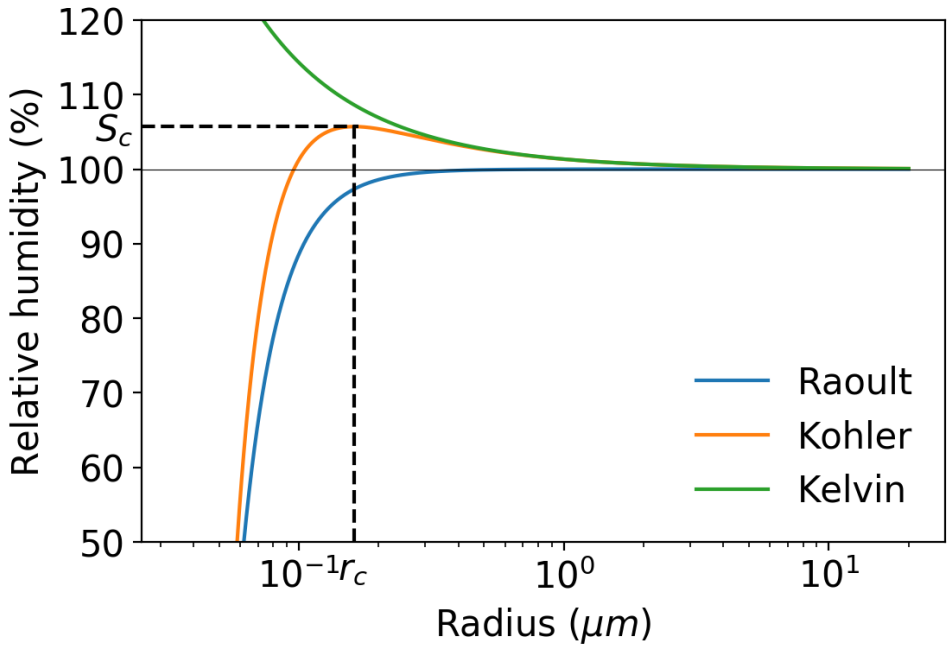

Figure 2 Example representation of how the Raoult and Kelvin effects modify the saturation water pressure. Both effects combined make the shape of the Köhler function.

Below a relative humidity of 100%, an aerosol particle will absorb moisture and grow as the relative humidity increases or shrink if the RH decreases. When the critical supersaturation is reached, the aerosol particle will reach a critical radious at which it activates into a water droplet that can grow indefinitely at the expense of the ambient moisture. This critical radius (r_c) and the supersaturation at which droplet activation will happen (S_c)can be obtained by differentiating the Köhler equation to obtain its maximum value:

$$\frac{\partial p}{\partial r} = 0; \quad (6) \qquad r_c = \sqrt{\frac{3B}{A}} \quad (7)$$

Substituting r_c into the Köhler equation leads to the saturation needed to activate an aerosol particle into a water droplet:

$$S_c = 1 + \sqrt{\frac{4A^3}{27B}} \quad (8)$$

Hence, for a certain aerosol population (assumed homogeneous in composition for simplicity), if the supersaturation in a cloud goes above the critical supersaturation, all the droplets with a radius larger than the critical radius will be activated into water droplets as long as there is enough available vapour. The condensation of water releases latent heat into the air mass, affecting its subsequent evolution. When the nucleated water droplets collide among each other the coalescence process takes place and several droplets can join forming larger rain droplets with faster fall speeds. These rain droplets precipitate in what is known as the warm rain process.

2. Formation of the ice phase

2.1. Ice nucleation

The evolution and properties of clouds become substantially more complex when they ice phase starts to compete with the water phase. When liquid water cools down below 0ºC, the ice phase becomes the thermodynamically stable phase of water. However, without the triggering of ice formation, water can instead persist in the liquid phase in a thermodynamically metastable state commonly referred as supercooling. The conversion from supercooled water to the ice phase begins with the formation of an aggregate of water molecules forming a similar structure to that of solid ice. This structure is known as an ice embryo and can occur by random fluctuations of molecules. When the embryo reaches a certain critical size, its growth at the expense of the liquid water becomes an energetically favourable process, forming an ice crystal. The triggering of the ice phase for pure water, commonly referred as homogeneous freezing, is a probabilistic phenomenon that depends strongly on the temperature [*Murray and Jensen*, 2010; *Riechers et al.*, 2013; *Koop and Murray*, 2016].

On atmospheric time-scales, the probability of ice formation occurring homogeneously in a liquid water droplet is negligibly small until temperatures are

lower than about -35^{o}C. Between these temperatures and 0^{o}C an external agent is needed to trigger the formation of the ice phase. This process is commonly called heterogeneous ice nucleation and the temperature range over which it can occur is referred to as the mixed-phase range.

Aerosol particles with the ability to nucleate ice will be called hereafter ice-nucleating particles (INPs) [*Vali et al.*, 2015a] and their composition, distribution and atmospheric implications are the main subject of this thesis.

There are different pathways through which INPs can form ice-crystals. If one of these aerosol particles triggers ice-nucleation from inside a supercooled water droplet it is said that it is acting through the condensation or immersion mode depending on whether the water was condensed onto the surface of the particle (condensation), or the particle was introduced in water (immersion). Some particles can also trigger the formation of ice by colliding with the surface of a water droplet, which is referred as the contact mode. A different pathway in which ice is formed without the presence of condensed supercooled liquid water can happen when water vapour deposits onto the surface of an aerosol particle and directly forms the ice-phase. This mode of nucleation is referred as the deposition mode. Figure 3 depicts the different nucleation pathways [*Kanji et al.*, 2017].

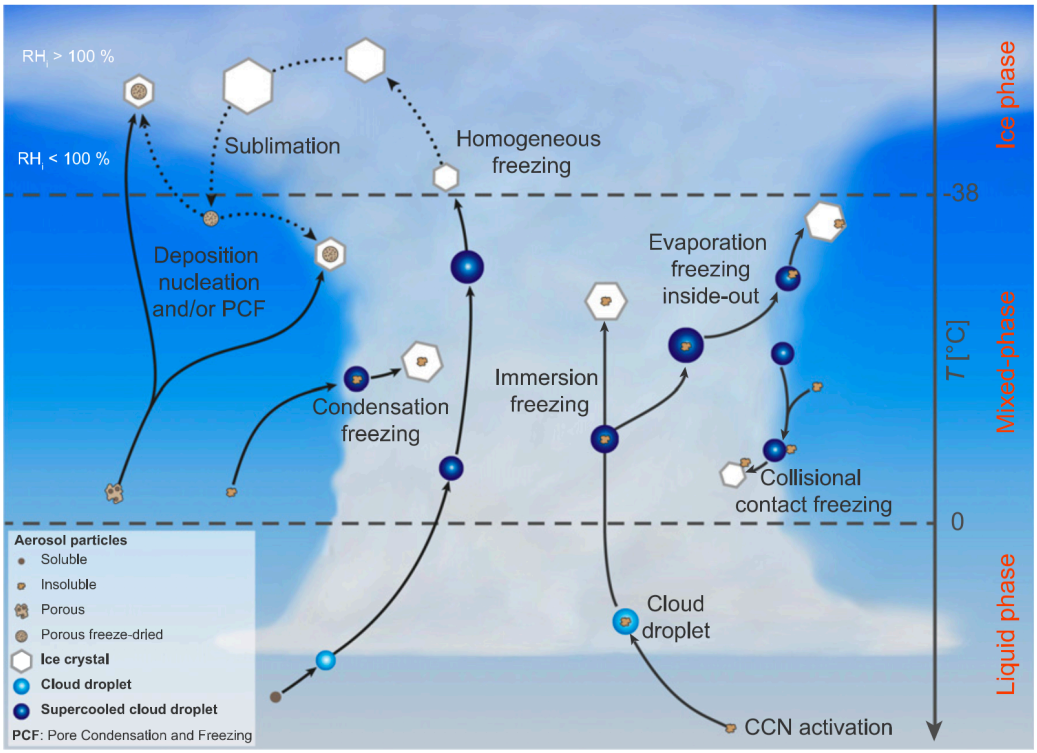

Figure 3 Schematic representation of the pathways in which ice-nucleation can occur. There are 4 main pathways, immersion freezing, condensation freezing, collisional contact freezing (also referred as contact nucleation) . Picture reproduced from [Kanji et al., 2017].

It is observed that in mixed-phase clouds the liquid phase appears prior freezing [*Field et al.*, 2004; *Ansmann et al.*, 2008; *Murray et al.*, 2012; *Westbrook and Illingworth*, 2013]. This suggest that the nucleation of ice directly from the gas phase is not relevant for these clouds. Hence, the immersion/condensation pathway is thought to be the most important in the mixed-phase range of temperatures, and it will be the main subject of this thesis.

Several modelling studies also found that deposition nucleation contributes little to the number of nucleation events in mixed-phase clouds [*Cui et al.*, 2006; *Philips et al.*, 2007; *Hoose et al.*, 2010a]. Contact nucleation is thought to not be significant in mixed-phase clouds [*Cui et al.*, 2006; *Philips et al.*, 2007], but some studies suggest that it might be important in some situations, particularly where droplets are evaporating [*Durant and Shaw*, 2005; *Ansmann et al.*, 2008; *Ladino Moreno et al.*, 2013].

2.2. The ice phase evolution

Liquid water in a supercooled state is commonly found in the atmosphere despite its intrinsic meta-stability. For example, satellite observations of cloud-top phase using LIDARs estimate that around 52% of all clouds in the globe are composed of supercooled water at -20ºC [*Choi et al.*, 2010]. This fraction varies significantly between regions and it is correlated negatively with the dust concentrations observed by satellite (Figure 4).

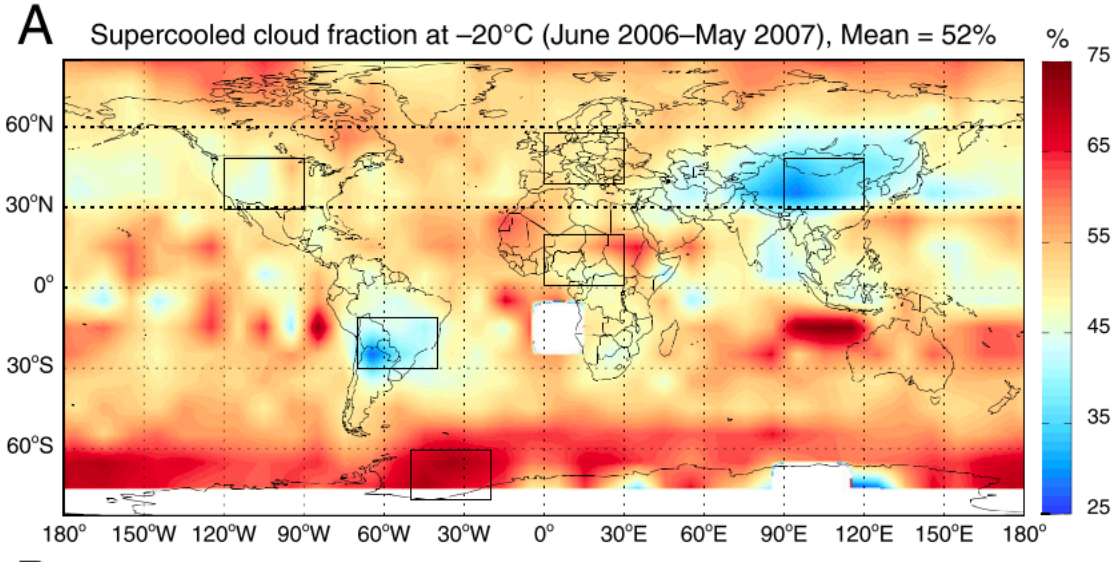

Figure 4 Supercooled liquid cloud fraction at -20ºC obtained from the National Aeronautics and Space Administration's (NASA) spaceborne instrument, cloud-aerosol lidar with orthogonal polarization (CALIOP). Image reproduced from Choi et al. [2010].

The phase of clouds has large atmospheric implications in terms its radiative properties and evolution [*Sassen and Khvorostyanov*, 2007]. Liquid clouds are typically composed of small droplets of about 10μm, whereas heterogeneously nucleated ice clouds, due to the smaller concentrations of INP in comparison with cloud condensation nuclei (CCN), tend to create much fewer ice crystals. Once the ice-crystals are formed, due to the lower saturation vapour pressure that ice has in comparison to liquid water, water vapour deposits preferentially on the surface of ice particles, enabling them to grow at the expense of ambient water vapour and condensed liquid water. This process in known as the Wegener-Bergeron-Findeisen

process [*Wegener*, 1923]. The preferential deposition of vapour on ice produces several changes to the cloud properties. First, because the condensed water is now accumulated in larger hydrometeors, its surface area is much smaller than when it is distributed across a larger population of smaller cloud droplets, making it less effective to reflect sunlight. Then, as the fall speed of these newly formed hydrometeors increases as they grow by deposition, they start to precipitate, colliding with water droplets that freeze in contact with the ice (riming process) depleting the cloud water content in what is called the cold-rain process. All these effects combined can change critically the properties of a mixed-phase clouds or make the cloud dissipate completely. A larger concentration of ice-nucleating particles will produce more ice-formation events, making these processes more efficient and hence decreasing the amount of sunlight that a cloud can reflect. More nucleation events can also lead to an ice cloud with more and smaller ice crystals, which will reflect more sunlight than a cloud with fewer and larger crystals. However, this effect is smaller than the caused by the phase transition [*Storelvmo et al.*, 2011], as typical cloud droplet concentrations are of the order of 100-1000 cm^{-3} [*H. Pruppacher*, 1997], whereas ice crystal number concentrations are typically about 4 to 5 orders of magnitude lower (around $1L^{-1}$ [*Gultepe et al.*, 2001]).

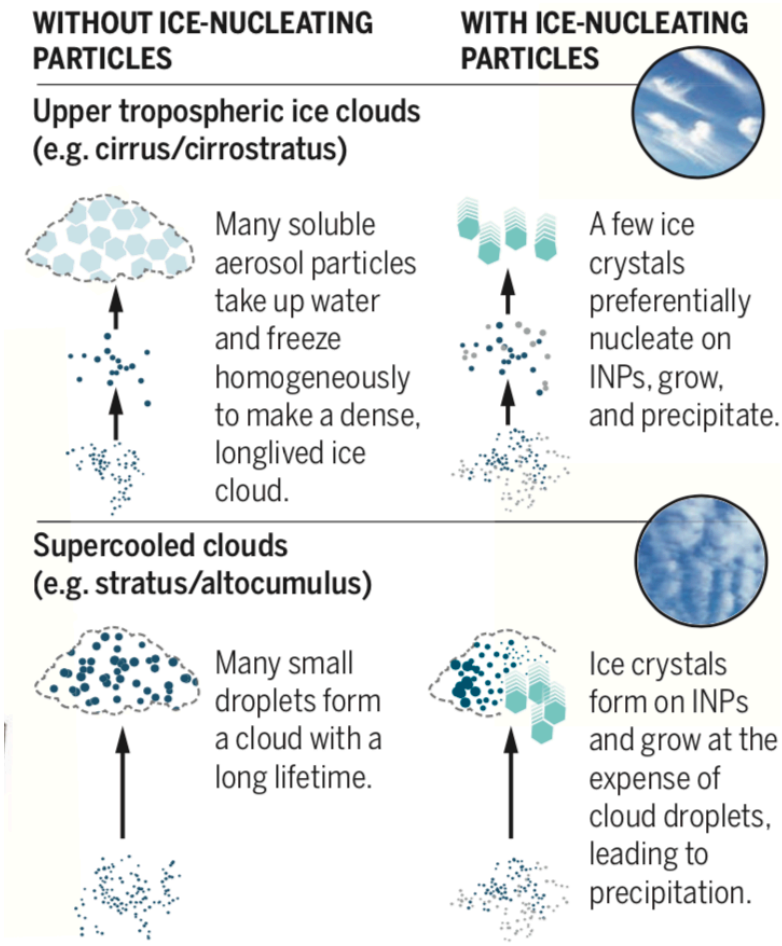

Figure 5. Example representation of the effect of INPs in upper tropospheric and supercooled clouds. For both high (ice) clouds and supercooled liquid clouds, heterogeneous ice nucleation produces few and large ice crystals that precipitate quicker, decreasing the lifetime of the clouds. Picture obtained from Murray [2017].

2.3. Ice nucleation in the atmosphere

Despite the importance of ice nucleation for mixed-phase clouds, the representation of cloud glaciation is currently very uncertain. Most global climate models tend to represent cloud glaciation with schemes that treat all mixed-phase clouds in the same manner, independently of the INP concentration [*McCoy et al.*, 2015a]. These schemes do not capture the important special variations in cloud glaciation temperatures [*McCoy et al.*, 2016] observed by satellite and ground lidars [*Choi et al.*, 2010; *Murray et al.*, 2012].

The concentration of ice-nucleating particles has been parameterized by using some parameterizations [*Fletcher*, 1962; *Cooper*, 1986; *Meyers et al.*, 1992] that use

temperature as the only variable to predict INP. These parameterizations were developed by fitting a temperature dependent function to several INP datasets. Meyers et al., [1992] also considered the supersaturation with respect to ice to develop a parameterization for condensation/deposition ice nucleation from CFDC observations in continental air masses. A more recent parameterization with an increase degree of complexity is the one developed in DeMott et al., [2010] in which several more datasets obtained from CFDC observations were used to fit the measured INP concentrations as function of temperature and the concentration of aerosol particles larger than 0.5 micrometers. Recent parameterizations typically predict INP using temperature and the composition and surface of the aerosol population from both laboratory and field observations [*Niemand et al.*, 2012; *Atkinson et al.*, 2013; *DeMott et al.*, 2015]. There are differences as large as several orders of magnitude when using these different parameterizations to predict INP at a given temperature, which makes ice nucleation a very uncertain process in climate models.

Some studies have previously attempted to represent the global distribution of ice-nucleating particles in the atmosphere based on the aerosol composition. For example, *Lohmann and Diehl* [2006] used CNT to simulate the distribution of dust and black carbon aerosols acting as ice-nucleating particles based on laboratory measurements. *Hoose et al.* [2010] included bacteria, pollen and fungal spores as ice-nucleating particles, finding that they contribute little to the total freezing events in the atmosphere in agreement with later studies [*Sesartic et al.*, 2013; *Spracklen and Heald*, 2014] . *Wang et al.* [2014] extended the model presented in *Hoose et al.* [2010], by including a distribution of contact angles to classical nucleation theory. [*Phillips et al.*, 2008] developed a framework to represent ice-nucleation based on observation of the INP composition from different field campaigns.

The question of how important the representation of ice nucleation is for cloud radiative properties in global models has also been addressed in some studies. For example, *DeMott et al.*, [2010] developed a parameterization of INP with new observations of atmospheric concentrations and used it to update the representation of INP in their model producing a change of 2.3W/m^2 in shortwave cloud forcing globally. *Yun and Penner* [2012] also obtained a change in top-of-the-atmosphere shortwave and longwave fluxes of about 3 to 8 W/m^2 depending on which

parameterizations were used for the different ice-nucleation modes. Similar studies of the effect of representing ice nucleation by various parameterizations obtained similar sensitivities [*Hoose et al.*, 2010a; *Tan et al.*, 2016; *Sagoo and Storelvmo*, 2017].

Despite the importance of ice nucleation for climate models, the observations of ice-nucleating particle concentrations, which are essential to evaluate models, are relatively scarce, with very little global coverage [*Vergara-Temprado et al.*, 2017] and more efforts are needed to constrain the model representation of INP and its effect on clouds.

3. Secondary ice processes

A different pathway through which the number of ice crystals in mixed-phase clouds can increase is through the so-called secondary ice processes, in which new ice crystals are generated from previously formed ice [*Field et al.*, 2016]. Some hypothesis that such types of processes could happen in mixed-phase clouds appeared in the 70s with experimental evidence of a secondary ice mechanism, the Hallet-Mossop process (H-M) [*Hallet and Mossop*, 1974]. Hallet and Mossop found that when using a rotating rod covered in rime to clash against supercooled water droplets in a chamber, the number of ice crystals in the chamber increased substantially as function of the amount of water mass rimmed. This process only worked at a narrow range of relatively high temperatures (-3^{o}C to -8^{o}C) in which ice crystals tend to grow in the form of needles. They explained their result by suggesting that small fragments of ice break as the riming process happens, ejecting small ice splinters. Once these small splinters are emitted, they find themselves in an ice supersaturated environment and therefore grow quickly to larger sizes potentially feeding back into the ice production process. The concentration of primary nucleated particles that is necessary to trigger and maintain this process is still very uncertain, but some estimates suggest that it can be as low as 10^{-5} to 10^{-3} particles per litre [*Beard*, 1992; *Crawford et al.*, 2012].

The experimental study presented by *Hallett and Mossop* [1974] was motivated by previous field observations of marine mixed-phase clouds in which the ice crystal concentrations at warm temperatures (<-10^{o}C) exceeded by about 4 orders of

magnitude the concentration of ice-nucleating particles in marine clouds [*Mossop*, 1970] . These early observations have subsequently been shown to be affected by instrumental ice-crystal shattering problems in which collisions between cloud ice-crystals and the measuring probe caused the crystals to break into many small pieces that were detected later by the instrument. This artifact could have caused the ice crystal number concentrations measured in the old studies to be overestimated by up to two orders of magnitude [*Korolev et al.*, 2013]. However, after correcting this instrumental artifact using new techniques [*Korolev and Field*, 2015], some more recent field studies show that the discrepancies between ice crystal number and ice-nucleating particles concentration still persist in clouds with warm tops [*Grosvenor et al.*, 2012], particularly those affected by strong updrafts [*Lawson and Gettelman*, 2014; *Ladino et al.*, 2017].

Some models use empirical representations of the H-M process as a secondary ice production mechanism. They typically relate the number of ice splinters ejected as a function of the rimed mass with a triangular function that peaks at -5^{o}C and decreases linearly up to -3^{o}C and down to -8^{o}C. The efficiency of this process depends strongly on the amount of supercooled water in the cloud and the efficiency of primary ice production processes because the riming particles that initiate the H-M process are nucleated as primary particles. In general, modelling studies do not agree on the importance of the H-M process for cloud evolution. While some studies suggest that this process could be important to represent the properties of the clouds [*Connolly et al.*, 2006; *Crawford et al.*, 2012] but does not affect precipitation rates, others found that it might affect precipitation by changing the vertical distribution of latent heat [*Clark et al.*, 2005]. In other studies, the H-M did not seem to affect substantially the evolution of the cloud system [*Dearden et al.*, 2016].
The large discrepancies between studies probably arise from the different evolution and properties of the various cloud systems studied and the uncertainties in the representation of this process and its interaction with other uncertain microphysical processes.

Some other secondary ice productions processes have been proposed such as the fragmentation of ice crystals by collisions amongst them [*Vardiman*, 1978;

Takahashi et al., 1995] or the shattering of droplets in the process of freezing [*Leisner et al.*, 2014], but their possible atmospheric relevance is also still uncertain.

4. INP effects on cirrus clouds and geoengineering

The term ice-nucleating particles is not only used for aerosols with the ability to trigger ice-nucleation from supercooled liquid water, but also for particles that can grow ice crystals on their surface when exposed to an ice supersaturated environment without the need for liquid water to condense first. This pathway for crystal formation is called deposition mode nucleation. In principle, several observational and modelling studies have found that this pathway seems not to be important for mixed-phase clouds, however its importance for cirrus cloud formation can be critical. Cirrus clouds form when water vapour condenses or deposits onto aerosol particles. If the saturation vapour pressure is higher than the supersaturation needed to condense liquid, liquid water condenses and freezes immediately homogeneously due to the low ambient temperature. If the saturation is below liquid supersaturation but above ice supersaturation, ice crystals can form heterogeneously on the surface of ice-nucleating particles. In general, the concentration of ice-nucleating particles in the atmosphere is always orders of magnitude lower than the concentration of aerosol particles. Hence, the way in which a cirrus cloud forms can substantially affect the properties of the clouds. If a cloud is formed through homogeneous freezing it will have many and smaller crystals than if it has been nucleated heterogeneously. In a similar way to the effect of having low or high concentrations of CCN particles in a liquid cloud, having smaller crystals increases the lifetime of the cloud and makes it more efficient at reflecting sunlight.

Cirrus clouds overall have a warming effect in the atmosphere. They are typically much optically thinner than low-level liquid clouds, which makes them almost transparent to shortwave radiation. However, they are good absorbers and reflectors of longwave radiation, making them opaque to the LW radiation emitted by the Earth's surface. As their temperature is low, they emit back to space much less longwave radiation than the surface behind them, causing an effect similar to

greenhouse gases in the atmosphere. This is the reason why an artificial modification of their properties has been proposed with the objective to make then thinner as a geoengineering technique to tackle future increases in greenhouse gases. This proposed method is called 'cirrus clouds thinning' (CCT) and was firstly proposed by *Mitchell and Finnegan* [2009]. The main idea of CCT is to emit large concentrations of efficient ice-nucleating particles acting in the deposition mode to change the way homogeneously nucleated cirrus clouds are formed. Heterogeneously nucleated clouds will be composed on fewer and larger crystals, therefore having shorter lifetimes and smaller optical thicknesses. These techniques have the advantage that they produce a similar effect on the radiative balance as a CO_2 decrease, so the combined effect of this technique and an increase in greenhouse gases in the water cycle is smaller than when using techniques focused on reflection of incoming sunlight [*Kristjánsson et al.*, 2015]. Some studies suggest that this method could work to offset greenhouse gas warming [*Storelvmo et al.*, 2013] while some others found no significant effect due to complex microphysical responses of their model [*Gasparini and Lohmann*, 2016]. Fundamental uncertainties in ice microphysics and its representation in models are likely responsible for these contradictory results [*Gasparini and Lohmann*, 2016]. Currently some observational studies suggest that most cirrus clouds nucleate heterogeneously in the present-day atmosphere [*Cziczo et al.*, 2013], which might limit the possible usefulness of this technique. However, homogeneously nucleated cirrus clouds are thought to be formed in high latitude winters and regions dominated by strong orographic updrafts [*Krämer et al.*, 2016], so it could still be a useful way to reduce warming in regions strongly affected by warming such as the Arctic [*Lohmann and Gasparini*, 2017].

5. Measuring ice nucleation in the laboratory and the atmosphere.

There has been a lot of interest in the area of experimental ice nucleation[*Hoose and Möhler*, 2012; *Murray et al.*, 2012; *Kanji et al.*, 2017]. One of the main goals of this research is to tackle some of the fundamental gaps in our understanding that modellers face when trying to represent and quantify ice nucleation in the atmosphere and draw firm conclusions on any hypothetical modification (naturally or anthropogenically driven) of the atmospheric INP distribution. Some of these

fundamental questions include issues such as what aerosols causes nucleation predominantly in the atmosphere or what approach represents better the process of ice-nucleation.

There are two main techniques to study the ability of different aerosols to nucleate ice from supercooled water and measure its concentration in the atmosphere. They can be grouped depending on whether the aerosols are introduced into the instrument as dry dispersions (dry-dispersion techniques) or are first suspended in water droplets (suspension techniques) [*Hiranuma et al.*, 2014]. Dry dispersion techniques expose aerosols to water saturation to form water droplets and then measure how many ice crystals form at a certain temperature. They typically expose the formed ice crystals to ice supersaturation to make then grow and detect separately from liquid droplets. Some examples of instruments using this technique are continuous flow diffusion chambers (CFDC) [*Noone et al.*, 1988] or cloud chambers [*Möhler et al.*, 2006]. In wet suspension techniques, a large population of aerosol particles are immersed in water droplets. The droplets are then cooled down on a cold stage and the fraction of droplets frozen at each temperature is recorded. An example of an instrument using this method can be found in *Whale et al.* [2014]. In dry-dispersion techniques, every droplet formed contains a single aerosol particle whereas in suspension techniques, every droplet may contain a whole population of aerosol particles. This difference makes both methods sensitive to different ranges of INP efficiencies.

Dry-dispersion techniques typically are able to detect very high INP efficiencies than can be reached at low temperatures, whereas in suspension techniques, because many aerosol particles are included in every droplet, their limit of detection is lower, making them able to measure much lower INP efficiencies at much warmer temperatures. However, impurities in water used in suspension techniques often make the droplets freeze at around -25^{o}C (depending on the droplet size used), making detection of INP activity at colder temperatures harder to access in these methods.

Both methods have been used to study the ice-nucleation efficiency of aerosol samples collected from the atmosphere and samples generated in laboratories. When the aerosols have been collected from the atmosphere, the concentration of ice-nucleating particles can be inferred from the number of nucleation events and the volume of the air sampled. Laboratory-generated samples, on the other hand, serve to study fundamental properties of an aerosol population such as the concentration of sites from where ice-nucleation can occur to then derive parameterizations of its ice-nucleation ability that can be used in models or for comparison in experimental and field studies.

5.1. Laboratory-derived parameterizations of ice-nucleation

Several parameterizations of the ice-nucleating ability of different aerosol species have been developed in recent years (Figure 6). Mineral dust particles, which are a well-known species for ice-nucleation, have been extensively studied. Several studies have quantified the ice-nucleating ability of different types of mineral dust such as illite [*Broadley et al.*, 2012], kaolinite [*Murray et al.*, 2011], Arizona test dust [*Connolly et al.*, 2009], different natural dust samples [*Niemand et al.*, 2012; *Ullrich et al.*, 2017], K-feldspar [*Atkinson et al.*, 2013; *Harrison et al.*, 2016] and several other mineral components of dust [*Atkinson et al.*, 2013].

Some modelling studies have determined the atmospheric relevance of dust and, in general, there is agreement that dust is an important component causing heterogeneous ice-nucleation in mixed-phase clouds [*Hoose et al.*, 2010a; *Niemand et al.*, 2012; *Atkinson et al.*, 2013; *Vergara-Temprado et al.*, 2017].

Biological aerosols have also received a lot of attention as they typically induce freezing at relatively warm temperatures, where secondary ice processes can start. Some of the existing data for bioaerosols include bacteria [*Mortazavi et al.*, 2008], pollen [*von Blohn et al.*, 2005], pollen fragments [*O'Sullivan et al.*, 2015], fungal spores [*Iannone et al.*, 2011] and soil dust with biological components [*O'Sullivan et al.*, 2016]. The importance of biological material for ice nucleation in the atmosphere is not clear. Some modelling studies have estimated that the contribution of bacteria, pollen and fungal material to atmospheric concentrations of ice-nucleating particles is small compared to that of dust [*Hoose et al.*, 2010b;

Spracklen and Heald, 2014]. Some studies show a decrease in the activity of atmospherically collected aerosol samples in farm environments after being exposed to heat [*Garcia et al.*, 2012], which suggest that a biological component might be an important component for triggering ice nucleation in those aerosol samples, however, it is unclear how much soil dust is emitted into the atmosphere.

Soot aerosols have also been the focus of several studies. Its relative importance in the atmosphere is not clear, as different experimental studies report INP efficiencies for BC particles that differ in orders of magnitude [*DeMott*, 1990; *Diehl and Mitra*, 1998; *Schill et al.*, 2016; *Ullrich et al.*, 2017]. Understanding the importance of this material for nucleating ice is critical to assess the possible role of human induced changes on cloud glaciation and the consequent climatic impacts. An extensive assessment of its relative importance will be presented on third chapter of this thesis.

Other aerosols that have been observed to nucleate ice in laboratory studies are ashes [*Umo et al.*, 2014], volcanic ashes [*Mangan et al.*, 2017] , lead-containing aerosols [*Cziczo et al.*, 2009], cellulose [*Hiranuma et al.*, 2015] and marine organic aerosols [*Wilson et al.*, 2015]. The second chapter of this thesis aims to understand the global importance of marine organic aerosols because of their potential role in controlling remote marine cloud systems, which cover much of the Earth. For an extensive discussion of different studies looking at ice nucleation by marine organic entities, see the introduction of the second chapter.

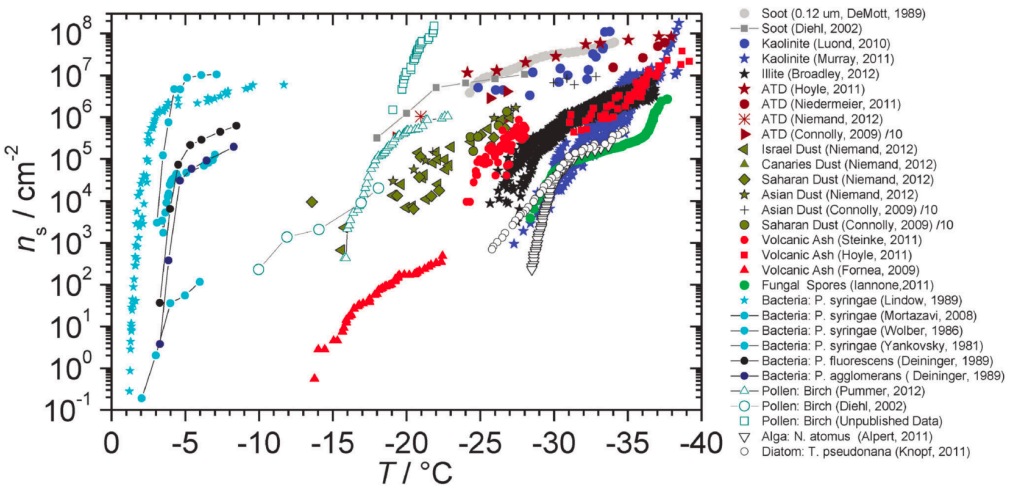

Figure 6. Experimental measured values of the density of active site from which ice nucleation can happen at different temperatures for several components. Plot reproduced from Murray et al.[2012] See the original paper for the references.

5.2. Atmospheric observations of INP concentrations

Measuring concentrations of ice-nucleating particles in different parts of the atmosphere and different times is a major challenge for the experimental ice-nucleation community. Currently, the observations of atmospheric INP concentrations are scarce with very little global and temporal coverage. Some field studies from the past century measured the atmospheric INP concentration in different locations [*Bigg*, 1953, 1973; *Fletcher*, 1962; *Rosinski et al.*, 1987, 1988] giving the first estimates of INP concentrations. After that, the need to develop empirical parameterizations of INP stimulated new investigations of the atmospheric concentrations of ice-nucleating particles, which focused mainly on the continental US region [*Phillips et al.*, 2008; *DeMott et al.*, 2010]. Currently, several groups are investing effort to extend the global coverage of INP observations, measuring INP concentrations in places such as the Alps [*Conen et al.*, 2015], Cape Verde [*Welti et al.*, 2017], remote marine environments [*DeMott et al.*, 2016], the Poles [*Ardon-Dryer et al.*, 2011] and China [*Yin et al.*, 2012] to mention just a few [See table 1 on Appendix C].

The overall picture from all these studies is that terrestrial environments tend to have INP concentrations that are orders of magnitude greater than remote marine environments [*DeMott et al.*, 2016], which has a strong influence on the way cloud glaciation happens in each environment. This continental/marine contrast in INP concentrations is currently not represented by most climate models [*McCoy et al.*, 2015a] and appears to have a large influence on the model performance [*McCoy et al.*, 2016]. By joining together some of the datasets currently available (Figure 7), it can be observed that the measured INP concentration spans about 8 orders of magnitude and can be as variable as 5 orders of magnitude for a given temperature (Figure 7). This variability is much greater than the observed for CCN concentrations. These values are probably underestimates of the real variability, as due to current instrumental limitations the observations are limited to short time periods in very few places.

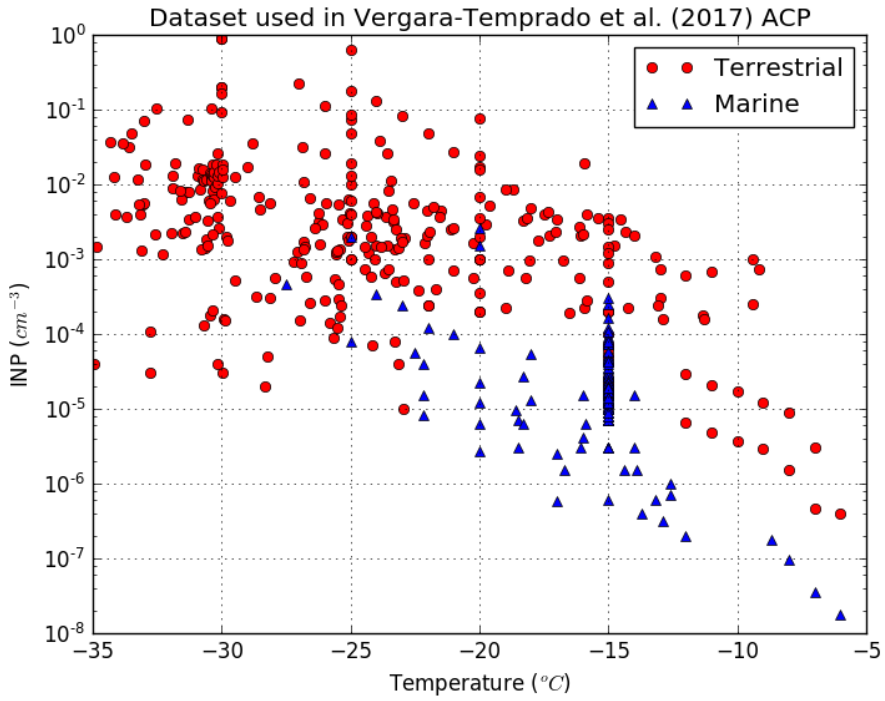

Figure 7 Global dataset of INP concentrations used in the second chapter of the thesis for model evaluation [Vergara-Temprado et al., 2017]. This dataset includes observations from filter measurements and CFDCs. The data points are classified between concentrations measured in terrestrial environments (circles) and marine environments (triangles).

5.3. Compositional analysis of ice-nucleating particles in the atmosphere.

To simulate ice-nucleating particles in global models, we need to know the chemical composition of the INP at cloud-level. Field studies have tried to address this question by two different approaches. Some studies take freshly nucleated ice crystals from mixed-phase clouds and separate them from ice crystal aggregates, liquid water droplets and interstitial aerosols. Then, by comparing the aerosol composition of the ice residuals to the background aerosol composition, it can be observed which aerosol components are enhanced in the ice crystals, assuming that these aerosols have been responsible for ice formation [*Cozic et al.*, 2008; *Pratt et al.*, 2009; *Kamphus et al.*, 2010; *Kupiszewski et al.*, 2016; *Schmidt et al.*, 2017]. Other studies follow a similar approach by taking an aerosol sample, testing its ice nucleating ability in a Continuous Flow Diffusion Chamber (CFDC) or a cloud chamber and then examining the composition of the aerosols inside the formed ice crystals [*Baustian et al.*, 2012; *Mccluskey et al.*, 2014].

Both methods have their advantages and inconveniences. The first method is in principle more representative of what nucleates ice in the cloud. However, scavenging of aerosol particles or activated cloud droplets by ice crystals (riming) can lead to the presence of aerosol particles inside the crystal that had no influence on the nucleation process. Also, the method cannot distinguish between ice crystals nucleated heterogeneously, homogeneously or formed through secondary ice processes, which could also lead to possible misclassifications. These problems are solved by using the second method (activating aerosols with an instrument), in which there is a much better control of the evolution of the aerosol population and the nucleation of ice crystals. However, this method does not observe crystals directly nucleated at ambient conditions (but under the conditions inside the instrument) and some instrumental artifacts such as size cut-offs or loss of particles through the inlet are still present.

Overall, most field studies show a consistent enhancement of dust particles over background air in the ice crystal residues, suggesting that dust is a principal

component for ice nucleation. This conclusion is backed up by several experimental studies of dust particles being efficient INPs in laboratory experiments [Connolly et al., 2009; Niemand et al., 2012; Atkinson et al., 2013], correlations between the amount of dust detected by satellite and the fraction of ice in mixed-phase clouds [Choi et al., 2010] and modelling studies [Hoose et al., 2010a; Niemand et al., 2012; Atkinson et al., 2013; Vergara-Temprado et al., 2017]. Aerosols with an organic signature have been also observed sometimes to be enhanced in ice crystal residues [Pratt et al., 2009]. However, these results should be interpreted with caution because new approaches have shown that single-particle mass spectrometry methods (SPMS) produce a large fraction of false positives when identifying organic material as it can be confused with phosphorous-rich types of mineral dust [Zawadowicz et al., 2017]

The role of BC is controversial, with a few studies showing an enhancement in ice-crystal residues [*Cozic et al.*, 2008; *Twohy et al.*, 2010] but several others not [*Kamphus et al.*, 2010; *Baustian et al.*, 2012; *Kupiszewski et al.*, 2016; *Schmidt et al.*, 2017]. The third chapter of this thesis will be an extended assessment dedicated to the potential role of BC particles acting as INP in the condensation/immersion mode.

6. Representations of ice-nucleation

There are two commonly used ways to represent and quantify the process of ice nucleation.

In the past, many studies have tried to explain ice-nucleation under the framework of classical nucleation theory (CNT) [*DeMott*, 1990; *Murray et al.*, 2011; *Broadley et al.*, 2012], in which the time dependence of ice nucleation is taken as an important factor determining the number of crystallization events. More recently, a description of ice nucleation has been used based on a deterministic approach, in which the time dependence is neglected and ice nucleation depends just on temperature and the particle composition [*Vali*, 1994, 2008; *Connolly et al.*, 2009; *Atkinson et al.*, 2013]. These two descriptions will be explained in detail in this section together with a discussion of the weaknesses and strengths of these two approaches.

6.1. Singular description

The singular description is based on the idea that ice nucleation occurs from specific active sites located randomly on the surface of the particle that trigger ice nucleation instantaneously when they reach a certain activation temperature [*Vali et al.*, 2015b]. The site density is assumed to be uniform across the particle surface, hence the probability of having a certain number of them on the surface of a particle can be calculated from a Poisson distribution.

$$F(k,\lambda) = \frac{e^{\lambda}\lambda^{k}}{k!} \quad (9)$$

where λ refers to the expected number of active sites, and F to the probability of finding k active sites. Under this framework, a particle will nucleate ice if, for a certain temperature, it has at least one active site. Hence, the probability of a particle to nucleate ice (p) can be calculated as the probability of having 1 or more active sites:

$$p = \sum_{1}^{\infty} F(k,\lambda) = 1 - F(0,\lambda) = 1 - e^{-\lambda} \quad (10)$$

For a sample of particles with the same composition and size, the fraction of particles with the ability to nucleate ice (commonly referred as the fraction frozen) is equal to the previously calculated probability. Using this framework, laboratory studies can quantify the density of active sites in their particles at different temperatures (n_s) depending on the fraction of droplets observed to freeze. For example, for a population of droplets containing identical populations of aerosol particles with a total aerosol surface area per droplet A_d, the expected number of active sites per droplet will be:

$$\lambda = n_s \cdot A_d \quad (11)$$

The density of active sites in this population of aerosols can be calculated from the experimentally observed fraction frozen (ff) as:

$$n_s(T) = -\frac{\ln\big(1 - ff(T)\big)}{A_d} \quad (12)$$

With the n_s values obtained from the experiments, one can then calculate what the concentration of INPs will be for those types of aerosols in the atmosphere just by knowing their concentration and size distribution. In the case of a lognormal distribution of aerosols, such as the ones used in many aerosol models, the INP concentration at a temperature T of a mode with mean radius r_m and standard deviation σ can be calculated as:

$$[INP](T) = [N]\int_0^{\infty}\left(1 - e^{-4\pi r^2 n_s(T)}\right)\frac{1}{r\ln(\sigma)\sqrt{2\pi}}e^{-\frac{(\ln(r)-\ln(r_m))^2}{2\ln(\sigma)^2}}dr \quad (13)$$

where $[N]$ is the number concentration of particles in the mode. As the integral has no analytical solution, numerical methods should be used to solve it. However, for the case when then probability of having more than an active site per particle is small, the concentration of ice-nucleating particles per mode can be approximated to just the number of active sites in the whole aerosol population (see appendix B for the derivation):

$$[INP](T) \approx [S] \cdot n_s(T) \quad (14)$$

where $[S]$ is the surface area density of the aerosol population in the atmosphere.

6.2. Classical nucleation theory

Classical nucleation theory (CNT) attempts to represent the process of ice nucleation as a stochastic process in which the rate of nucleation events is defined by temperature and the ability of the surface of the aerosol particle to nucleate ice, which is quantified in terms of a contact angle [*H. Pruppacher*, 1997; *Seinfeld and Pandis*, 2006; *Lamb and Verlinde*, 2011]. CNT was initially developed to explain homogeneous freezing events of pure water droplets. In a supercooled water droplet, clusters of molecules form randomly across the droplet and dissipate quickly. When one of these clusters reaches a critical size, it becomes stable and can grow to an ice crystal. The Gibbs free energy of forming a cluster (ΔG_{cl}) is the sum of the Gibbs free energy needed to create the surface (ΔG_s) (positive as it is an unfavourable process) and the energy to create the bulk (ΔG_v) (negative as it is favourable) [*Seinfeld and Pandis*, *2006*]:

$$\Delta G_{cl} = \Delta G_s - \Delta G_v \quad (15)$$

The interfacial Gibbs free energy can be expressed as:

$$\Delta G_s = 4\pi r^2 \gamma. \quad (16)$$

where r is the radio of the cluster and γ the interfacial energy between ice and water. The equivalent for the bulk of the cluster is:

$$\Delta G_v = \frac{4\pi r^3}{3v} k_B T \ln S \quad (17)$$

where v is the volume of a water molecule, k_B is the Boltzmann constant, T is the temperature and S is the saturation ratio with respect to ice. The critical radius r_{crit} at which the cluster will grow favourable can be calculated as the maximum of the total Gibbs free energy of the cluster ($\frac{d\Delta G_{cl}}{dr} = 0$):

$$r_{crit} = \frac{2\gamma v}{k_B T \ln S} \quad (18)$$

And the Gibbs free energy to form a cluster:

$$\Delta G = \frac{16\pi\gamma^3 v^2}{3(k_B T \ln S)} \quad (19)$$

The rate of homogeneous nucleation events (J_h) can be calculated with the Arrhenius equation:

$$J_h = A \exp\left(\frac{-\Delta G}{k_B\, T}\right) \quad (20)$$

where A is a pre-exponential factor that can be obtain by fitting experimental data or derived theoretically from the kinetic equations of clusters of molecules agglomerating.

Classical nucleation theory can be adapted for heterogeneous nucleation by the addition of a term that lowers the Gibbs free energy need for nucleation to occur,

referred as the contact angle. The equation for the rate of freezing events is represented as:

$$J = A \exp\left(\frac{-\Delta G \cdot f}{k_B T}\right) \quad (21)$$

where f is a factor accounting for the contact angle (θ) of ice on particle surface in the form:

$$f = \frac{1}{4}(2 + \cos\theta)(1 - \cos\theta)^2 \quad (22)$$

It is not clear what the physical meaning of the contact angle is, so it is obtained for different aerosol samples as a fitting factor to experimental ice-nucleation results.

A more extended approach is sometimes used to account for the variability observed in ice-nucleation efficiencies among particles with the same composition. With this approach, a distribution of contact angles is used to account for the ice-nucleating ability of a particular material instead of just a single value [*Marcolli et al.*, 2007; *Eidhammer et al.*, 2009; *Broadley et al.*, 2012; *Niedermeier et al.*, 2015; *Savre and Ekman*, 2015b].

This approach has the advantage that the heterogeneity observed in natural samples, in which some particles nucleate ice much more efficiently than others, is much better represented.

6.3. Discussion of the two approaches

Fundamentally, ice nucleation is a stochastic process strongly dependent on temperature and less strongly on time and the surface area of aerosol material in contact with the water.

The stochastic and singular approaches presented here represent this process in quite different ways. In CNT, when a single contact angle is used, it is assumed that for a given aerosol sample, if two equal concentrations of this sample are immersed in two different water droplets and maintained at the same temperature, both droplets will have the same probability of freezing in time and you will just need to wait long

enough for both of them to freeze. In case they thaw and cool down again to the same temperature, the time at which they will freeze will be independent of how long it took for them to freeze previously. This happens because ice nucleation is seen as a stochastic process that will depend probabilistically on time and the surface area in contact with the water.

The singular description takes a different approach, and predicts a very different behaviour. Under the singular description, if two water droplets containing the same concentration of aerosols are cooled down to a certain temperature, the probability of them to freeze will be the same, but this probability will depend on whether there is an active site on the surface of the aerosol sample or not. For example, under this approach, it could be possible that just one of the droplets freezes once cooled down to a certain temperature, while the other does not, and that behaviour will prevail independently on how much time the droplets are maintained at that temperature. In case the droplets are thawed and cooled down to the same temperature again, the singular description will predict that the droplet that froze previously will freeze again once the 'critical' temperature is reached. This happens because the triggering of the previous freezing event depends on the specific active site in the immersed aerosols, and this site will get active again once their activation temperature is reached. The droplet that did not freeze previously will be expected to prevail again in a supercooled state as the material inside does not contain any of these specific active sites.

Which one of these descriptions represents better the reality has been the subject of debate. In past studies, an approach based on classical nucleation theory has been preferred to the singular description as way of representing atmospheric ice nucleation in models [*Hoose et al.*, 2010b; *Spracklen and Heald*, 2014; *Savre and Ekman*, 2015a, 2015b] . However, several laboratory observations support the idea that ice nucleation is a process that is not being triggered randomly across the surface of a particle but that comes from certain specific sites on the surface of a particle that become active at a certain temperature. For example, *Vali* [2008] showed that repeated cycles of freezing and melting of water droplets with soil dust

inside them, made them nucleate at very similar temperatures (less than a degree difference). *Marcolli et al.* [2007] showed that a CNT description with a single contact angle cannot account for the freezing behaviour of mineral dust particles. *Kiselev et al.* [2017] observed directly the formation of ice crystals on feldspar surfaces with an electron scanning microscope showing that the crystals appeared on surface defects, which also supports the singular description of ice nucleation. Some other studies also show a behaviour of several aerosol samples following a singular description approach [*Dorsey*, 1938; *Vali*, 1994]. However, for some materials, it has been shown that a CNT description can account for the freezing behaviour observed in the laboratory. Some examples are silver iodide [*Vonnegut and Baldwin*, 1984] or kaolinite [*Murray et al.*, 2011]. So, the question of which description is better will largely depend on the sample.

Currently, most of the relevant materials for ice nucleation show a much stronger particle to particle variability than dependence on time [*Connolly et al.*, 2009; *Niemand et al.*, 2012; *Atkinson et al.*, 2013; *Herbert et al.*, 2014; *Wilson et al.*, 2015], supporting a representation based on the singular description. However, time will also play a role in ice nucleation, and neglecting it is not desirable. That is why some people have tried to expand the singular description with schemes that take time into account such as the Framework for Reconciling Observable Stochastic Time-dependence (FROST) presented in *Herbert et al.* [2014], that takes into account the cooling rate when quantifying the ice-nucleation ability of the samples.

7. Ice-nucleating aerosols

7.1. Dust aerosols

As discussed previously, dust is a well-known ice-nucleating particle thought to have a first-order importance in the atmosphere for nucleating ice heterogeneously. Hence, it is important to understand its properties, emissions, and evolution in the atmosphere to estimate its atmospheric importance for ice-nucleation.

Dust is predominantly emitted from the large deserts of the world and then distributed by atmospheric transport through the atmosphere [*Kok et al.*, 2017].

Emissions of dust particles from high-latitude regions can also play an important role in modifying local dust concentrations but do not play an important role on a global scale [*Bullard et al.*, 2016] . Dust is mainly emitted from dry soils in what is called the saltation process. In the soil, small dust fragments become attached to larger aggregates by strong inter-particle cohesive forces [*Kok et al.*, 2012]. When wind speeds reach a certain value, the drag force becomes strong enough to lift into the atmosphere large dust particles of hundreds of micrometres. These particles fall quickly to the surface, crashing with aggregates and ejecting smaller particles (<50μm) that can be suspended into the atmosphere and transported in the form of aerosol particles.

Once dust particles are emitted into the atmosphere, they have important effects on climate. First, they are able to reflect and absorb solar radiation, cooling the surface and warming the atmosphere which modifies the thermodynamic vertical structure, affecting cloud formation and atmospheric circulation [*Kok et al.*, 2017]. They can act as cloud condensation nuclei, affecting cloud droplet number concentrations over desert regions although its global effect is small compared with other aerosol components [*Manktelow et al.*, 2010; *Karydis et al.*, 2011]. They can also influence cloud properties globally by acting as ice-nucleating particle as discussed previously.

Dust can be removed from the atmosphere by several mechanisms. Large dust particles, due to their size, have large fall speeds and can be deposited to the ground by the action of gravity. This process is referred as dry deposition and it is the most important removal process for super micron dust particles [*Mann et al.*, 2010]. Another way dust particles can by removed from the atmosphere is from the so-called wet scavenging processes, in which dust particles are remove by precipitation after being activated to water droplets, or by impaction with falling hydro-meteors. Wet removal processes are more important for submicron particles for which, given their size, their fall speeds are small (less than a millimetre per second) which makes gravitational deposition negligible.

Once deposited, dust particles still play a relevant role in the Earth system by providing nutrients for different ecosystems. For example, the deposition of

bioavailable iron from dust particles into the ocean is hypothesised to affect ocean productivity [*Martin et al.*, 1991], which affects the biogeochemical cycles of carbon and nitrogen [*Mahowald*, 2011] . Dust deposited in soil also can serve as a source of phosphorous, which affects ecosystem productivity [*Okin et al.*, 2004]. When deposited on ice surfaces, it changes the surface-albedo promoting a faster melting of the ice [*Flanner et al.*, 2008; *Painter et al.*, 2010].

The composition of dust particles emitted from different parts of the world varies depending on the soil mineralogical composition. This modifies dust radiative properties and the amount of minerals that can fertilize oceans and soils once deposited. Some studies have attempt to represent the difference in dust composition from different parts of the world [*Perlwitz et al.*, 2015; *Scanza et al.*, 2015] in atmospheric models. An approach to doing that is to consider that the composition of emitted dust particles is similar to the mineralogical composition of wet-sieved dust extracted from the soil [*Claquin et al.*, 1999]. More recent approaches take into account the differences between the wet-sieved soils mineralogical composition and the emitted dust fraction [*Perlwitz et al.*, 2015].

7.2. Sea-spray and marine organic aerosols.

Another aerosol component known to nucleate ice and thought to be relevant in the atmosphere is the organic part of marine emitted sea-spray aerosols [*Wilson et al.*, 2015], in which I will focus later in this thesis.

Sea-spray aerosols are emitted from the so-called bubble-bursting process [*Blanchard and Woodcock, 1957*] . When waves break in the ocean forming whitecaps, air bubbles are entrained into the sea. As the bubbles rise and reach the surface they produce the emission of small jet and film drops of sea-water into the atmosphere. Once these drops are emitted they start to evaporate water content, increasing the salinity until an equilibrium is reached, forming what is called a sea-spray particle. During the bubble-bursting process, as bubbles rise, they scavenge organic material in the water that is then emitted together with the drops. Wind speed is the main driver of this process [*Gong*, 2003], with stronger winds

enhancing the production of whitecaps, and hence, the emissions of sea-spray aerosols. Different parameterizations of sea-spray have been developed to be used in models [*Gong*, 2003; *Mårtensson et al.*, 2003; *Ovadnevaite et al.*, 2014] in which the parameterized sea-spray size distributions is dependent on windspeed and sometimes, on some other parameters such as wave height or temperature. However, none of these parameterizations aim to predict organic/inorganic fractions on the emitted sea-spray.

Super-micron sea-spray particles are typically composed of inorganic material, with very small fractions of organics [*Facchini et al.*, 2008]. However, in the submicron ranges, organic material can account for up to 80% of the sea-spray composition [*O'Dowd et al.*, 2008; *Rinaldi et al.*, 2013]. Representing the organic fraction of sea-spray and its seasonality has been suggested to be important for climate by interacting with clouds as cloud condensation nuclei and ice-nucleating particles [*Wilson et al.*, 2015]. Satellite observations suggest that the biogenic sources of marine aerosols could increase the reflected SW radiation of Southern Ocean clouds by up to 10 W/m^2 by increasing the cloud droplet number concentration [*McCoy et al.*, 2015b]. Modelling studies have also shown how the inclusion of marine organic emissions affect the indirect radiative effect on clouds [*O'Dowd et al.*, 2004; *Partanen et al.*, 2014].

The marine organic component of sea-spray is found partly to be composed of soluble and insoluble material. The soluble part (water-soluble organic material, WSOM) is typically measured next to the surface having a downward flux, together with sulphate aerosols [*O'Dowd et al.*, 2008]. In contrast, the insoluble part (water insoluble organic mass WIOM) is observed to have an upwards flux from the ocean. These observations suggest that the insoluble part is being emitted primarily from the ocean in addition to sea-spray while the soluble part is likely to be formed in the atmosphere through secondary processes. Studies using artificially generated aerosols in a wave tank with sea water during periods of phytoplankton blooms found a similar behaviour [*Facchini et al.*, 2008].

The mixing state of marine organic aerosols with sea-salt depends strongly on their size [*Prather et al.*, 2013]. At submicron sizes it has been found that the organic component is mainly mixed with sea-salt down to about 0.1μm where externally mixed organic components can start to dominate. This difference arises from the two ways in which marine aerosols are emitted. Film drops tend to produce smaller externally mixed aerosols while jet drops produce larger and internally mixed particles [*Wang et al.*, 2017].

The relation between the organic mass fraction in sea-spray and the organic content of the ocean is still not clear. In their study of atmospheric marine organic matter at Mace Head (Ireland), *O'Dowd et al.* [2004, 2015] found a strong correlation between the chlorophyll-a content on the ocean surface upwind from the measurement station and the organic mass fraction in submicron sea-spray particles. This finding has also been corroborated by some other studies at Mace Head [*Rinaldi et al.*, 2013] and some other parts of the world [*Sciare et al.*, 2009]. However, in some other studies this correlation between the organic mass fraction and chlorophyll-a could not be found [*Quinn et al.*, 2014]. It has been hypothesised that the discordant conclusions obtained in these studies arise from the differences in organic composition in different regions [*Burrows et al.*, 2014].

The organic mass fraction found in submicron sea-spray has been parameterized in several studies. Some studies made use of atmospheric measurements of WIOM to relate it with the chlorophyll-a content on the surface of the ocean from where sea-spray particles where emitted [*O'Dowd et al.*, 2008; *Gantt et al.*, 2011; *Rinaldi et al.*, 2013]. Chlorophyll-a is typically used in these studies as a marker of biological activity in the ocean based on the correlations previously discussed. These studies typically present a negative dependence between OMF and wind speed at the surface of the ocean to account for the mixing of the sea-surface microlayer in bulk sea water when winds are strong. Other authors have suggested that the reservoir of organic carbon in sea-water could be a better proxy for parameterizing the OMF, and suggested to use a constant organic enrichment factor to calculate the fraction of organic mass in nascent sea-spray [*Quinn et al.*, 2014]. *Burrows et al.* [2014]

presented a framework to model the absorption of organic matter by the surface of the bubbles based on the properties of different organic species found in sea-water. With that approach, the emissions of organic matter in the bubble bursting process depend not just on the organic content of the ocean, but also on how surface-active the different organic components are in each region of the ocean.

8. Research questions

8.1. Marine organic and K-feldspar as ice-nucleating particles

Historically a major limitation of studies looking at the global distribution of ice-nucleating particles [*Lohmann*, 2002; *Phillips et al.*, 2008, 2013; *Hoose et al.*, 2010b; *Yun and Penner*, 2012; *Sesartic et al.*, 2013; *Yun et al.*, 2013; *Spracklen and Heald*, 2014] has been the evaluation of their simulated concentrations with ambient measurements of the INP concentration. The comparison between CNT studies and atmospheric INP concentrations is not straight forward, as a certain time has to be used to integrate the number of freezing events to an INP concentration. However, using the singular description, the comparison becomes straight forward, as time do not influence the simulated concentrations.

Recently laboratory advances on measuring the ice nucleating activity of K-feldspar, the ice active component of desert dust [*Atkinson et al., 2013*], and marine organic aerosols [*Wilson et al., 2015*] have given new knowledge to the community that currently has not being incorporated in models.

Here, I will use the new information about the ice-nucleating ability of these two species to investigate its relative importance in the atmosphere and evaluate the model with the most recent atmospheric observations of ice-nucleating particles. This work aims to estimate what fraction of the atmospheric observations can be explained with these two species and determine where within model and measurement uncertainties we can identify locations where other species or unrepresented processes might be affecting the INP concentration.

8.2. Black carbon as ice-nucleating particle

Several modelling studies have simulated the concentration of BC particles acting as ice-nucleating particles in the immersion mode [*Phillips et al.*, 2008, 2013, *Hoose et al.*, 2010a, 2010b; *Fan et al.*, 2012; *Yun and Penner*, 2012; *Wang et al.*, 2014; *Savre and Ekman*, 2015b] based on old laboratory studies of its ice-nucleating ability [*DeMott*, 1990; *Diehl and Mitra*, 1998]. Simulating these concentrations correctly is important to quantify any possible role that anthropogenic emissions of BC particles could have in affecting cloud glaciation [*Lohmann*, 2002]. However, new studies of BC particles acting as INPs in the immersion mode could not reproduce the results from previous studies which arises the question of is BC an actual relevant ice-nucleating particle in the atmosphere. Here, we will use new and old laboratory observations to assess the possible role that BC particles can have in the atmosphere and study the realism of these representations against field observations. This will help us better understand if humans have influenced substantially the atmospheric distribution of INPs through BC emissions and subsequently affected cloud, which is being mentioned in IPCC reports [*Boucher et al.*, 2013] as an important unknown that affects our ability to quantify human induced radiative forcing.

8.3. Impacts of improving the representation of INP on climate models

There are orders of magnitude differences in the atmospheric concentration of ice-nucleating particles from terrestrial environments to remote marine places. Most climate models do not account for these differences, which could lead to biases in the representation of cloud microphysics. For example, climate models tend to have a recursive cloud radiative bias in the remote marine region of the Southern Ocean, where our new modelling estimates suggest that the concentrations of INP will be substantially lower than in northern hemisphere terrestrial environments. The current model bias consists in modelled clouds that reflect too little solar radiation, and the main cloud type responsible for this bias has been identified as low-level clouds in the cold sector of the cyclones that are typically within the mixed-phase range of temperatures. A number of ice nucleation events much larger than in reality could be depleting the liquid of these clouds too efficiently making them reflect

much less solar radiation. So, our hypothesis is, can the right representation of the low concentrations of ice-nucleating particles present in the Southern Ocean improve the modelled radiative properties of these clouds and explain a large fraction of the bias. This is the hypothesis I address on the fourth chapter.

References:

Ackerman, A. S. (2000), Reduction of Tropical Cloudiness by Soot, *Science (80-.).*, *288*(5468), 1042–1047, doi:10.1126/science.288.5468.1042.

Albrecht, B. A.: (1989), Aerosols, cloud microphysics, and fractional cloudiness, *Science***245**, 1227–1230.

Ansmann, A. et al. (2008), Influence of Saharan dust on cloud glaciation in southern Morocco during the Saharan Mineral Dust Experiment, *J. Geophys. Res.*, *113*(D4), D04210, doi:10.1029/2007JD008785.

Ardon-Dryer, K., Z. Levin, and R. P. Lawson (2011), Characteristics of immersion freezing nuclei at the South Pole station in Antarctica, *Atmos. Chem. Phys.*, *11*(8), 4015–4024, doi:10.5194/acp-11-4015-2011.

Atkinson, J. D., B. J. Murray, M. T. Woodhouse, T. F. Whale, K. J. Baustian, K. S. Carslaw, S. Dobbie, D. O'Sullivan, and T. L. Malkin (2013), The importance of feldspar for ice nucleation by mineral dust in mixed-phase clouds., *Nature*, *498*(7454), 355–8, doi:10.1038/nature12278.

Baustian, K. J., D. J. Cziczo, M. E. Wise, K. A. Pratt, G. Kulkarni, A. G. Hallar, and M. A. Tolbert (2012), Importance of aerosol composition, mixing state, and morphology for heterogeneous ice nucleation: A combined field and laboratory approach, *J. Geophys. Res. Atmos.*, *117*(D6), n/a-n/a, doi:10.1029/2011JD016784.

Beard, K. V. (1992), Ice initiation in warm-base convective clouds: An assessment of microphysical mechanisms, *Atmos. Res.*, *28*(2), 125–152, doi:10.1016/0169-8095(92)90024-5.

Bigg, E. K. (1953), The formation of atmospheric ice crystals by the freezing of droplets, *Q. J. R. Meteorol. Soc.*, *79*(342), 510–519, doi:10.1002/qj.49707934207.

Bigg, E. K. (1973), Ice Nucleus Concentrations in Remote Areas, *J. Atmos. Sci.*, *30*(6), 1153–1157, doi:10.1175/1520-0469(1973)030<1153:INCIRA>2.0.CO;2.

Blanchard, D.C. , Woodcock, A.H. (1957) Bubble formation and modification in the sea and its meteorological significance. Tellus, 9

von Blohn, N., S. K. Mitra, K. Diehl, and S. Borrmann (2005), The ice nucleating ability of pollen: Part III: New laboratory studies in immersion and contact freezing modes including more pollen types, *Atmos. Res.*, *78*(3–4), 182–189, doi:10.1016/j.atmosres.2005.03.008.

Boucher, O. et al. (2013), Clouds and Aerosols, *Clim. Chang. 2013 Phys. Sci. Basis. Contrib. Work. Gr. I to Fifth Assess. Rep. Intergov. Panel Clim. Chang.*, 571–

657, doi:10.1017/CBO9781107415324.016.

Broadley, S. L., B. J. Murray, R. J. Herbert, J. D. Atkinson, S. Dobbie, T. L. Malkin, E. Condliffe, and L. Neve (2012), Immersion mode heterogeneous ice nucleation by an illite rich powder representative of atmospheric mineral dust, *Atmos. Chem. Phys.*, *12*(1), 287–307, doi:10.5194/acp-12-287-2012.

Bullard, J. E. et al. (2016), High-latitude dust in the Earth system, *Rev. Geophys.*, *54*(2), 447–485, doi:10.1002/2016RG000518.

Burrows, S. M., O. Ogunro, a. a. Frossard, L. M. Russell, P. J. Rasch, and S. Elliott (2014), A physically-based framework for modelling the organic fractionation of sea spray aerosol from bubble film Langmuir equilibria, *Atmos. Chem. Phys. Discuss.*, *14*(July), 5375–5443, doi:10.5194/acpd-14-5375-2014.

Carslaw, K. S. et al. (2013), Large contribution of natural aerosols to uncertainty in indirect forcing., *Nature*, *503*(7474), 67–71, doi:10.1038/nature12674.

Choi, Y.-S., R. S. Lindzen, C.-H. Ho, and J. Kim (2010), Space observations of cold-cloud phase change., *Proc. Natl. Acad. Sci. U. S. A.*, *107*(25), 11211–6, doi:10.1073/pnas.1006241107.

Claquin, T., M. Schulz, and Y. J. Balkanski (1999), Modeling the mineralogy of atmospheric dust sources, *J. Geophys. Res.*, *104*(D18), 22243, doi:10.1029/1999JD900416.

Clark, P. D., T. W. Choularton, P. R. a. Brown, P. R. Field, a. J. Illingworth, and R. J. Hogan (2005), Numerical modelling of mixed-phase frontal clouds observed during the CWVC project, *Q. J. R. Meteorol. Soc.*, *131*(608), 1677–1693, doi:10.1256/qj.03.210.

Conen, F., S. Rodríguez, C. Hüglin, S. Henne, E. Herrmann, N. Bukowiecki, and C. Alewell (2015), Atmospheric ice nuclei at the high-altitude observatory Jungfraujoch, Switzerland, *Tellus B*, *67*(1), 1–10, doi:10.3402/tellusb.v67.25014.

Connolly, P. J., A. J. Heymsfield, and T. W. Choularton (2006), Modelling the influence of rimer surface temperature on the glaciation of intense thunderstorms: The rime–splinter mechanism of ice multiplication, *Q. J. R. Meteorol. Soc.*, *132*(621C), 3059–3077, doi:10.1256/qj.05.45.

Connolly, P. J., O. Möhler, P. R. Field, H. Saathoff, R. Burgess, T. Choularton, and M. Gallagher (2009), Studies of heterogeneous freezing by three different desert dust samples, *Atmos. Chem. Phys.*, *9*(8), 2805–2824, doi:10.5194/acp-9-2805-2009.

Cooper, W. A. (1986), Ice Initiation in Natural Clouds. In: Precipitation Enhancement—A Scientific Challenge., *Meteorol. Monogr.*

Cozic, J., S. Mertes, B. Verheggen, D. J. Cziczo, S. J. Gallavardin, S. Walter, U. Baltensperger, and E. Weingartner (2008), Black carbon enrichment in atmospheric ice particle residuals observed in lower tropospheric mixed phase clouds, *J. Geophys. Res. Atmos.*, *113*(15), 1–11, doi:10.1029/2007JD009266.

Crawford, I. et al. (2012), Ice formation and development in aged, wintertime cumulus over the UK: observations and modelling, *Atmos. Chem. Phys.*, *12*(11), 4963–4985, doi:10.5194/acp-12-4963-2012.

Cui, Z., K. S. Carslaw, Y. Yin, and S. Davies (2006), A numerical study of aerosol effects on the dynamics and microphysics of a deep convective cloud in a continental environment, *J. Geophys. Res.*, *111*(D5), D05201, doi:10.1029/2005JD005981.

Cziczo, D. J. et al. (2009), Inadvertent climate modification due to anthropogenic lead, *Nat. Geosci.*, *2*(5), 333–336, doi:10.1038/ngeo499.

Cziczo, D. J., K. D. Froyd, C. Hoose, E. J. Jensen, M. Diao, M. A. Zondlo, J. B. Smith, C. H. Twohy, and D. M. Murphy (2013), Clarifying the Dominant Sources and Mechanisms of Cirrus Cloud Formation, *Science (80-.).*, *340*(6138), 1320–1324, doi:10.1126/science.1234145.

Dearden, C., G. Vaughan, T. Tsai, and J.-P. Chen (2016), Exploring the Diabatic Role of Ice Microphysical Processes in Two North Atlantic Summer Cyclones, *Mon. Weather Rev.*, *144*(4), 1249–1272, doi:10.1175/MWR-D-15-0253.1.

DeMott, P. J. (1990), An Exploratory Study of Ice Nucleation by Soot Aerosols, *J. Appl. Meteorol.*, *29*, 1072–1079, doi:10.1175/1520-0450(1990)029<1072:AESOIN>2.0.CO;2.

DeMott, P. J., a J. Prenni, X. Liu, S. M. Kreidenweis, M. D. Petters, C. H. Twohy, M. S. Richardson, T. Eidhammer, and D. C. Rogers (2010), Predicting global atmospheric ice nuclei distributions and their impacts on climate., *Proc. Natl. Acad. Sci. U. S. A.*, *107*(25), 11217–11222, doi:10.1073/pnas.0910818107.

DeMott, P. J. et al. (2015), Integrating laboratory and field data to quantify the immersion freezing ice nucleation activity of mineral dust particles, *Atmos. Chem. Phys.*, *15*(1), 393–409, doi:10.5194/acp-15-393-2015.

DeMott, P. J. et al. (2016), Sea spray aerosol as a unique source of ice nucleating particles, *Proc. Natl. Acad. Sci.*, *113*(21), 5797–5803, doi:10.1073/pnas.1514034112.

Diehl, K., and S. K. Mitra (1998), A laboratory study of the effects of a kerosene-burner exhaust on ice nucleation and the evaporation rate of ice crystals, *Atmos. Environ.*, *32*(18), 3145–3151, doi:10.1016/S1352-2310(97)00467-6.

Dorsey, N. E. (1938), Supercooling and freezing of water, *J. Res. Natl. Bur. Stand.*,

20(6), 799–808.

Durant, A. J., and R. A. Shaw (2005), Evaporation freezing by contact nucleation inside-out, *Geophys. Res. Lett.*, *32*(20), 1–4, doi:10.1029/2005GL024175.

Eidhammer, T., P. J. DeMott, and S. M. Kreidenweis (2009), A comparison of heterogeneous ice nucleation parameterizations using a parcel model framework, *J. Geophys. Res.*, *114*(D6), D06202, doi:10.1029/2008JD011095.

Facchini, M. C. et al. (2008), Primary submicron marine aerosol dominated by insoluble organic colloids and aggregates, *Geophys. Res. Lett.*, *35*(17), L17814, doi:10.1029/2008GL034210.

Fan, S. M., J. P. Schwarz, J. Liu, D. W. Fahey, P. Ginoux, L. W. Horowitz, H. Levy, Y. Ming, and J. R. Spackman (2012), Inferring ice formation processes from global-scale black carbon profiles observed in the remote atmosphere and model simulations, *J. Geophys. Res. Atmos.*, *117*(23), 1–12, doi:10.1029/2012JD018126.

Field, P. R., R. J. Hogan, P. R. A. Brown, A. J. Illingworth, T. W. Choularton, P. H. Kaye, E. Hirst, and R. Greenaway (2004), Simultaneous radar and aircraft observations of mixed-phase cloud at the 100 m scale, *Q. J. R. Meteorol. Soc.*, *130*(600), 1877–1904, doi:10.1256/qj.03.102.

Field, P. R. et al. (2016), Chapter 7. Secondary Ice Production - current state of the science and recommendations for the future, *Meteorol. Monogr.*, AMSMONOGRAPHS-D-16-0014.1, doi:10.1175/AMSMONOGRAPHS-D-16-0014.1.

Flanner, M. G., C. S. Zender, P. G. Hess, N. M. Mahowald, T. H. Painter, V. Ramanathan, and P. J. Rasch (2008), Springtime warming and reduced snow cover from carbonaceous particles, *Atmos. Chem. Phys. Discuss.*, *8*(6), 19819–19859, doi:10.5194/acpd-8-19819-2008.

Fletcher, N. H. (1962), The Physics of Rainclouds, *Cambridge Univ. Press*.

Gantt, B., N. Meskhidze, M. C. Facchini, M. Rinaldi, D. Ceburnis, and C. D. O'Dowd (2011), Wind speed dependent size-resolved parameterization for the organic mass fraction of sea spray aerosol, *Atmos. Chem. Phys.*, *11*(16), 8777–8790, doi:10.5194/acp-11-8777-2011.

Garcia, E., T. C. J. Hill, A. J. Prenni, P. J. DeMott, G. D. Franc, and S. M. Kreidenweis (2012), Biogenic ice nuclei in boundary layer air over two U.S. High Plains agricultural regions, *J. Geophys. Res. Atmos.*, *117*(D18), n/a-n/a, doi:10.1029/2012JD018343.

Gasparini, B., and U. Lohmann (2016), Why cirrus cloud seeding cannot substantially cool the planet, *J. Geophys. Res. Atmos.*, *121*(9), 4877–4893,

doi:10.1002/2015JD024666.

Girard, E., and N. Sokhandan Asl (2014), Relative importance of acid coating on ice nuclei in the deposition and contact modes for wintertime Arctic clouds and radiation, *Meteorol. Atmos. Phys.*, *123*(1–2), 81–92, doi:10.1007/s00703-013-0298-9.

Gong, S. L. (2003), A parameterization of sea-salt aerosol source function for sub- and super-micron particles, *Global Biogeochem. Cycles*, *17*(4), n/a-n/a, doi:10.1029/2003GB002079.

Grosvenor, D. P., T. W. Choularton, T. Lachlan-Cope, M. W. Gallagher, J. Crosier, K. N. Bower, R. S. Ladkin, and J. R. Dorsey (2012), In-situ aircraft observations of ice concentrations within clouds over the Antarctic Peninsula and Larsen Ice Shelf, *Atmos. Chem. Phys.*, *12*(23), 11275–11294, doi:10.5194/acp-12-11275-2012.

Gultepe, I., G. A. Isaac, and S. G. Cober (2001), Ice crystal number concentration versus temperature for climate studies, *Int. J. Climatol.*, *21*(10), 1281–1302, doi:10.1002/joc.642.

Gultepe, I. et al. (2007), Fog Research: A Review of Past Achievements and Future Perspectives, *Pure Appl. Geophys.*, *164*(6–7), 1121–1159, doi:10.1007/s00024-007-0211-x.

H. Pruppacher, J. K. (1997), Microphysics of Clouds and Precipitation 2nd ed - H.,

HALLETT, J., and S. C. MOSSOP (1974), Production of secondary ice particles during the riming process, *Nature*, *249*(5452), 26–28, doi:10.1038/249026a0.

Harrison, A. D., T. F. Whale, M. A. . Carpenter, M. A. Holden, L. Neve, D. O'Sullivan, J. Vergara Temprado, and B. J. Murray (2016), Not all feldspar is equal: a survey of ice nucleating properties across the feldspar group of minerals, *Atmos. Chem. Phys. Discuss.*, (February), 1–26, doi:10.5194/acp-2016-136.

Herbert, R. J., B. J. Murray, T. F. Whale, S. J. Dobbie, and J. D. Atkinson (2014), Representing time-dependent freezing behaviour in immersion mode ice nucleation, *Atmos. Chem. Phys.*, *14*(16), 8501–8520, doi:10.5194/acp-14-8501-2014.

Hiranuma, N. et al. (2014), A comprehensive laboratory study on the immersion freezing behavior of illite NX particles: a comparison of seventeen ice nucleation measurement techniques, *Atmos. Chem. Phys. Discuss.*, *14*, accepted, doi:10.5194/acpd-14-22045-2014.

Hiranuma, N. et al. (2015), Ice nucleation by cellulose and its potential contribution to ice formation in clouds, *Nat. Geosci.*, *8*(4), 273–277, doi:10.1038/ngeo2374.

Hoose, C., and O. Möhler (2012), Heterogeneous ice nucleation on atmospheric aerosols: A review of results from laboratory experiments, *Atmos. Chem. Phys.*, *12*(20), 9817–9854, doi:10.5194/acp-12-9817-2012.

Hoose, C., J. E. Kristjánsson, J.-P. Chen, and A. Hazra (2010a), A Classical-Theory-Based Parameterization of Heterogeneous Ice Nucleation by Mineral Dust, Soot, and Biological Particles in a Global Climate Model, *J. Atmos. Sci.*, *67*(8), 2483–2503, doi:10.1175/2010JAS3425.1.

Hoose, C., J. E. Kristjánsson, and S. M. Burrows (2010b), How important is biological ice nucleation in clouds on a global scale?, *Environ. Res. Lett.*, *5*(2), 24009, doi:10.1088/1748-9326/5/2/024009.

Iannone, R., D. I. Chernoff, A. Pringle, S. T. Martin, and A. K. Bertram (2011), The ice nucleation ability of one of the most abundant types of fungal spores found in the atmosphere, *Atmos. Chem. Phys.*, *11*(3), 1191–1201, doi:10.5194/acp-11-1191-2011.

Kamphus, M., M. Ettner-Mahl, T. Klimach, F. Drewnick, L. Keller, D. J. Cziczo, S. Mertes, S. Borrmann, and J. Curtius (2010), Chemical composition of ambient aerosol, ice residues and cloud droplet residues in mixed-phase clouds: Single particle analysis during the cloud and aerosol characterization experiment (CLACE 6), *Atmos. Chem. Phys.*, *10*(16), 8077–8095, doi:10.5194/acp-10-8077-2010.

Kanji, Z. A., L. A. Ladino, H. Wex, Y. Boose, M. Burkert-Kohn, D. J. Cziczo, and M. Krämer (2017), Overview of Ice Nucleating Particles, *Meteorol. Monogr.*, *58*, 1.1-1.33, doi:10.1175/AMSMONOGRAPHS-D-16-0006.1.

Karydis, V. a., P. Kumar, D. Barahona, I. N. Sokolik, and a. Nenes (2011), On the effect of dust particles on global cloud condensation nuclei and cloud droplet number, *J. Geophys. Res. Atmos.*, *116*(23), doi:10.1029/2011JD016283.

Kiselev, A., F. Bachmann, P. Pedevilla, S. J. Cox, A. Michaelides, D. Gerthsen, and T. Leisner (2017), Active sites in heterogeneous ice nucleation—the example of K-rich feldspars, *Science (80-.).*, *355*(6323), 367–371, doi:10.1126/science.aai8034.

Köhler, H. (1936), The nucleus in and the growth of hygroscopic droplets, *Trans. Faraday Soc.*, *32*(0), 1152–1161, doi:10.1039/TF9363201152.

Kok, J. F., E. J. R. Parteli, T. I. Michaels, and D. B. Karam (2012), The physics of wind-blown sand and dust, *Reports Prog. Phys.*, *75*(10), 106901, doi:10.1088/0034-4885/75/10/106901.

Kok, J. F., D. A. Ridley, Q. Zhou, R. L. Miller, C. Zhao, C. L. Heald, D. S. Ward, S. Albani, and K. Haustein (2017), Smaller desert dust cooling effect estimated from analysis of dust size and abundance, *Nat. Geosci.*, (March),

doi:10.1038/ngeo2912.

Koop, T., and B. J. Murray (2016), A physically constrained classical description of the homogeneous nucleation of ice in water, , *211915*, 1–27, doi:10.1063/1.4962355.

Korolev, A., and P. R. Field (2015), Assessment of the performance of the inter-arrival time algorithm to identify ice shattering artifacts in cloud particle probe measurements, *Atmos. Meas. Tech.*, *8*(2), 761–777, doi:10.5194/amt-8-761-2015.

Korolev, A. V., E. F. Emery, J. W. Strapp, S. G. Cober, and G. A. Isaac (2013), Quantification of the effects of shattering on airborne ice particle measurements, *J. Atmos. Ocean. Technol.*, *30*(11), 2527–2553, doi:10.1175/JTECH-D-13-00115.1.

Krämer, M. et al. (2016), A microphysics guide to cirrus clouds-Part 1: Cirrus types, *Atmos. Chem. Phys.*, *16*(5), 3463–3483, doi:10.5194/acp-16-3463-2016.

Kristjánsson, J. E., H. Muri, and H. Schmidt (2015), The hydrological cycle response to cirrus cloud thinning, *Geophys. Res. Lett.*, *42*(24), 10807–10815, doi:10.1002/2015GL066795.

Kupiszewski, P. et al. (2016), Ice residual properties in mixed-phase clouds at the high-alpine Jungfraujoch site, *J. Geophys. Res. Atmos.*, *121*(20), 12,343-12,362, doi:10.1002/2016JD024894.

Ladino, L. A., A. Korolev, I. Heckman, M. Wolde, A. M. Fridlind, and A. S. Ackerman (2017), On the role of ice-nucleating aerosol in the formation of ice particles in tropical mesoscale convective systems, *Geophys. Res. Lett.*, *44*(3), 1574–1582, doi:10.1002/2016GL072455.

Ladino Moreno, L. A., O. Stetzer, and U. Lohmann (2013), Contact freezing: A review of experimental studies, *Atmos. Chem. Phys.*, *13*(19), 9745–9769, doi:10.5194/acp-13-9745-2013.

Lamb, D., and J. Verlinde (2011), *Physics and Chemistry of Clouds*, Cambridge University Press, Cambridge.

Lawson, R. P., and A. Gettelman (2014), Impact of Antarctic mixed-phase clouds on climate., *Proc. Natl. Acad. Sci. U. S. A.*, *111*(51), 18156–61, doi:10.1073/pnas.1418197111.

Leisner, T., T. Pander, P. Handmann, and A. Kiselev (2014), Secondary ice processes upon heterogeneous freezing of cloud droplets, *4th Conf. Cloud Phys. Atmos. Radiat.*

Lohmann, U. (2002), A glaciation indirect aerosol effect caused by soot aerosols, *Geophys. Res. Lett.*, *29*(4), 1052, doi:10.1029/2001GL014357.

Lohmann, U. (2006), Aerosol effects on clouds and climate, *Space Sci. Rev.*, *125*(1–4), 129–137, doi:10.1007/s11214-006-9051-8.

Lohmann, U., and K. Diehl (2006), Sensitivity studies of the importance of dust ice nuclei for the indirect aerosol effect on stratiform mixed-phase clouds, *J. Atmos. Sci.*, 968–982.

Lohmann, U., and B. Gasparini (2017), A cirrus cloud climate dial?, *Science (80-.).*, *357*(6348), 248–249, doi:10.1126/science.aan3325.

Mahowald, N. (2011), Aerosol Indirect Effect on Biogeochemical Cycles and Climate, *Science (80-.).*, *334*(6057), 794–796, doi:10.1126/science.1207374.

Mangan, T. P., J. D. Atkinson, J. W. Neuberg, D. O'Sullivan, T. W. Wilson, T. F. Whale, L. Neve, N. S. Umo, T. L. Malkin, and B. J. Murray (2017), Heterogeneous Ice nucleation by soufriere hills volcanic ash immersed in water droplets, *PLoS One*, *12*(1), 1–11, doi:10.1371/journal.pone.0169720.

Manktelow, P. T., K. S. Carslaw, G. W. Mann, and D. V. Spracklen (2010), The impact of dust on sulfate aerosol, CN and CCN during an East Asian dust storm, *Atmos. Chem. Phys.*, *10*(2), 365–382, doi:10.5194/acp-10-365-2010.

Mann, G. W., K. S. Carslaw, D. V. Spracklen, D. a. Ridley, P. T. Manktelow, M. P. Chipperfield, S. J. Pickering, and C. E. Johnson (2010), Description and evaluation of GLOMAP-mode: a modal global aerosol microphysics model for the UKCA composition-climate model, *Geosci. Model Dev.*, *3*(2), 519–551, doi:10.5194/gmd-3-519-2010.

Marcolli, C., S. Gedamke, T. Peter, and B. Zobrist (2007), Efficiency of immersion mode ice nucleation on surrogates of mineral dust, *Atmos. Chem. Phys. Discuss.*, *7*(4), 9687–9716, doi:10.5194/acpd-7-9687-2007.

Mårtensson, E. M., E. D. Nilsson, G. de Leeuw, L. H. Cohen, and H.-C. Hansson (2003), Laboratory simulations and parameterization of the primary marine aerosol production, *J. Geophys. Res.*, *108*, 1–12, doi:10.1029/2002JD002263.

Martin, J. H., M. Gordon, and S. E. Fitzwater (1991), The case for iron, *Limnol. Oceanogr.*, *36*(8), 1793–1802, doi:10.4319/lo.1991.36.8.1793.

Mccluskey, C. S., P. J. Demott, A. J. Prenni, E. J. T. Levin, G. R. Mcmeeking, A. P. Sullivan, T. C. J. Hill, S. Nakao, C. M. Carrico, and S. M. Kreidenweis (2014), Characteristics of atmospheric ice nucleating particles associated with biomass burning in the US: Prescribed burns and wildfire, *J. Geophys. Res. Atmos.*, 458–470, doi:10.1002/2014JD021980.Received.

McCoy, D. T., D. L. Hartmann, M. D. Zelinka, P. Ceppi, and D. P. Grosvenor (2015a), Mixed-phase cloud physics and Southern Ocean cloud feedback in climate models, *J. Geophys. Res. Atmos.*, *120*, 9539–9554,

doi:10.1002/2015JD023603.Received.

McCoy, D. T., S. M. Burrows, R. Wood, D. P. Grosvenor, S. M. Elliott, P.-L. Ma, P. J. Rasch, and D. L. Hartmann (2015b), Natural aerosols explain seasonal and spatial patterns of Southern Ocean cloud albedo, *Sci. Adv.*, *1*(6), e1500157–e1500157, doi:10.1126/sciadv.1500157.

McCoy, D. T., I. Tan, D. L. Hartmann, M. D. Zelinka, and T. Storelvmo (2016), On the relationships among cloud cover, mixed-phase partitioning, and planetary albedo in GCMs, *J. Adv. Model. Earth Syst.*, *8*(2), 650–668, doi:10.1002/2015MS000589.

Meyers, M. P., P. J. DeMott, and W. R. Cotton (1992), New Primary Ice-Nucleation Parameterizations in an Explicit Cloud Model, *J. Appl. Meteorol.*, *31*(7), 708–721, doi:10.1175/1520-0450(1992)031<0708:NPINPI>2.0.CO;2.

Mitchell, D. L., and W. Finnegan (2009), Modification of cirrus clouds to reduce global warming, *Environ. Res. Lett.*, *4*(4), 45102, doi:10.1088/1748-9326/4/4/045102.

Möhler, O. et al. (2006), Efficiency of the deposition mode ice nucleation on mineral dust particles, *Atmos. Chem. Phys.*, *6*(10), 3007–3021, doi:10.5194/acp-6-3007-2006.

Mortazavi, R., C. T. Hayes, and P. A. Ariya (2008), Ice nucleation activity of bacteria isolated from snow compared with organic and inorganic substrates, *Environ. Chem.*, *5*(6), 373, doi:10.1071/EN08055.

Mossop, S. C. (1970), Concentrations of Ice Crystals in Clouds, *Bull. Am. Meteorol. Soc.*, *51*(6), 474–479, doi:10.1175/1520-0477(1970)051<0474:COICIC>2.0.CO;2.

Murray, B. J. (2017), Cracking the problem of ice nucleation, *Science (80-.).*, *355*(6323).

Murray, B. J., and E. J. Jensen (2010), Homogeneous nucleation of amorphous solid water particles in the upper mesosphere, *J. Atmos. Solar-Terrestrial Phys.*, *72*(1), 51–61, doi:10.1016/j.jastp.2009.10.007.

Murray, B. J., S. L. Broadley, T. W. Wilson, J. D. Atkinson, and R. H. Wills (2011), Heterogeneous freezing of water droplets containing kaolinite particles, *Atmos. Chem. Phys.*, *11*(9), 4191–4207, doi:10.5194/acp-11-4191-2011.

Murray, B. J., D. O'Sullivan, J. D. Atkinson, and M. E. Webb (2012), Ice nucleation by particles immersed in supercooled cloud droplets, *Chem. Soc. Rev.*, *41*(19), 6519, doi:10.1039/c2cs35200a.

Myhre, G. et al. (2013a), Anthropogenic and Natural Radiative Forcing, *Clim. Chang. 2013 Phys. Sci. Basis. Contrib. Work. Gr. I to Fifth Assess. Rep.*

Intergov. Panel Clim. Chang., 659–740, doi:10.1017/CBO9781107415324.018.

Myhre, G. et al. (2013b), Radiative forcing of the direct aerosol effect from AeroCom Phase II simulations, *Atmos. Chem. Phys.*, *13*(4), 1853–1877, doi:10.5194/acp-13-1853-2013.

Niedermeier, D., S. Augustin-bauditz, S. Hartmann, H. Wex, and F. Stratmann (2015), Can we define an asymptotic value for the ice active surface site density for heterogeneous ice nucleation ?, *J. Geophys. Res. Atmos.*, *120*(May), 5036–5046, doi:10.1002/2014JD022814.The.

Niemand, M. et al. (2012), A Particle-Surface-Area-Based Parameterization of Immersion Freezing on Desert Dust Particles, *J. Atmos. Sci.*, *69*(10), 3077–3092, doi:10.1175/JAS-D-11-0249.1.

Noone, K. J., J. A. Ogren, J. Heintzenberg, R. J. Charlson, and D. S. Covert (1988), Design and calibration of a counterflow virtual impactor for sampling of atmospheric fog and cloud droplets, *Aerosol Sci. Technol.*, *8*(3), 235–244, doi:10.1080/02786828808959186.

O'Dowd, C., M. Facchini, and F. Cavalli (2004), Biogenically driven organic contribution to marine aerosol, *Nature*, *431*(October), 0–4, doi:10.1038/nature02970.1.

O'Dowd, C. et al. (2015), Connecting marine productivity to sea-spray via nanoscale biological processes: Phytoplankton Dance or Death Disco?, *Sci. Rep.*, *5*(October), 14883, doi:10.1038/srep14883.

O'Dowd, C. D., B. Langmann, S. Varghese, C. Scannell, D. Ceburnis, and M. C. Facchini (2008), A combined organic-inorganic sea-spray source function, *Geophys. Res. Lett.*, *35*, 1–5, doi:10.1029/2007GL030331.

O'Sullivan, D., B. J. Murray, J. F. Ross, T. F. Whale, H. C. Price, J. D. Atkinson, N. S. Umo, and M. E. Webb (2015), The relevance of nanoscale biological fragments for ice nucleation in clouds, *Sci. Rep.*, *5*, 8082, doi:10.1038/srep08082.

O'Sullivan, D., B. J. Murray, J. Ross, and M. E. Webb (2016), The adsorption of fungal ice-nucleating proteins on mineral dusts: a terrestrial reservoir of atmospheric ice-nucleating particles, *Atmos. Chem. Phys. Discuss.*, (January), 1–22, doi:10.5194/acp-2015-1018.

Okin, G. S., N. Mahowald, O. A. Chadwick, and P. Artaxo (2004), Impact of desert dust on the biogeochemistry of phosphorus in terrestrial ecosystems, *Global Biogeochem. Cycles*, *18*(2), doi:10.1029/2003GB002145.

Ovadnevaite, J., a. Manders, G. de Leeuw, D. Ceburnis, C. Monahan, a.-I.

Partanen, H. Korhonen, and C. D. O'Dowd (2014), A sea spray aerosol flux parameterization encapsulating wave state, *Atmos. Chem. Phys.*, *14*(4), 1837–1852, doi:10.5194/acp-14-1837-2014.

Painter, T. H., J. S. Deems, J. Belnap, A. F. Hamlet, C. C. Landry, and B. Udall (2010), Response of Colorado River runoff to dust radiative forcing in snow, *Proc. Natl. Acad. Sci.*, *107*(40), 17125–17130, doi:10.1073/pnas.0913139107.

Partanen, a.-I. et al. (2014), Global modelling of direct and indirect effects of sea spray aerosol using a source function encapsulating wave state, *Atmos. Chem. Phys.*, *14*(21), 11731–11752, doi:10.5194/acp-14-11731-2014.

Perlwitz, J. P., C. Perez Garcia-Pando, and R. L. Miller (2015), Predicting the mineral composition of dust aerosols Part 1: Representing key processes, *Atmos. Chem. Phys. Discuss.*, *15*(3), 3493–3575, doi:10.5194/acpd-15-3493-2015.

Philips, V. T. J., L. J. Donner, and S. T. Garner (2007), Nucleation Processes in Deep Convection Simulated by a Cloud-System-Resolving Model with Double-Moment Bulk Microphysics, *J. Atmos. Sci.*, *64*, 738–761, doi:10.1175/JAS3869.1.

Phillips, V. T. J., P. J. DeMott, and C. Andronache (2008), An Empirical Parameterization of Heterogeneous Ice Nucleation for Multiple Chemical Species of Aerosol, *J. Atmos. Sci.*, *65*(9), 2757–2783, doi:10.1175/2007JAS2546.1.

Phillips, V. T. J., P. J. Demott, C. Andronache, K. a. Pratt, K. a. Prather, R. Subramanian, and C. Twohy (2013), Improvements to an Empirical Parameterization of Heterogeneous Ice Nucleation and Its Comparison with Observations, *J. Atmos. Sci.*, *70*(2), 378–409, doi:10.1175/JAS-D-12-080.1.

Prather, K. a et al. (2013), Bringing the ocean into the laboratory to probe the chemical complexity of sea spray aerosol., *Proc. Natl. Acad. Sci. U. S. A.*, *110*(19), 7550–5, doi:10.1073/pnas.1300262110.

Pratt, K. a., P. J. DeMott, J. R. French, Z. Wang, D. L. Westphal, A. J. Heymsfield, C. H. Twohy, A. J. Prenni, and K. a. Prather (2009), In situ detection of biological particles in cloud ice-crystals, *Nat. Geosci.*, *2*(6), 398–401, doi:10.1038/ngeo521.

Quinn, P. K., T. S. Bates, K. S. Schulz, D. J. Coffman, a. a. Frossard, L. M. Russell, W. C. Keene, and D. J. Kieber (2014), Contribution of sea surface carbon pool to organic matter enrichment in sea spray aerosol, *Nat. Geosci.*, *7*(3), 228–232, doi:10.1038/ngeo2092.

Ramanathan, V., R. D. Cess, E. F. Harrison, P. Minnis, B. R. Barkstrom, E. Ahmad, and D. Hartmann (1989), Cloud-Radiative Forcing and Climate: Results from

the Earth Radiation Budget Experiment, *Science (80-.).*, *243*(4887), 57–63, doi:10.1126/science.243.4887.57.

Riechers, B., F. Wittbracht, A. Hütten, and T. Koop (2013), The homogeneous ice nucleation rate of water droplets produced in a microfluidic device and the role of temperature uncertainty, *Phys. Chem. Chem. Phys.*, *15*(16), 5873, doi:10.1039/c3cp42437e.

Rinaldi, M. et al. (2013), Is chlorophyll- a the best surrogate for organic matter enrichment in submicron primary marine aerosol?, *J. Geophys. Res. Atmos.*, *118*(10), 4964–4973, doi:10.1002/jgrd.50417.

Rosinski, J., P. L. Haagenson, C. T. Nagamoto, and F. Parungo (1987), Nature of ice-forming nuclei in marine air masses, *J. Aerosol Sci.*, *18*(3), 291–309, doi:10.1016/0021-8502(87)90024-3.

Rosinski, J., P. L. Haagenson, C. T. Nagamoto, B. Quintana, F. Parungo, and S. D. Hoyt (1988), Ice-forming nuclei in air masses over the Gulf of Mexico, *J. Aerosol Sci.*, *19*(5), 539–551, doi:10.1016/0021-8502(88)90206-6.

Sagoo, N., and T. Storelvmo (2017), Testing the sensitivity of past climates to the indirect effects of dust, *Geophys. Res. Lett.*, *44*(11), 5807–5817, doi:10.1002/2017GL072584.

Sassen, K., and V. I. Khvorostyanov (2007), Microphysical and radiative properties of mixed-phase altocumulus: A model evaluation of glaciation effects, *Atmos. Res.*, *84*(4), 390–398, doi:10.1016/j.atmosres.2005.08.017.

Savre, J., and A. M. L. Ekman (2015a), Large-eddy simulation of threemixed-phase cloud events during ISDAC: Conditions for persistent heterogeneous ice formation, *J. Geophys. Res.*, *120*(15), 7699–7725, doi:10.1002/2014JD023006.

Savre, J., and a M. L. Ekman (2015b), A theory-based parameterization for heterogeneous ice nucleation and implications for the simulation of ice processes in atmospheric models, *J. Geophys. Res. Atmos.*, *120*(10), 4937–4961, doi:10.1002/2014JD023000.

Scanza, R. A., N. Mahowald, S. Ghan, C. S. Zender, J. F. Kok, X. Liu, Y. Zhang, and S. Albani (2015), Modeling dust as component minerals in the Community Atmosphere Model: Development of framework and impact on radiative forcing, *Atmos. Chem. Phys.*, *15*(1), 537–561, doi:10.5194/acp-15-537-2015.

Schill, G. P. et al. (2016), Ice nucleating particle emissions from photochemically-aged diesel and biodiesel exhaust, *Geophys. Res. Lett.*, 1–8, doi:10.1002/2016GL069529.

Schmidt, S., J. Schneider, T. Klimach, S. Mertes, L. P. Schenk, P. Kupiszewski, J. Curtius, and S. Borrmann (2017), Online single particle analysis of ice particle

residuals from mountain-top mixed-phase clouds using laboratory derived particle type assignment, *Atmos. Chem. Phys.*, *17*(1), 575–594, doi:10.5194/acp-17-575-2017.

Sciare, J., O. Favez, R. Sarda-Estève, K. Oikonomou, H. Cachier, and V. Kazan (2009), Long-term observations of carbonaceous aerosols in the Austral Ocean atmosphere: Evidence of a biogenic marine organic source, *J. Geophys. Res.*, *114*(D15), D15302, doi:10.1029/2009JD011998.

Seinfeld, J. H., and S. N. Pandis (2006), Atmospheric Chemistry and Physics, from Air Pollution to Climate Change,

Sesartic, A., U. Lohmann, and T. Storelvmo (2013), Modelling the impact of fungal spore ice nuclei on clouds and precipitation, *Environ. Res. Lett.*, *8*(1), 14029, doi:10.1088/1748-9326/8/1/014029.

Spracklen, D. V., and C. L. Heald (2014), The contribution of fungal spores and bacteria to regional and global aerosol number and ice nucleation immersion freezing rates, *Atmos. Chem. Phys.*, *14*(17), 9051–9059, doi:10.5194/acp-14-9051-2014.

Storelvmo, T., J. E. Kristjánsson, and U. Lohmann (2008), Aerosol Influence on Mixed-Phase Clouds in CAM-Oslo, *J. Atmos. Sci.*, *65*(10), 3214–3230, doi:10.1175/2008JAS2430.1.

Storelvmo, T., C. Hoose, and P. Eriksson (2011), Global modeling of mixed-phase clouds: The albedo and lifetime effects of aerosols, *J. Geophys. Res.*, *116*(D5), D05207, doi:10.1029/2010JD014724.

Storelvmo, T., J. E. Kristjansson, H. Muri, M. Pfeffer, D. Barahona, and A. Nenes (2013), Cirrus cloud seeding has potential to cool climate, *Geophys. Res. Lett.*, *40*(1), 178–182, doi:10.1029/2012GL054201.

Takahashi, T., Y. Nagao, and Y. Kushiyama (1995), Possible High Ice Particle Production during Graupel–Graupel Collisions, *J. Atmos. Sci.*, *52*(24), 4523–4527, doi:10.1175/1520-0469(1995)052<4523:PHIPPD>2.0.CO;2.

Tan, I., T. Storelvmo, and M. D. Zelinka (2016), Observational constraints on mixed-phase clouds imply higher climate sensitivity, *Science (80-.).*, *352*(6282), 224–227, doi:10.1126/science.aad5300.

Twohy, C. H. et al. (2010), Relationships of Biomass-Burning Aerosols to Ice in Orographic Wave Clouds, *J. Atmos. Sci.*, *67*(8), 2437–2450, doi:10.1175/2010JAS3310.1.

Twomey, S. (1974), Pollution and the planetary albedo, *Atmos. Environ.*, *8*(12), 1251–1256, doi:10.1016/0004-6981(74)90004-3.

Ullrich, R., C. Hoose, O. Möhler, M. Niemand, R. Wagner, K. Höhler, N.

Hiranuma, H. Saathoff, and T. Leisner (2017), A New Ice Nucleation Active Site Parameterization for Desert Dust and Soot, *J. Atmos. Sci.*, *74*(3), 699–717, doi:10.1175/JAS-D-16-0074.1.

Umo, N. S., B. J. Murray, M. T. Baeza-Romero, J. M. Jones, a. R. Lea-Langton, T. L. Malkin, D. O'Sullivan, J. M. C. Plane, and a. Williams (2014), Ice nucleation by combustion ash particles at conditions relevant to mixed-phase clouds, *Atmos. Chem. Phys. Discuss.*, *14*(21), 28845–28883, doi:10.5194/acpd-14-28845-2014.

Vali, G. (1994), Freezing Rate Due to Heterogeneous Nucleation, *J. Atmos. Sci.*, *51*(13), 1843–1856, doi:10.1175/1520-0469(1994)051<1843:FRDTHN>2.0.CO;2.

Vali, G. (2008), Repeatability and randomness in heterogeneous freezing nucleation, *Atmos. Chem. Phys. Discuss.*, *8*(1), 4059–4097, doi:10.5194/acpd-8-4059-2008.

Vali, G., P. J. DeMott, O. Möhler, and T. F. Whale (2015a), Technical Note: A proposal for ice nucleation terminology, *Atmos. Chem. Phys.*, *15*(18), 10263–10270, doi:10.5194/acp-15-10263-2015.

Vali, G., P. J. DeMott, O. Möhler, and T. F. Whale (2015b), Technical Note: A proposal for ice nucleation terminology, *Atmos. Chem. Phys.*, *15*(18), 10263–10270, doi:10.5194/acp-15-10263-2015.

Vardiman, L. (1978), Ice Crystal Multiplication in Convective Elements of Winter Orographic Clouds,

Vergara-Temprado, J. et al. (2017), Contribution of feldspar and marine organic aerosols to global ice nucleating particle concentrations, *Atmos. Chem. Phys.*, *17*(5), 3637–3658, doi:10.5194/acp-17-3637-2017.

Vonnegut, B., and M. Baldwin (1984), Repeated nucleation of a supercooled water sample that contains silver iodide particles, *J. Clim. Appl. Meteorol.*, *23*(3), 486–490, doi:10.1175/1520-0450(1984)023<0486:RNOASW>2.0.CO;2.

Wang, X. et al. (2017), The role of jet and film drops in controlling the mixing state of submicron sea spray aerosol particles, *Proc. Natl. Acad. Sci.*, *114*(27), in press, doi:10.1073/PNAS.1702420114.

Wang, Y., X. Liu, C. Hoose, and B. Wang (2014), Different contact angle distributions for heterogeneous ice nucleation in the Community Atmospheric Model version 5, *Atmos. Chem. Phys.*, *14*(19), 10411–10430, doi:10.5194/acp-14-10411-2014.

Wegener, A. (1923), *Thermodynamik Der Atmosphäre*.

Welti, A., K. Müller, Z. L. Fleming, and F. Stratmann (2017), Concentration and

variability of ice nuclei in the subtropic, maritime boundary layer, *Atmos. Chem. Phys. Discuss.*, (August), 1–18, doi:10.5194/acp-2017-783.

Westbrook, C. D., and A. J. Illingworth (2013), The formation of ice in a long-lived supercooled layer cloud, *Q. J. R. Meteorol. Soc.*, *139*(677), 2209–2221, doi:10.1002/qj.2096.

Whale, T. F., B. J. Murray, D. O'Sullivan, N. S. Umo, K. J. Baustian, J. D. Atkinson, and G. J. Morris (2014), A technique for quantifying heterogeneous ice nucleation in microlitre supercooled water droplets, *Atmos. Meas. Tech. Discuss.*, *7*(9), 9509–9536, doi:10.5194/amtd-7-9509-2014.

Wilson, T. W. et al. (2015), A marine biogenic source of atmospheric ice-nucleating particles, *Nature*, *525*(7568), 234–238, doi:10.1038/nature14986.

Yin, J., D. Wang, and G. Zhai (2012), An evaluation of ice nuclei characteristics from the long-term measurement data over North China, *Asia-Pacific J. Atmos. Sci.*, *48*(2), 197–204, doi:10.1007/s13143-012-0020-8.

Yun, Y., and J. E. Penner (2012), Global model comparison of heterogeneous ice nucleation parameterizations in mixed phase clouds, *J. Geophys. Res. Atmos.*, *117*(7), 1–23, doi:10.1029/2011JD016506.

Yun, Y., J. E. Penner, and O. Popovicheva (2013), The effects of hygroscopicity on ice nucleation of fossil fuel combustion aerosols in mixed-phase clouds, *Atmos. Chem. Phys.*, *13*(8), 4339–4348, doi:10.5194/acp-13-4339-2013.

Zawadowicz, M. A., K. D. Froyd, D. M. Murphy, and D. J. Cziczo (2017), Improved identification of primary biological aerosol particles using single-particle mass spectrometry, *Atmos. Chem. Phys.*, *17*(11), 7193–7212, doi:10.5194/acp-17-7193-2017.

Zelinka, M. D., D. A. Randall, M. J. Webb, and S. A. Klein (2017), Clearing clouds of uncertainty, *Nat. Clim. Chang.*, *7*(10), 674–678, doi:10.1038/nclimate3402.

Chapter 2 Manuscript "Contribution of feldspar and marine organic aerosols to global ice nucleating particle concentrations"

Authors: **Jesús Vergara-Temprado[1], Benjamin J. Murray[1], TheodoreW.Wilson[1], Daniel O'Sullivan[1], Jo Browse[1,2], Kirsty J. Pringle[1], Karin Ardon-Dryer[3], Allan K. Bertram[4], Susannah M. Burrows[5], Darius Ceburnis[6], Paul J. DeMott[7], Ryan H. Mason[4], Colin D. O'Dowd[6], Matteo Rinaldi[8], and Ken S. Carslaw[1]**

[1]Institute for Climate and Atmospheric Science, School of Earth and Environment, University of Leeds, Woodhouse Lane, Leeds, LS2 9JT, UK

[2]College of Life and Environmental Sciences, University of Exeter, Penryn, TR10 9EZ, UK [3]Department of System Biology, Harvard University, Harvard Medical School, Boston, USA [4]Department of Chemistry, University of British Columbia, Vancouver, BC, V6T1Z1, Canada [5]Pacific Northwest National Laboratory, Atmospheric Sciences and Global Change Division,

P.O. Box 999 MS K-24, Richland, WA 99352, USA

[6]School of Physics and Centre for Climate and Air Pollution Studies, Ryan Institute, National University of Ireland Galway, Galway, Ireland

[7]Department of Atmospheric Science, Colorado State University, Fort Collins, CO 80523-1371, USA

[8]Italian National Research Council (CNR), Institute of Environmental Sciences and Climate (ISAC), via P. Gobetti 101, 40129 Bologna, Italy

Correspondence to: Jesús Vergara-Temprado (eejvt@leeds.ac.uk)

Received: 14 September 2016 – Discussion started: 21 September 2016 Revised: 16 February 2017 – Accepted: 1 March 2017 – Published: 15 March 2017

Abstract

Ice-nucleating particles (INPs) are known to affect the amount of ice in mixed-phase clouds, thereby influencing many of their properties. The atmospheric INP concentration changes by orders of magnitude from terrestrial to marine environments, which typically contain much lower concentrations. Many modelling studies use parameterizations for heterogeneous ice nucleation and cloud ice processes that do not account for this difference because they were developed based on INP measurements made predominantly in terrestrial environments without considering the aerosol composition. Errors in the assumed INP concentration will influence the simulated amount of ice in mixed-phase clouds, leading to errors in top-of-atmosphere radiative flux and ultimately the climate sensitivity of the model. Here we develop a global model of INP concentrations relevant for mixed-phase clouds based on laboratory and field measurements of ice nucleation by K-feldspar (an ice-active component of desert dust) and marine organic aerosols (from sea spray). The simulated global distribution of INP concentrations based on these two species agrees much better with currently available ambient

measurements than when INP concentrations are assumed to depend only on temperature or particle size. Underestimation of INP concentrations in some terrestrial locations may be due to the neglect of INPs from other terrestrial sources. Our model indicates that, on a monthly average basis, desert dusts dominate the contribution to the INP population over much of the world, but marine organics become increasingly important over remote oceans and they dominate over the Southern Ocean. However, day-to-day variability is important. Because desert dust aerosol tends to be sporadic, marine organic aerosols dominate the INP population on many days per month over much of the mid- and high-latitude North- ern Hemisphere. This study advances our understanding of which aerosol species need to be included in order to adequately describe the global and regional distribution of INPs in models, which will guide ice nucleation researchers on where to focus future laboratory and field work.

1. Introduction

In the absence of aerosol particles which can act as ice- nucleating particles (INPs), liquid water droplets can supercool to temperatures below −37 ◦C [*Riechers et al.*, 2013; *Herbert et al.*, 2015]. It is well-known that ice formation frequently occurs at much higher temperatures in many clouds, indicating that INPs are prevalent in the atmosphere [*Choi et al.*, 2010; *Rosenfeld et al.*, 2011]. In supercooled and mixed-phase clouds (containing ice and water) INPs cause clouds to glaciate, which leads to changes in many cloud properties such as cloud lifetime, their radiative effect on the atmosphere, and the formation of precipitation through the Wegener–Bergeron–Findeisen process [*Murphy and Koop*, 2005; *Korolev*, 2007] and possibly cloud ice multiplication processes [*Hallet and Mossop*, 1974]. In the mixed-phase cloud regime, the dominant freezing mechanism is thought to be through INPs that are immersed within cloud droplets, known as immersion freezing [*Westbrook and Illingworth*, 2011; *Field et al.*, 2012; *Murray et al.*, 2012]. Hence, this is the pathway we focus on in this study. Heterogeneous freezing in climate models and operational numerical weather prediction models is usually based on parameterizations that depend on the temperature [*Young*, 1974; *Meyers et al.*, 1992] or the size distribution of aerosol particles as well as the temperature [*DeMott et al.*, 2010]. These parameterizations treat aerosol particles all around the globe and across seasons as having the same ice-nucleating properties irrespective of the aerosol chemical composition. This is an unrealistic assumption that may affect the realism of mixed-phase clouds in models. Over the Southern Ocean clouds tend to persist in a supercooled state more commonly than models predict [*Bodas-Salcedo et al.*, 2014], which might be related to the very low INP concentrations that exist in this region but are not simulated in models [*Bigg*, 1973; *DeMott et al.*, 2016]. It has been shown that fewer INPs in the Southern Ocean lead to less ice and more supercooled water in model clouds, with a significant impact on the radiative properties of the clouds [*Tan et al.*, 2016]. The variability between different models in the representation of cloud glaciation can lead to differences of tens of degrees in the temperature at which clouds glaciate [*McCoy et al.*, 2015]. A better representation of mixed-phase clouds in climate models is important for climate prediction. For example, *Tan et al.*, [2016] concluded that the response of global mean surface temperature to a doubling of CO2 is more than one degree greater

when mixed-phase clouds are better represented. This cloud-phase feedback is particularly sensitive to the amount of supercooled liquid in Southern Ocean mixed-phase clouds while most current models are biased relative to measurements [*McCoy et al.*, 2015]. In the future, regional and global climate models will include improved representations of cloud processes [*Bauer et al.*, 2015], including ice processes, so an improved representation of heterogeneous ice nucleation will be required to make the models more physically realistic and correct some of the main biases. In particular, studies have shown that clouds are sensitive to INP concentrations, which could affect the radiative balance of the atmosphere [*Zeng et al.*, 2009; *DeMott et al.*, 2010; *Hoose et al.*, 2010a; *Wang et al.*, 2014; *Tan et al.*, 2016]. The reliability of such studies will depend on being able to relate the changes in cloud proper- ties to emitted aerosol species so that we can attribute future changes in weather and climate to particular aerosol sources. Global aerosol models have, for many years, been based on transported aerosol species from different sources, which enables aerosol radiative forcing to be related to anthropogenic and natural emissions and their effects on cloud droplet formation [*Ghan and Schwartz*, 2007; *Carslaw et al.*, 2013; *Rap et al.*, 2013; *Kodros et al.*, 2015]. Our ability to achieve the same level of realism for ice formation has been much more difficult to achieve, partly because it has been challenging to identify species-specific ice-nucleating properties [*Hoose and Möhler*, 2012; *Murray et al.*, 2012] and model them on a global scale.

Previous studies have simulated heterogeneous ice nucleation on a global scale accounting for different aerosol species [*Lohmann and Diehl*, 2006; *Hoose et al.*, 2010a; *Sesartic et al.*, 2012; *Spracklen and Heald*, 2014]. These studies used classical nucleation theory to calculate nucleation rates using contact angles derived from laboratory data for each INP species. This approach has the advantage that the time dependence of ice nucleation is represented (although temperature is the main driver of nucleation), but when a single contact angle is used to describe ice nucleation by a single aerosol species, particle-to-particle variability is not represented [*Herbert et al.*, 2014] as long-time integration will eventually allow all particles to nucleate ice.

Classical nucleation theory can be extended with a distribution of contact angles to account for differences in the ice- nucleating ability between different particles

within the same material [*Marcolli et al.*, 2007; *Eidhammer et al.*, 2009; *Niedermeier et al.*, 2011; *Broadley et al.*, 2012; *Herbert et al.*, 2014] and has been applied in models [*Wang et al.*, 2014]. In addition, it has been shown that representation of the time evolution of the distribution of contact angles is necessary to improve the representation of ice formation in a cloud- resolving model under some conditions using classical nucleation theory [*Savre and Ekman*, 2015].

The alternative to describing ice nucleation by classical nucleation theory is to use a singular approximation [*Vali and Snider*, 2015] in which the time dependence of nucleation is assumed to be of secondary importance compared to the particle-to-particle variability (just a fraction of particles nucleates ice). This approach has been used to define the population of INPs in previous model studies [*Niemand et al.*, 2012; *Atkinson et al.*, 2013; *Wilson et al.*, 2015].

The ice-nucleating efficiency using the singular description is defined by a temperature-dependent density (i.e. per unit surface area) of active sites, ($n_s(T)$) which represents a spectrum of active sites with variable characteristic ice nucleation temperatures. The temperature-dependent number of active sites per surface area can also be normalized to an- other parameter characteristic of the aerosol population (such as mass or volume; *Murray et al.*, 2012). From this density of active sites, one can calculate what fraction of the particles will nucleate ice at a certain temperature (See Appendix B). In the case of having different aerosol species, a different density of active sites for every species has to be defined in order to account for their different abilities in nucleating ice. The singular description of ice nucleation is consistent with many laboratory studies showing that particle-to-particle variability is the main factor driving the measured spectrum of INP concentrations with temperature [*Vali*, 2008; *Herbert et al.*, 2014; *Vali and Snider*, 2015] for most of the known atmospherically relevant ice-nucleating species. However, it should be borne in mind that time dependence could play a role in long-lived stable mixed-phase clouds where ice crystals are produced over a long period of time [*Morrison et al.*, 2011; *Murray et al.*, 2011; *Westbrook and Illingworth*, 2013; *Herbert et al.*, 2014]. Nevertheless, the singular approach for ice nucleation can be used to approximate INP concentrations, which can be calculated with knowledge of the number, size distribution and density of ac- tive sites of the relevant INP species. Mineral dust is considered to be the dominant ice- nucleating

species in many parts of the world [*Hoose et al.*, 2010a; *Ardon-Dryer and Levin*, 2014; *DeMott et al.*, 2015; *Boose et al.*, 2016]. Satellite measurements have shown a negative correlation between the amount of supercooled water and dust concentration [*Choi et al.*, 2010], suggesting that dust is important for cloud glaciation. The ice-nucleating ability of dust has been quantified in several studies [*Koehler et al.*, 2010; *Broadley et al.*, 2012; *Niemand et al.*, 2012; *Augustin-Bauditz et al.*, 2014]. *Atkinson et al. [2013]* found that K-feldspars are far more effective at nucleating ice than any of the other minerals in desert dust, which is supported by several later studies [*O'Sullivan et al.*, 2014; *Wex et al.*, 2014; *Whale et al.*, 2014; *Emersic et al.*, 2015; *Niedermeier et al.*, 2015; *Zolles et al.*, 2015; *Harrison et al.*, 2016]. Therefore, the representation of K-feldspar in atmospheric models is important for obtaining a realistic representation of ice nucleation by mineral dust. We have previously represented ice nucleation on a global scale by K-feldspar aerosols [*Atkinson et al.*, 2013; *Wilson et al.*, 2015]. In this study, we will take a similar approach to estimate the contribution of K-feldspar aerosol to global INP concentrations. Some marine aerosol particles act as ice-nucleating particles. Early evidence for a relationship between phytoplankton and marine INPs was found by *Schnell and Vali*, [1975, 1976], who observed active INPs at temperatures as high as−4 ◦C in resuspended biological material, largely from phytoplankton filtered from bulk sea water. A relationship between the amount of biological material and the INP concentration was also measured in seawater and fog water by *Schnell*, [1977]. More recent studies have measured ice nucleation by Thalassiosira Pseudonana (a ubiquitous species of phytoplankton) diatom cells [*Knopf et al.*, 2010; *Alpert et al.*, 2011] and exudates [*Wilson et al.*, 2015]. However, these studies measured ice nucleation at significantly lower temperatures than those measured by *Schnell and Vali*, [1975, 1976], suggesting that more active INPs could be associated with phytoplankton material in the ocean. This would be supported by a previous measurement of ice-nucleating bacteria associated with phytoplankton cultures [*Fall and Schnell*, 1985]. Further evidence for the biological origin of marine INPs is the heat sensitivity of some types of organic INPs; i.e. the temperature at which they nucleate ice is reduced after heating to 100 ◦C [*Schnell and Vali*, 1975, 1976; *Wilson et al.*, 2015] . The likelihood of a marine source of INPs was high- lighted in studies that measured INP concentrations in environments remote from other sources of INPs [*Bigg*, 1973; *Schnell*, 1982; *Rosinski et al.*, 1986,

1987, 1988; Bigg, 1996]. The first global simulation of marine INP concentrations [*Burrows et al.*, 2013] suggested that marine organics were likely to be the dominant source of INPs over remote marine regions such as the Southern Ocean. Other studies provide further strong evidence that there is a marine source of atmospheric INPs with a biological origin. For example, INP production associated with phytoplankton blooms has been measured in laboratory experiments that use artificially generated sea-spray aerosol from wave and bubble tanks [*Wang et al.*, 2015; *DeMott et al.*, 2016]. *DeMott et al. [2016]* measured the INP concentrations in laboratory-generated sea spray as being consistent with measurements made by *Bigg [1973]* as well as with measurements of ambient INP concentrations in marine-influenced air. *Wilson et al. [2015]* found that the sea-surface microlayer is enriched with INPs compared to subsurface seawater at the same locations. The sea-surface microlayer is enriched with surface active organic material similar to that found in sea spray [*Aller et al.*, 2005; *Russell et al.*, 2010; *Gantt et al.*, 2011; *Orellana et al.*, 2011; *Cunliffe et al.*, 2013; *Quinn et al.*, 2014; *Cochran et al.*, 2016]. A correlation between total organic carbon content and the temperature at which microlayer droplets froze was measured [*Wilson et al.*, 2015]. All the above evidence suggests the existence of a marine organic source of ice-nucleating particles that we will attempt to represent in this paper.

Here we conduct a modelling study of global immersion-mode INP concentrations based on recently developed laboratory-based parameterizations of the ice-nucleating ability of two species: marine organic matter and potassium feldspar (K-feldspar). The objectives of our study are to (i) determine the ability of laboratory-measured INP efficiencies to explain the global distribution of INP concentrations as a function of activation temperature, (ii) quantify the relative importance of these two sources of INPs in different locations, (iii) determine what fraction of global INP concentrations can be explained by these two sources and (iv) deter- mine whether, within model and measurement uncertainties, we can use the model results to draw conclusions about additional important sources of INPs.

2. Methods

2.1. Global modelling

We use the GLOMAP-mode global aerosol model described in *Mann et al.* [2010]. The model has a horizontal latitude–longitude grid spacing of 2.8°×2.8° and 31 pressure levels from the surface to 10 hPa. The species represented in the baseline version are sulphate, sea salt, black carbon, particulate organic matter and dust. In this study, we focus on the representation of two species of relevance to INPs: the K- feldspar component of dust and the organic component of primary marine sea-spray aerosols. Aerosol chemical component mass concentrations and the particle number con- centration are represented by seven internally mixed lognormal modes (four soluble and three insoluble). Aerosol microphysical processes in the model include nucleation of new particles by gas-to-particle conversion, growth by coagulation and condensation of low-volatility gases, dry de- position at the surface and below-cloud (impaction) and in- cloud (nucleation) wet scavenging. Nucleation scavenging is suppressed for ice clouds, which are assumed to glaciate at −15ºC. A discussion of the nucleation scavenging assumptions in our model is included in *Browse et al.*, [2012]. Scavenging of aerosols by marine drizzle clouds is also included in the model to improve the predicted concentration in polar regions, as shown in *Browse et al.*, [2012]. The model uses wind, temperature and humidity fields from the European Centre for Medium-Range Weather Forecasts (ECMWF). We ran the model from the year 2000 to 2001 in order to reach a steady state aerosol distribution before running the model and then used data from 2001 to 2002.

2.2. Representation of feldspar

Feldspar is emitted in the model as a fraction of the mass of dust (derived from AEROCOM emissions; *Dentener and Kinne*, [2006]). The model has been shown to reproduce dust mass concentrations within an order of magnitude [*Mann et al.*, 2010; *Huneeus et al.*, 2011]. The fraction of feldspar emitted is assumed to be equal to the fraction by mass of this mineral found in the soils in the arid emission regions. This assumption has been shown to be a close approximation of the fraction of the mineral emitted in the form of aerosols [*Lafon et al.*, 2004; *Nickovic et al.*, 2012]. How- ever, new studies suggest that there is a difference between the fraction of the

minerals found in the soil after wet sieving and the aerosolized fraction [*Perlwitz et al.*, 2015]. This difference is considered to be small (around a factor of 2) compared to other errors in our representation of the ice- nucleating ability of K-feldspar such as differences in the density of active sites of different types of K-feldspar (around a factor of 6; *Harrison et al.* [2016]). Feldspar is emitted into the insoluble accumulation and coarse modes with fractions corresponding to the clay and silt size range [*Lafon et al.*, 2004; *Nickovic et al.*, 2012], similar to the method followed in *Atkinson et al. [2013]*. However, once in the atmosphere, dust particles (including feldspar) are aged by condensation of sulfates and secondary organic aerosol material and moved into the soluble modes, which are subject to wet scavenging. This process was not represented in *Atkinson et al. [2013]*, and was likely one of the causes of the overestimation of dust concentrations in re- mote locations as discussed in *Atkinson et al. [2013]*. With this wet scavenging process being active, the concentration of feldspar in remote places such as the Southern Ocean is several orders of magnitude smaller than the concentrations simulated by *Atkinson et al. [2013]*. However, the concentrations closer to source regions are very similar to *Atkinson et al. [2013]*. Feldspar tends to reside in the larger particles because it is found mainly in the silt fraction (r >1 μm; *Claquin et al.*, [1999]). It is therefore removed more rapidly from the atmosphere compared with other minerals that occur preferentially in the clay fraction because removal by dry deposition increases with particle size. Relatively rapid scavenging of large feldspar-containing particles means that it is trans- ported shorter distances compared with smaller dust particles.

2.3. Representation of marine organic aerosols

Submicron marine organic aerosols are usually parameterized by relating the organic mass fraction observed in sea spray to some variables such as seawater chlorophyll content or wind speed [*Gantt et al.*, 2011; *Rinaldi et al.*, 2013; *O'Dowd et al.*, 2015]. With those parameterizations, the flux of marine organic mass can be calculated in a model with the flux of submicron sea salt following Eq. A5 (see Appendix A). The performance of any parameterization in reproducing observations of marine organic mass concentrations will therefore depend on the emission fluxes

of submicron sea spray, which is a highly uncertain model-dependent process. *Mann et al.* [2014] showed that models can have differences of more than a factor of 6 in the simulated concentration of particles with a diameter larger than 100nm in the Southern Ocean. Other uncertainties affecting the modelled concentrations of marine organic aerosols can arise from removal processes or some other aspect of the model such as the parameterization of convection and cloud microphysical processes, or model grid and temporal resolution, as well as uncertainties related to the organic mass fraction parameterization. Therefore, the performance of any parameterization in an aerosol model will be affected by the uncertainties related to these processes. It is therefore necessary to evaluate and adjust the modelled marine organic concentrations to match observations. To represent primary marine organic aerosols in GLOMAP mode, we developed a parameterization of the organic mass fraction of submicron sea-spray particles and adjusted it to fit the observations of water insoluble organic matter (WIOM) at Amsterdam Island (37.48°S, 77.34°E) and Mace Head (53.33°N, 9.9°W). We use observations from only these two stations due to the limited availability of long-term measurements of marine WIOM. It is thought that most primary marine organic emissions are formed of water-insoluble components [*Facchini et al.*, 2008]. The marine organic component is assumed to be internally mixed with sea salt. The sea-salt emissions in our model are dependent on the surface wind speed (10m above the surface) and follow the parameterization of *Gong*, [2003], which is an extension of *Monahan et al.* [1986]. The development of our new organic mass fraction parameterization, explained in detail in Appendix A, assumes that the organic mass fraction of the sea-spray particles depends on wind speed and the chlorophyll content of seawater. The organic emission parameterization includes a positive dependence of WIOM mass fraction on chlorophyll [*Gantt et al.*, 2011; *Rinaldi et al.*, 2013; *O'Dowd et al.*, 2015], but a negative dependence on wind speed. Thus, the WIOM is essentially diluted in the sea-spray particles when the total sea-spray emission flux is high, which may be caused by a limited supply of organic material in the surface ocean but effectively limitless salt [*Gantt et al.*, 2011]. This parameterization is similar to previous chlorophyll-based parameterizations such as *Rinaldi et al.* [2013] and *Gantt et al.*, [2011] but adjusted in order to fit the observations in Amsterdam Island and Mace Head when applied in our model. Our model agrees with the observed WIOM concentrations within a factor of 2 (Fig. 1) which is a small factor compared with

other uncertainties related to the calculation of INP concentrations such as the uncertainty related to the parameterization of the number of INP per gram of organic carbon in sea water (around an order of magnitude; *Wilson et al. [2015]*). The mixed organic-salt sea-spray particles are emitted into the accumulation mode and treated as water-soluble particles with respect to their cloud condensation nuclei activity, and hence they are removed by nucleation scavenging when they enter a precipitating cloud. This treatment of primary marine organic mass as being internally mixed with sea salt and able to activate to cloud droplets is consistent with other previous studies [*Vignati et al.*, 2010; *Fuentes et al.*, 2011; *Orellana et al.*, 2011; *Ovadnevaite et al.*, 2011; *Burrows et al.*, 2013; *Partanen et al.*, 2014]. Simulated surface concentrations of marine organic aerosol mass are shown in Fig. 2.

2.4. Calculation of INP concentrations

To quantify INP concentrations from the modelled aerosol distributions we use the singular description. This method assumes that the time dependence of ice nucleation plays a secondary role and that specific particles have a characteristic temperature at which they nucleate ice. The spectrum of ice-nucleating properties is often represented as a surface area density of active sites dependent on temperature, which is appropriate for solid particles like dust [*Atkinson et al., 2013*]. For marine organic material the active site density is defined per unit mass of organic material in the particle [*Wilson et al., 2015*]. The method for calculating ice-nucleating particle concentrations from the simulated aerosol size distributions is explained in Appendix B.

To represent the ice-nucleating ability of K-feldspar we assume that 35%of the total feldspar is K-feldspar, as assumed in *Atkinson et al.* [*2013*], then we apply the parameterization for n_s shown in *Atkinson et al.* [*2013*]. Our method assumes that different varieties of K-feldspar nucleate ice with the same efficiency. Different studies have shown that the values of ns for most types of K-feldspar tend to agree with the values shown in *Atkinson et al.* [*2013*] within a factor of 2 to 4 [*O'Sullivan et al.*, 2014; *Whale et al.*, 2014; *Emersic et al.*, 2015; *Niedermeier et al.*, 2015; *Zolles et al.*, 2015; *Harrison et al.*, 2016]. However, it should be borne in mind that a minority of feldspar samples are either much more active or much less active than indicated by *Atkinson et al. [2013]*. Nevertheless, the Atkinson parameterization is a

good approximation of the majority of K-feldspars that have been studied in the laboratory. Assuming that feldspar particles are externally mixed in terms of their mineralogy, we can use the laboratory parameterizations to calculate the INP concentration for each soluble mode, following Eq. B9, as a function of activation temperature (see Appendix B for the derivation). For marine organic aerosols, we use the parameterization shown in *Wilson et al. [2015]*, and apply it to our distributions of simulated marine organic aerosol mass. We are assuming that the organic material found in the sea-surface microlayer is representative of the organic material in sea-spray aerosols and that this material has the same ice-nucleating ability as sea-surface microlayer material. For marine organic particles, the density of active sites per particle is always small ($\lambda<0.1$ see Appendix B) for the whole temperature range covered by the parameterization (−6 to −27 ◦C) and all realistic sizes of particle (submicron particles). This means that we can calculate the INP concentration in a simplified way following Eq. 1 (see Appendix B for the derivation).

$$[INP](T) \approx \lambda(T) \cdot [N] \quad (1)$$

It should be noted that extrapolating this parameterization to lower temperatures, or for bigger particles, may lead to unrealistically high concentrations of INPs because Eq. 1 is no longer valid. There are two distinct ways of presenting simulated INP concentrations – either according to the concentration that an INP counter would measure or the concentration of potential INPs under ambient conditions. An INP is defined as a particle which has the potential to nucleate ice if exposed to a specific set of conditions (much like a CCN is defined at a specific supersaturation). For the immersion/condensation mode, the INP concentration we quote are for water saturation and for a defined activation temperature. The two ways of quoting INP concentrations (Fig. 3) are at a specific activation temperature T ($[INP]_T$), which is appropriate for comparison with an INP instrument set to measure at that temperature, or $[INP]_{ambient}$ for which the activation temperature is set to the local ambient temperature.

In Fig. 4 (top) we show the INP concentration for an activation temperature of −20°C ($[INP]_{-20}$) at the 600 hPa pressure level, which is what would be measured by an INP

instrument set to this temperature. Throughout much of the globe, especially through the tropics, the temperature at this pressure level will never reach −20°C, so the INPs at this altitude that can be active at −20°C or warmer would not fulfil their potential to nucleate ice. However, if the air at a particular altitude was drawn into a convective system, the INPs it contains would activate higher in the cloud. Hence, when considering a deep convective cloud or a frontal cloud in which air is moved vertically through all the temperature range of mixed- phase clouds, it is the spectrum of $[INP]_T$ (a spectrum over activation temperature) which is the pertinent quantity (see Fig. 3 for an illustration). In addition, when comparing measurements of INP concentration to our modelled [INP], we compare these quantities at specific activation temperatures. Hence, Fig. 4 (top) provides the [INP] to compare it to a measurement of [INP] for which the activation temperature in a measurement was −20°C. In Fig. 4 (bottom) we plot the [INP] for which the activation temperature is set to the local atmospheric temperature. $[INP]_{ambient}$ is useful for identifying regions in the atmosphere where we might expect cloud glaciation in stratus- type mixed-phase clouds. Non-deep convective clouds with minimal vertical extent, such as altostratus, altocumulus or high-latitude stratus, form in air parcels which have not been vertically transported large distances, in contrast to deep convection or frontal systems. Based on Fig. 4 (bottom), we would expect K- feldspar to contribute much more to midlatitude, mid-level (600 hPa), mixed-phase clouds in the Northern Hemisphere than in the Southern Hemisphere. Both $[INP]_T$ and $[INP]_{ambient}$ are useful ways of looking at the global INP distribution, but in order to understand the impact of these INP species on clouds, we would need a model in which the INP fields are coupled to cloud microphysics and dynamics. This is beyond the remit of this study, where our goal is to understand the global distribution of INPs and evaluate the model against measurements. To calculate $[INP]_{ambient}$, we use the daily mean temperatures obtained from ECMWF and the daily mean concentrations (mass and number concentrations) predicted by the model. The daily values are then averaged to calculate monthly and annual mean values of INPs. The concentrations of $[INP]_{ambient}$ at temperatures lower than the temperature limit of the parameterizations (−25°C for K-feldspar and −27°C for marine organics) are set at the value defined by the concentration at the limiting temperature of each parameterization. This is consistent with studies that caution against extrapolating singular parameterizations outside the range in which measurements were made. For

example, *Niedermeier et al. [2015]* showed that the density of active sites on the surface of K-feldspar particles plateaus below about −25 ◦C and a simple extrapolation of the parameterization of *Atkinson et al. [2013]* would lead to substantial errors.

3. Results

3.1. Simulated global INP distributions

Simulated INP concentrations at the surface are shown in Fig. 5 for an activation temperature of −15°C. Feldspar dominates the INP concentration in environments influenced by terrestrial dust emission sources such as the Sahara and the Asian dust belt. However, concentrations fall rapidly with distance from dust sources because the large-sized feldspar- containing dust particles are rapidly removed from the atmosphere (Fig. 5a). The concentrations of INPs from K-feldspar and marine organics are summarized in Fig. 5. Comparison with panels a and b reveals that INPs from deserts far out- number INPs from sea spray throughout much of the low latitudes and midlatitudes, which are strongly influenced by desert dust, while marine organics are becoming more important over the world's remote oceans, such as the Southern Ocean.

Figure 6 shows the $[INP]_{ambient}$ concentration of marine organics and K-feldspar for the different seasons. Feldspar dominates $[INP]_{ambient}$ on a monthly mean basis across the Northern Hemisphere, while marine organic aerosols tend to be important in southern high latitudes, such as those corresponding to the Southern Ocean and Antarctica. The seasonal mean results in Fig. 6 have to be interpreted with caution since high dust concentrations are often associated with episodic dust plumes. Hence, the seasonal mean may not reflect the relative contributions of desert dust and sea-spray INPs on a day-to-day basis. In addition, day-to-day fluctuations in temperature can drive large changes in $[INP]_{ambient}$ which are not necessarily representative of the typical concentrations of active ice-nucleating particles, but will greatly affect the monthly mean value of $[INP]_{ambient}$, as the INP concentration increases exponentially with temperature. To account for such variability, Fig. 7 shows the percentage of days per season when the concentration of $[INP]_{ambient}$ from marine organics is greater than the concentration from K-feldspar. Overall, over the

Northern Hemisphere, marine organic INP concentrations are greater than K-feldspar INP concentrations between 10 and 30% of the days when the temperature is within the mixed-phase range (0 to −37◦C) and the total concentration of $[INP]_{ambient}$ is larger than $10^{-4}L^{-1}$. This large influence of marine organic INP is hidden when looking at the monthly mean values shown in Fig. 6 as the feldspar monthly mean concentrations are dominated by short periods during which a dust plume occurs. It is striking that the contribution of marine organics is more important than K-feldspar on a significant fraction of days in the Northern Hemisphere because in these zonal mean plots we are averaging across the Eurasian and North American continents where the influence of marine organics is minor. In fact, Fig. 7 suggests that marine organics are more important than K-feldspar in the Norther Hemisphere, for example, on 10–40% of days at 600 hPa.

In the Southern Hemisphere, the dominance of marine organic aerosols is more prevalent. On a monthly mean basis and on the large majority of days, marine organic aerosols are the dominant INPs from March through to November (Fig. 6b–d). On the other hand, K-feldspar cannot always be ruled out as an important source of INPs in the southern high latitudes in the period from March to November, since there are still several days per month (10 to 60%) when the concentration of transported K-feldspar INPs dominates over marine organics (Fig. 6). Conversely, during December to February at southern high latitudes, K-feldspar mineral dust is more important on more days than marine organic aerosols (Fig. 7a). This is related to higher dust concentrations during the austral summer.

3.2. Comparison with observations and other parameterizations

Some climate models determine heterogeneous freezing using parameterizations that depend only on the temperature, [*McCoy et al.*, 2015] such as the scheme of *Meyers et al.* [1992]. This type of parameterization does not account for spatial or temporal variations in the aerosol loading and does not differentiate between different aerosol species; both of these factors actually determine INP concentrations. Other parameterizations such as *DeMott et al. [2010]* use empirical evidence from extensive atmospheric measurements to define INP concentrations in terms of the

aerosol particle concentration above a defined size. Such parameterizations implicitly account for the fact that many INP-active species are present in larger particles, such as in dust [*Niemand et al.*, 2012] and biological particles[*Tobo et al.*, 2013]. In addition, larger particles are more likely to carry nanoscale or smaller ice active materials [*O'Sullivan et al.*, 2015].

Nevertheless, size-based parameterizations of INP concentration do not account for the source of the particles or differences between marine and terrestrial aerosols, so they may not capture variations and long-term trends driven by changes in aerosol emissions since different aerosol types have different ice-nucleating abilities. In Fig. 8 we compare several singular INP parameterizations with observations (See Figure 9a and Appendix C). Panel a compares the observed values of $[INP]_T$ to those predicted by the scheme of *Meyers et al.* [*1992*], which relates $[INP]_T$ to temperature and is independent of aerosol properties. This is clearly a poor representation of many INP measurements in the atmosphere (Table 1). Figure 8b shows the $[INP]_T$ predicted by the parameterization of *DeMott et al.* [*2010*], in which $[INP]_T$ is predicted on the basis of the concentration of particles larger than 0.5μm diameter, $n_{aer,0.5}$, and temperature. This parameterization tends to overpredict $[INP]_T$, although multiplicative scaling of the simulated values would greatly improve its performance as it has a better correlation coefficient (Table 1). We also note that in our analysis we use the annual mean naer,0.5 from our model (without the contribution of sea-salt aerosols), whereas *DeMott et al.* [*2010*] used $n_{aer,0.5}$ from measurements coincident with their INP measurements and obtained a better representation of the $[INP]_T$ data (some of which is included in Fig. 8). Sulfate aerosols contribute significantly to the simulated $n_{aer,0.5}$ in remote places impacting *DeMott et al.* [*2010*] over oceans.

Figure 8c shows how our model compares with observed $[INP]_T$ using the desert dust parameterization from *Niemand et al.* [*2012*] (with no additional marine organic INPs). In this case some observations are overestimated by a factor 100–1000, especially those in marine regions (triangles). A similar trend is observed when this parameterization is extrapolated at higher temperatures. This overprediction is partly caused by the implicit assumption that all components of dust particle nucleate ice with the same efficiency. Feldspars exist mainly in the large dust particles (silt fraction) so they are not transported as efficiently to remote

locations as the clay minerals; consequently, transported desert dust is less important as INP in remote locations. Finally, we compare our two-species representation of INPs with the same $[INP]_T$ data set Fig. 8d. The observations used in this comparison are within the range of temperatures of the parameterizations (−5 to −27°C). In this case our representation of INPs (Fig. 8d) is able to reproduce 56.7% of the observations within an order of magnitude and 74% within 1.5 orders of magnitude (Table 1). When the parameterizations are extrapolated outside their temperature range, they still perform similarly (Table 1). Looking at the performance of the different ways of representing INPs within the smallest temperature range shared by the all the parameterizations (−12 to −25°C), our representation of INPs is able to reproduce 61.6% of the data points within an order of magnitude and 78.7%within 1.5 orders of magnitude. These values are greater than that obtained when using the other three parameterizations used for this study (Table 1). The contributions of K-feldspar and marine organics to the simulated INP concentrations of each data point are illustrated in Fig. 9b. Marine organics explain more than 90% of the INP concentrations in marine-influenced environments and some terrestrial environments with low concentrations of INPs (corresponding to high temperature observations). K-Feldspar, however, explains most of the observations in terrestrial regions. The large biases observed when using species independent parameterizations over marine regions are largely corrected, as most marine influenced INP concentrations are simulated within an order of magnitude (72%of marine points), although some biases are still apparent. Figure 10 shows the location and temperature of the observations with a bias greater than 1.5 orders of magnitude. Figure 10a suggests that the main positive bias occurs at low temperatures (<−20°C) in locations far from K-feldspar emission sources, where it is transported. It is possible that processes such as atmospheric ageing by acids play a role in modifying the efficiency of K-feldspar aerosols in nucleating ice [*Augustin-Bauditz et al.*, 2014] or that we overestimate the amount of feldspar particles that are transported. One possible explanation for this is that we do not model the preferential removal of INPs during cloud glaciation and precipitation; hence K-feldspar aerosol transported over long distances may contain fewer INPs than our model simulations [*Haga et al.*, 2013, 2014; *Stopelli et al.*, 2015]. Figure 10b shows that the model underestimates high-temperature INP concentrations (~−5 to −15°C)

over terrestrial locations, which might indicate that we are missing some terrestrial source that affects the INP concentration. Some of the possible candidates for these particles could be bacteria [*Maki and Willoughby*, 1978; *Möhler et al.*, 2008; *Hartmann et al.*, 2013], fungal material [*Pouleur et al.*, 1992; *Morris et al.*, 2013; *Fröhlich-Nowoisky et al.*, 2015; *O'Sullivan et al.*, 2015, 2016], agricultural dust [*Garcia et al.*, 2012; *O'Sullivan et al.*, 2014; *Tobo et al.*, 2014] or biological nanoscale fragments attached to mineral dust particles [*Fröhlich-Nowoisky et al.*, 2015; *O'Sullivan et al.*, 2015, 2016; *Pummer et al.*, 2015]. However, size-resolved INP measurements in several terrestrial locations suggest that a large proportion (40–90%) of INPs are commonly associated with larger particles (diameter>2.5 μm; *Mason et al.* [2016]). Such large particles are likely to have short atmospheric lifetimes, so they are less likely to be transported to cloud altitudes than smaller particles and are more likely to be transported shorter distances. In summary, the overall agreement between the two-species model and observations is good, but there are significant discrepancies. These discrepancies indicate that processes such as ageing and preferential INPs in-cloud removal could be important and also that we could be missing high-temperature terrestrial sources of INPs in the model.

4. Conclusions

This study is a step towards the inclusion of ice-nucleating particles in weather and climate models in a way that accounts for the aerosol chemical composition using laboratory-derived parameterizations under the singular description. We find that marine organic aerosols dominate the concentration of INPs in remote locations like the Southern Ocean on many days, whereas feldspar particles are the dominant species for ice nucleation in places influenced by the terrestrial emission sources. However, even over Northern Hemisphere regions influenced by dust, marine organic INP concentrations exceed K-feldspar INP concentrations on 10– 30% of the days when the temperature is within the mixed- phase range and the total concentration of INPs is larger than 10^{-4} L^{-1}. Similarly, K-feldspar cannot be ruled out as an important source of INPs in the southern high latitudes because there are several days per month when the concentration of transported K-feldspar INP dominates over the prevailing marine organics. K-feldspar in our model can reproduce 70% of the observations of INPs in terrestrial locations at low

temperatures (T <−15°C) within 1.5 orders of magnitude. Because K- feldspar is mainly a coarse aerosol type, it is scavenged more rapidly than the clay fraction of desert dusts, and therefore has substantially smaller influence on remote marine environments in contrast with *Atkinson et al. [2013]* where dust was not subject to wet removal. For remote locations, we find that marine organic aerosols acting as INPs are able to reproduce a majority (80%) of the observations within an order of magnitude. Our model of INPs based on emitted and transported aerosol species provides a reasonable explanation of measured global INP concentrations, but there are some important biases. The two-species model overestimates the concentrations of INPs in marine locations that are influenced by the transport of K-feldspar-containing dust particles by around 1.5 orders of magnitude, although it is difficult to draw firm conclusions from the small number of observations. Nevertheless, the bias points to the possible importance of missing processes, such as the effect of atmospheric processing of feldspar particles, a preferential scavenging of INPs as proposed in *Stopelli et al. [2015]*, or a possible overestimation of the transport of this aerosol type. The model also underestimates measured INP concentrations at high temperatures in some terrestrial locations. This bias is most likely to be explained by neglecting the contribution of some terrestrial biogenic aerosol species such as soil dust, fungal spores and bacteria. The model bias is large at the surface, but some studies show that some of these species are not important for ice nucleation once in the atmosphere [*Hoose et al.*, 2010b; *Spracklen and Heald*, 2014] because of their low simulated concentrations above the surface for heterogeneous ice nucleation. These species, however, could be important for triggering secondary production ice processes, such as the Hallett–Mossop process, due to its high nucleation temperatures. In addition, other unknown sources of ice-nucleating particles, such as biological fragments attached to mineral dust particles [*O'Sullivan et al.*, 2015, 2016], could help explain underestimated INP concentrations in the model. In summary, our results suggest that the inclusion of both marine organic and feldspar emissions are required to accurately simulate global INP concentrations. However, there are still large uncertainties to be resolved, such as the importance of acid coating affecting the INP ability of K-feldspar [*Sullivan et al.*, 2010; *Wex et al.*, 2014] or the relative importance of soot for ice nucleation in the atmosphere, which could lead to a possible anthropogenic effect on clouds. Finally, we suggest that further experimental studies on the ice-nucleating ability of different aerosol species,

followed by modelling studies of their importance in the atmosphere, will be crucial for determining the possible importance of other species for ice nucleation under atmospheric conditions. In addition, more INP measurements in the ambient atmosphere for different environments and seasons are necessary to better evaluate and constrain models. Among those, exploratory studies about the composition and type of ice-nucleating particles in terrestrial environments at high temperatures will be crucial to determine which species need to be included in models.

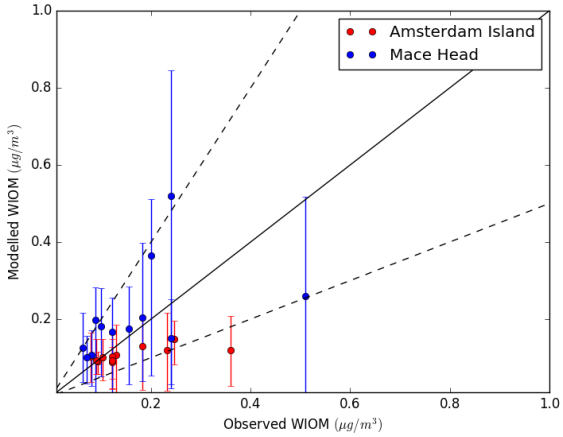

Figure 1. Evaluation of modelled water-insoluble organic matter (WIOM) mass concentration with monthly mean observations at Mace Head (53.33ºN, 9.9ºW) and Amsterdam Island (37.48ºS, 77.34ºE). The dashed lines correspond to a difference of a factor of 2 between modelled and observed values. The error bars correspond to the simulated daily variability within a month (maximum and minimum values). Variability in the observed values is not shown because the measurements were made with filter samples which were collected over 1 week, and therefore they do not represent the day-to-day variability.

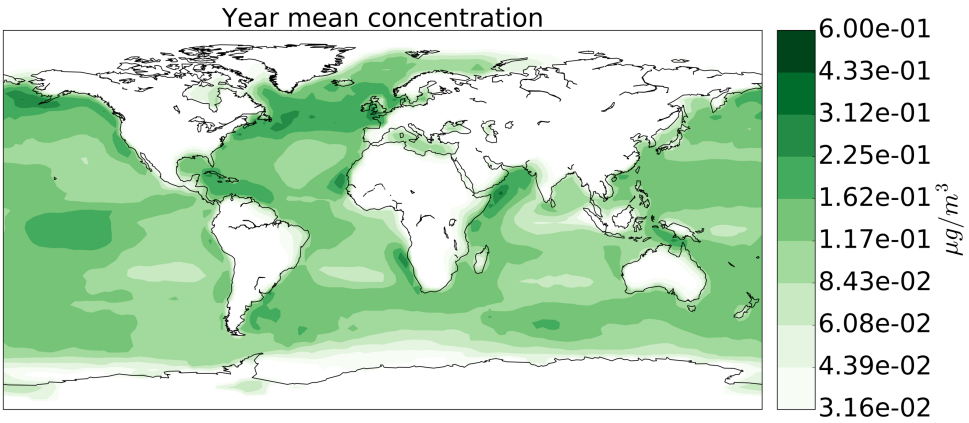

Figure 2. Annual mean modelled mass concentration of submicron marine organic aerosol at surface level.

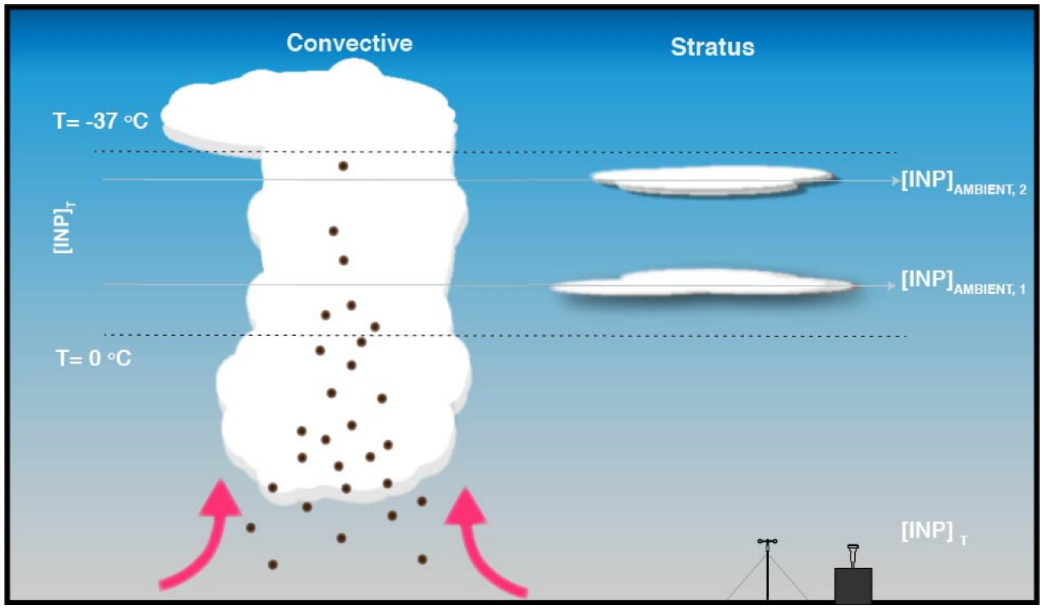

Figure 3. Illustration of the two ways in which we display INP concentrations. It is important to bear in mind that INPs are defined as particles with the potential to nucleate ice and their concentration is quoted for a specific set of conditions. $[INP]_{ambient}$, where ambient denotes the local atmospheric temperature, is a useful way of looking at the INP concentration relevant to non-deep convective mixed-phase clouds. $[INP]_T$, on the other hand, has utility in representing the spectrum of INP concentrations over temperature that will influence clouds with a large vertical extent such as deep-convective systems. Moreover $[INP]_T$ is the relevant quantity when comparing modelled and observed INP concentrations, since measurements are made by exposing particles to controlled temperatures within the instrumentation.

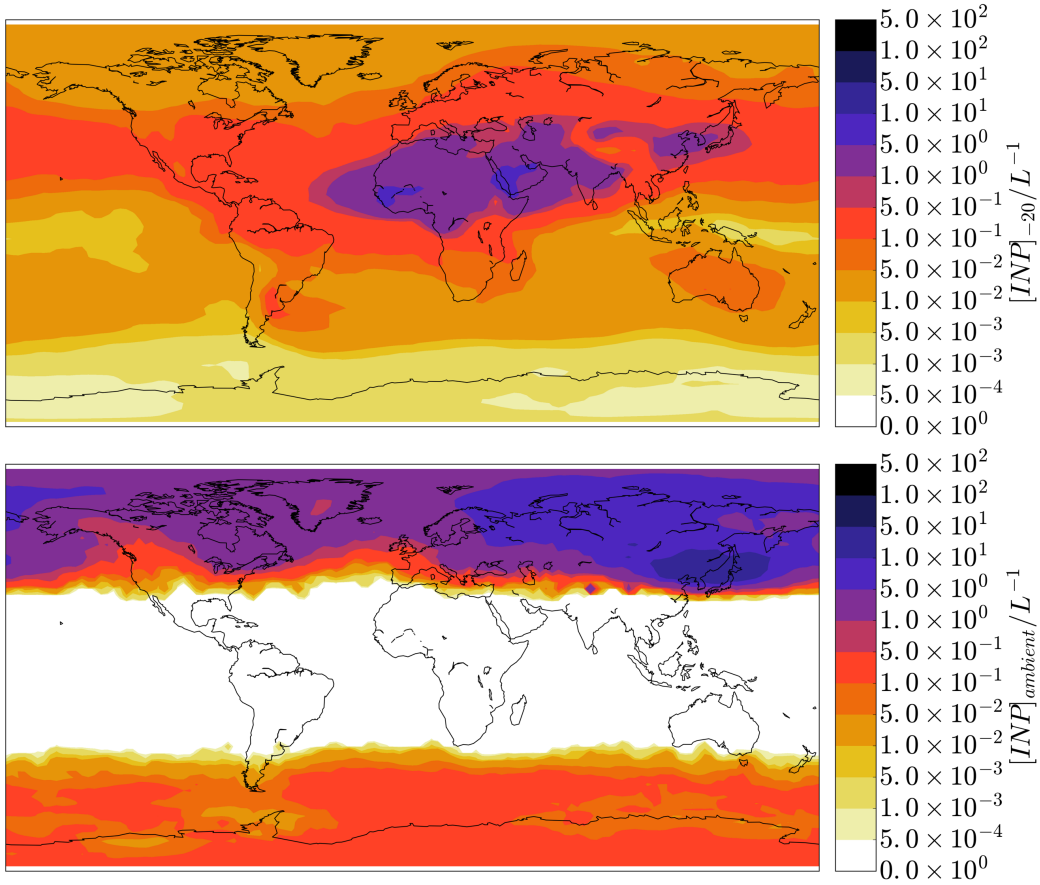

Figure 4. Annual mean K-feldspar INP distribution using GLOMAP mode at a pressure level of 600 hpa. Top panel shows the concentration of ice-nucleating particles active at a temperature of −20°C ($[INP]_T$) whereas the bottom panel shows the INP concentration at local ambient temperature ($[INP]_{ambient}$).

convection.

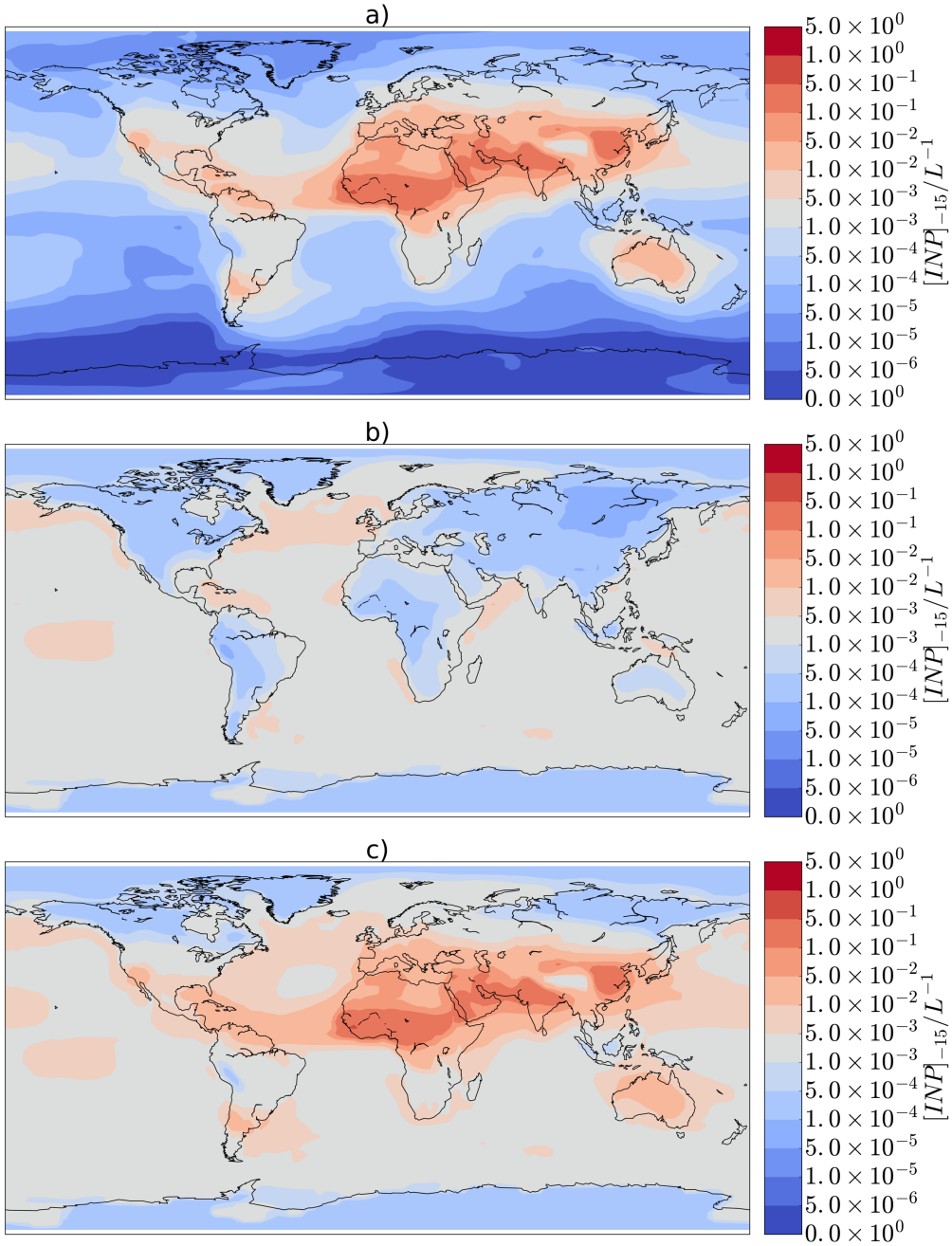

Figure 5. Annual mean distributions of ice-nucleating particles concentrations, for an activation temperature of −15ºC based on feldspar (a) and marine organics (b). Panel (c) shows the total INP concentration obtained by summing the INP concentrations from K-feldspar and marine organics. We show $[INP]_T$ for a T of −15ºC because this is a temperature used by many instruments. The number of INP that activate to ice crystals ($[INP]_{ambient}$) at the surface will be zero over much of the globe, because these particles will only become important at high altitudes. Surface concentrations are shown because this is where most observations of atmospheric INP concentrations are made.

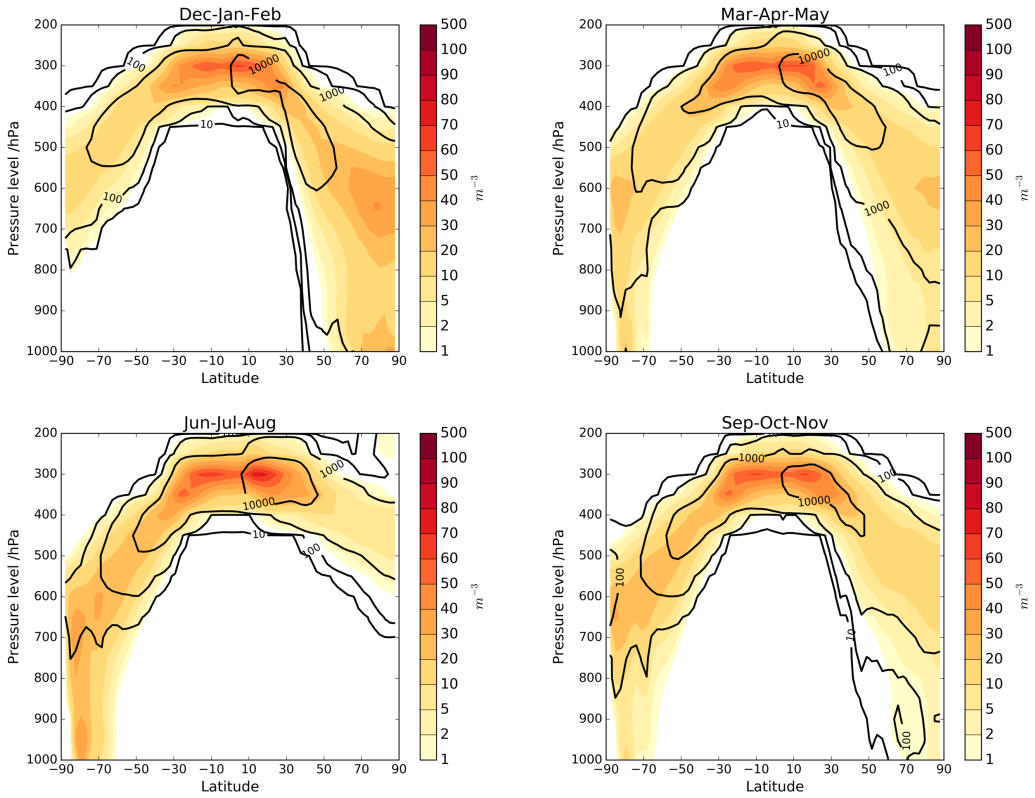

Figure 6. Zonal mean profiles of $[INP]_{ambient}$ for every month of the year. The black contour lines correspond to the INP concentration of K-feldspar aerosols (m^{-3}), while the colour map shows the INP concentration of marine organic aerosol. The values correspond to seasonal mean values calculated using daily concentrations and temperatures and averaged across latitudes.

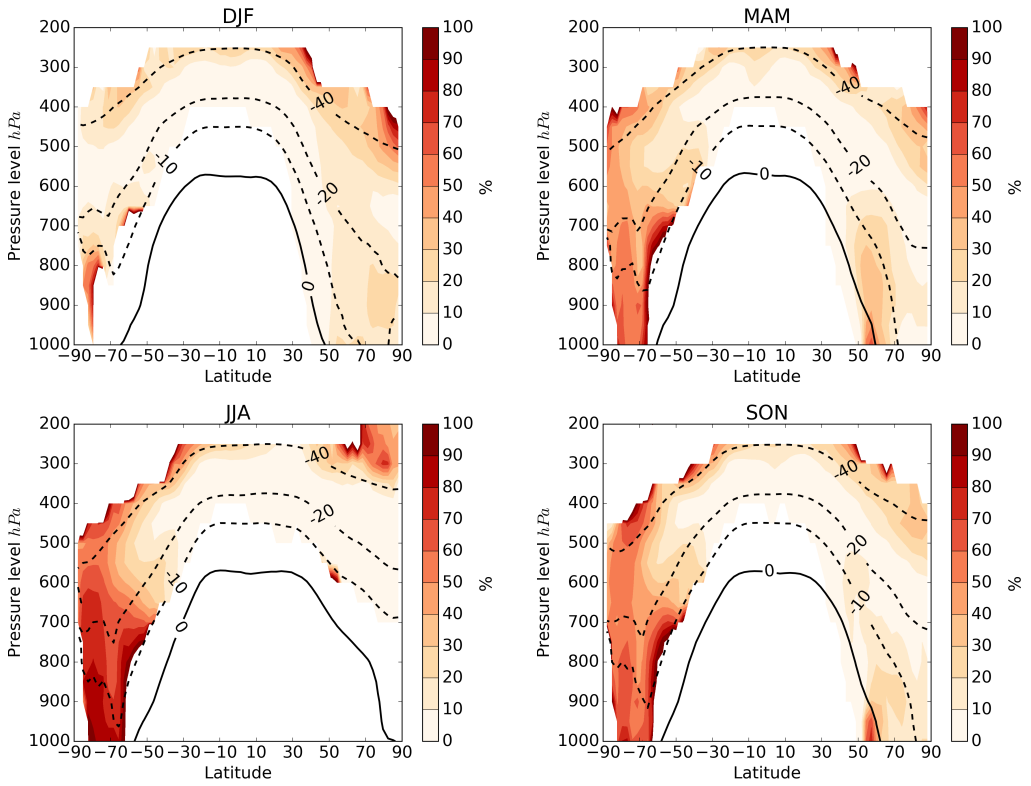

Figure 7. Percentage of days when $[INP]_{ambient}$ from marine organic aerosols is greater than from K-feldspar. The number of days have been calculated only for times and locations where the total $[INP]_{ambient}$ concentration is larger than $0.1 m^{-3}$. The black contour lines represent seasonal mean isotherms in degrees centigrade.

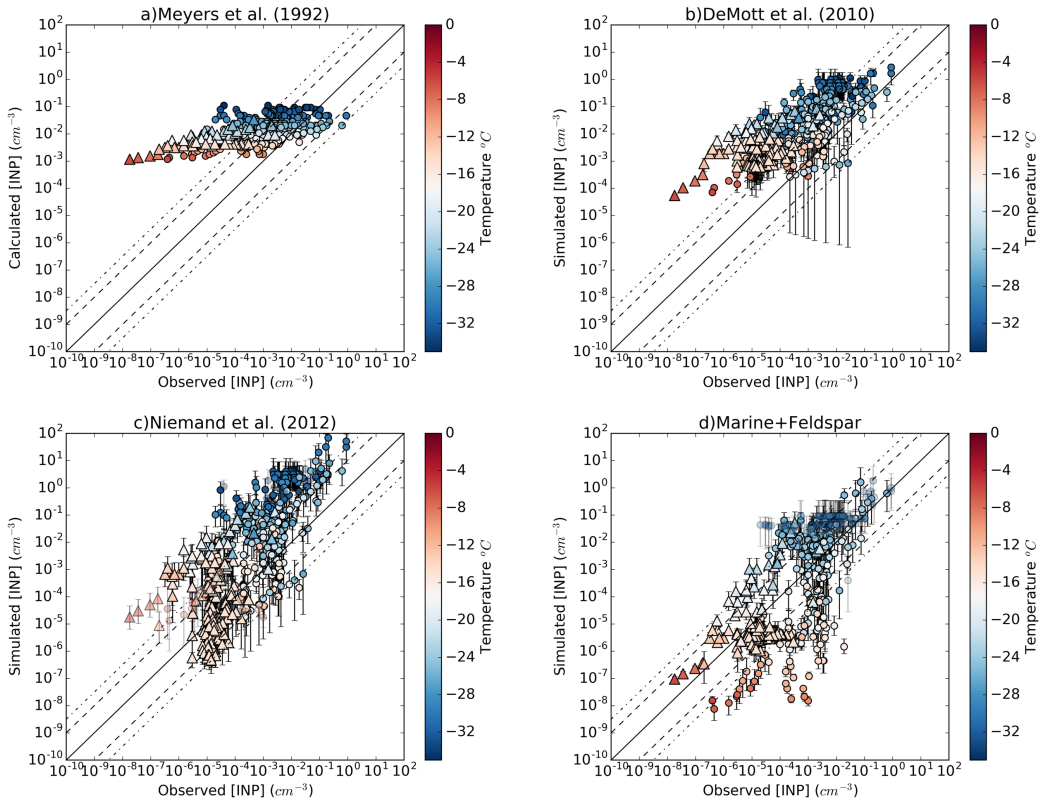

Figure 8. Comparison of the performance of a variety of INP parameterizations tested against field measurements shown in Figure 9 and appendix C. (a–d) Modelled INP concentration values when using (a) Meyers parameterization [*Meyers et al., 1992*], (b) DeMott's parameterization [*DeMott et al., 2010*] combined with a global aerosol simulation using GLOMAP-mode, (c) Niemand dust parameterization [*Niemand et al., 2012*] and (d) our two- species representation based on feldspar [*Atkinson et al., 2013*] and marine organic aerosols [*Wilson et al., 2015*]. Triangles represent marine influenced regions and points terrestrial environments. The light shaded points in (d) and (e) are for data points outside the temperature range of the parameterizations. The dashed lines represent one order of magnitude of difference between modelled and observed and the dashed- dotted lines 1.5 orders of magnitude. The simulated values correspond to an annual mean concentration and the error bars correspond to the simulated seasonality of INPs calculated with monthly mean values. For each individual observation, we calculated the INP concentration at the temperature corresponding to the temperature that aerosol particles were exposed to in the INP instruments. The locations of the data point are shown in Fig. 9.

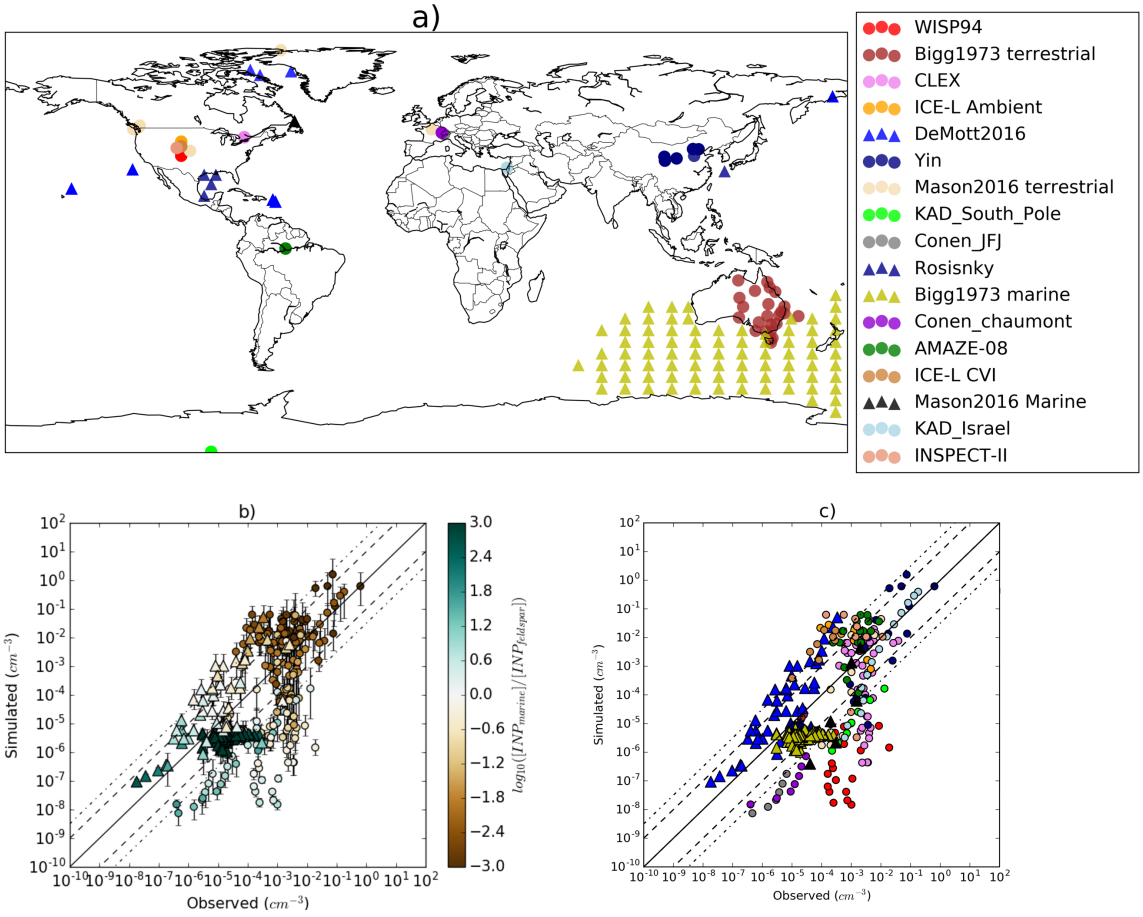

Figure 9. (a) Location of the data used for comparison in Fig. 8. (b) Same as Fig. 8d but showing the relative contribution (in orders of magnitude) of each aerosol species to the simulated concentration. (c) Same as (b) but distinguishes between the different campaigns shown in (a) (with the same colours and symbols). References to the data sets used are shown in Appendix C.

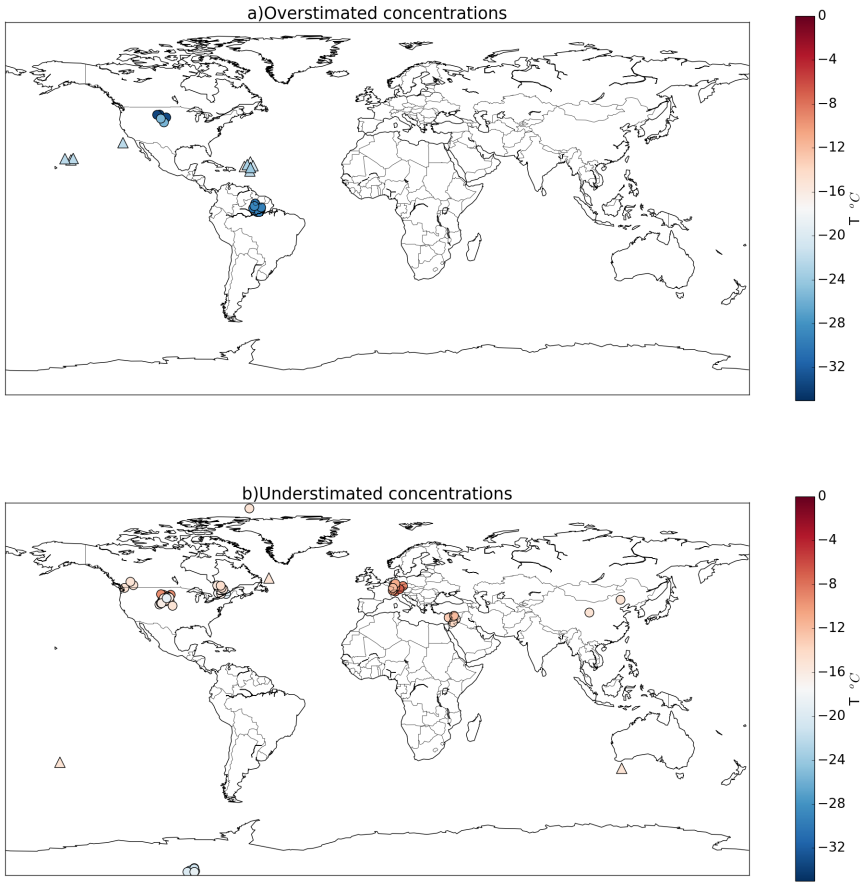

Figure 10. Overestimation and underestimation of places according to our two-species-based parameterization of INP *[Atkinson et al., 2013; Wilson et al., 2015]*. (a) Shows the places where we overestimate the values of INPs by more than 1.5 orders of magnitude. (b) Similar to (a) but for places where the concentration is underestimated by more than 1.5 orders of magnitude. The location of the points has been moved randomly in the plot for purpose of visualization so it can be seen when the bias affects a single data point or a whole data set.

Parameterization	Temperature range	Data points	Pt1	Pt1.5	R	Pt1*	Pt1.5*	R^*	Pt1**	Pt1.5**	R^{**}
Meyers et al. (1992)	0 to −37 °C	479	35.5 %	51 %	0.57	35.5 %	51 %	0.57	27.4 %	39.4 %	0.47
DeMott et al. (2010)	0 to −37 °C	479	24 %	39.2 %	0.67	24 %	39.2 %	0.67	23.6 %	38.3 %	0.42
Niemand et al. (2012)	−12 to −33 °C	438	33.7 %	53 %	0.58	31.7 %	53 %	0.64	46.9 %	70 %	0.41
Marine and K-feldspar	−6 to −25 °C	354	56.7 %	74 %	0.62	54.9 %	75.9 %	0.64	61.6 %	78.7 %	0.5

Table 1. Statistical performance of the different parameterizations. Pt1 and Pt1.5 are the percentages of data points reproduced within an order of magnitude and 1.5 orders of magnitude in the temperature range of every parameterization. The number of data points used for calculating these values is shown under the data points column. The values with $*$ show the same calculation but include data points outside the temperature range of the parameterizations. These values give an idea of the performance that you would expect if you extrapolate the parameterizations in a climate model. The values with $**$ are for data points within the smallest temperature range shared by the four parameterizations (−12 to −25 ◦C). The correlation coefficient has been calculated with the logarithm of the values as INP concentrations vary logarithmically with temperature.

References:

Aller, J. Y., M. R. Kuznetsova, C. J. Jahns, and P. F. Kemp (2005), The sea surface microlayer as a source of viral and bacterial enrichment in marine aerosols, *J. Aerosol Sci.*, *36*(5–6), 801–812, doi:10.1016/j.jaerosci.2004.10.012.

Alpert, P. a., J. Y. Aller, and D. a. Knopf (2011), Ice nucleation from aqueous NaCl droplets with and without marine diatoms, *Atmos. Chem. Phys. Discuss.*, *11*(3), 8291–8336, doi:10.5194/acpd-11-8291-2011.

Ardon-Dryer, K., and Z. Levin (2014), Ground-based measurements of immersion freezing in the eastern Mediterranean, *Atmos. Chem. Phys.*, *14*(10), 5217–5231, doi:10.5194/acp-14-5217-2014.

Atkinson, J. D., B. J. Murray, M. T. Woodhouse, T. F. Whale, K. J. Baustian, K. S. Carslaw, S. Dobbie, D. O'Sullivan, and T. L. Malkin (2013), The importance of feldspar for ice nucleation by mineral dust in mixed-phase clouds., *Nature*, *498*(7454), 355–8, doi:10.1038/nature12278.

Augustin-Bauditz, S., H. Wex, S. Kanter, M. Ebert, D. Niedermeier, F. Stolz, a. Prager, and F. Stratmann (2014), The immersion mode ice nucleation behavior of mineral dusts: A comparison of different pure and surface modified dusts, *Geophys. Res. Lett.*, *41*(20), 7375–7382, doi:10.1002/2014GL061317.

Bauer, P., A. Thorpe, and G. Brunet (2015), The quiet revolution of numerical weather prediction, *Nature*, *525*(7567), 47–55, doi:10.1038/nature14956.

Bigg, E. K. (1973), Ice Nucleus Concentrations in Remote Areas, *J. Atmos. Sci.*, *30*(6), 1153–1157, doi:10.1175/1520-0469(1973)030<1153:INCIRA>2.0.CO;2.

Bigg, E. K. (1996), Ice forming nuclei in the high Arctic, *Tellus B*, *48*(2), 223–233, doi:10.1034/j.1600-0889.1996.t01-1-00007.x.

Bodas-Salcedo, A., K. D. Williams, M. A. Ringer, I. Beau, J. N. S. Cole, J.-L. Dufresne, T. Koshiro, B. Stevens, Z. Wang, and T. Yokohata (2014), Origins of the Solar Radiation Biases over the Southern Ocean in CFMIP2 Models*, *J. Clim.*, *27*(1), 41–56, doi:10.1175/JCLI-D-13-00169.1.

Boose, Y., B. Sierau, M. I. García, S. Rodríguez, A. Alastuey, C. Linke, M. Schnaiter, P. Kupiszewski, Z. A. Kanji, and U. Lohmann (2016), Ice nucleating particles in the Saharan Air Layer, *Atmos. Chem. Phys. Discuss.*, (March), 1–36, doi:10.5194/acp-2016-192.

Broadley, S. L., B. J. Murray, R. J. Herbert, J. D. Atkinson, S. Dobbie, T. L. Malkin, E. Condliffe, and L. Neve (2012), Immersion mode heterogeneous ice nucleation by an illite rich powder representative of atmospheric mineral dust, *Atmos. Chem. Phys.*, *12*(1), 287–307, doi:10.5194/acp-12-287-2012.

Browse, J., K. S. Carslaw, S. R. Arnold, K. Pringle, and O. Boucher (2012), The scavenging processes controlling the seasonal cycle in Arctic sulphate and black carbon aerosol, *Atmos. Chem. Phys.*, *12*(15), 6775–6798, doi:10.5194/acp-12-6775-2012.

Burrows, S. M., C. Hoose, U. Pöschl, and M. G. Lawrence (2013), Ice nuclei in marine air: biogenic particles or dust?, *Atmos. Chem. Phys.*, *13*(1), 245–267, doi:10.5194/acp-13-245-2013.

Carslaw, K. S. et al. (2013), Large contribution of natural aerosols to uncertainty in indirect forcing., *Nature*, *503*(7474), 67–71, doi:10.1038/nature12674.

Choi, Y.-S., R. S. Lindzen, C.-H. Ho, and J. Kim (2010), Space observations of cold-cloud phase change., *Proc. Natl. Acad. Sci. U. S. A.*, *107*(25), 11211–6, doi:10.1073/pnas.1006241107.

Claquin, T., M. Schulz, and Y. J. Balkanski (1999), Modeling the mineralogy of atmospheric dust sources, *J. Geophys. Res.*, *104*(D18), 22243, doi:10.1029/1999JD900416.

Cochran, R. E., T. Jayarathne, E. A. Stone, and V. H. Grassian (2016), Selectivity Across the Interface: A Test of Surface Activity in the Composition of Organic-Enriched Aerosols from Bubble Bursting, *J. Phys. Chem. Lett.*, *7*(9), 1692–1696, doi:10.1021/acs.jpclett.6b00489.

Cunliffe, M., A. Engel, S. Frka, B. Gašparović, C. Guitart, J. C. Murrell, M. Salter, C. Stolle, R. Upstill-Goddard, and O. Wurl (2013), Sea surface microlayers: A unified physicochemical and biological perspective of the air ocean interface, *Prog. Oceanogr.*, *109*, 104–116, doi:10.1016/j.pocean.2012.08.004.

DeMott, P. J., a J. Prenni, X. Liu, S. M. Kreidenweis, M. D. Petters, C. H. Twohy, M. S. Richardson, T. Eidhammer, and D. C. Rogers (2010), Predicting global atmospheric ice nuclei distributions and their impacts on climate., *Proc. Natl. Acad. Sci. U. S. A.*, *107*(25), 11217–11222, doi:10.1073/pnas.0910818107.

DeMott, P. J. et al. (2015), Integrating laboratory and field data to quantify the immersion freezing ice nucleation activity of mineral dust particles, *Atmos. Chem. Phys.*, *15*(1), 393–409, doi:10.5194/acp-15-393-2015.

DeMott, P. J. et al. (2016), Sea spray aerosol as a unique source of ice nucleating particles, *Proc. Natl. Acad. Sci.*, *113*(21), 5797–5803, doi:10.1073/pnas.1514034112.

Dentener, F., and S. Kinne (2006), Emissions of primary aerosol and precursor gases in the years 2000 and 1750 prescribed data-sets for AeroCom, ... *Phys.*, (year 1750), 4321–4344.

Eidhammer, T., P. J. DeMott, and S. M. Kreidenweis (2009), A comparison of

heterogeneous ice nucleation parameterizations using a parcel model framework, *J. Geophys. Res.*, *114*(D6), D06202, doi:10.1029/2008JD011095.

Emersic, C., P. J. Connolly, S. Boult, M. Campana, and Z. Li (2015), Investigating the discrepancy between wet-suspension and dry-dispersion derived ice nucleation efficiency of mineral particles, *Atmos. Chem. Phys. Discuss.*, *15*(1), 887–929, doi:10.5194/acpd-15-887-2015.

Facchini, M. C. et al. (2008), Primary submicron marine aerosol dominated by insoluble organic colloids and aggregates, *Geophys. Res. Lett.*, *35*(17), L17814, doi:10.1029/2008GL034210.

Fall, R., and R. C. Schnell (1985), Association of an ice-nucleating pseudomonad with cultures of the marine dinoflagellate, <I>Heterocapsa niei</I>, *J. Mar. Res.*, *43*(1), 257–265, doi:10.1357/002224085788437370.

Field, P. R., A. J. Heymsfield, B. J. Shipway, P. J. DeMott, K. a. Pratt, D. C. Rogers, J. Stith, and K. a. Prather (2012), Ice in Clouds Experiment Layer Clouds. Part II: Testing Characteristics of Heterogeneous Ice Formation in Lee Wave Clouds, *J. Atmos. Sci.*, *69*(3), 1066–1079, doi:10.1175/JAS-D-11-026.1.

Fröhlich-Nowoisky, J., T. C. J. Hill, B. G. Pummer, P. Yordanova, G. D. Franc, and U. Pöschl (2015), Ice nucleation activity in the widespread soil fungus Mortierella alpina, *Biogeosciences*, *12*(4), 1057–1071, doi:10.5194/bg-12-1057-2015.

Fuentes, E., H. Coe, D. Green, and G. McFiggans (2011), On the impacts of phytoplankton-derived organic matter on the properties of the primary marine aerosol Part 2: Composition, hygroscopicity and cloud condensation activity, *Atmos. Chem. Phys.*, *11*(6), 2585–2602, doi:10.5194/acp-11-2585-2011.

Gantt, B., N. Meskhidze, M. C. Facchini, M. Rinaldi, D. Ceburnis, and C. D. O'Dowd (2011), Wind speed dependent size-resolved parameterization for the organic mass fraction of sea spray aerosol, *Atmos. Chem. Phys.*, *11*(16), 8777–8790, doi:10.5194/acp-11-8777-2011.

Garcia, E., T. C. J. Hill, A. J. Prenni, P. J. DeMott, G. D. Franc, and S. M. Kreidenweis (2012), Biogenic ice nuclei in boundary layer air over two U.S. High Plains agricultural regions, *J. Geophys. Res. Atmos.*, *117*(D18), n/a-n/a, doi:10.1029/2012JD018343.

Ghan, S. J., and S. E. Schwartz (2007), Aerosol Properties and Processes: A Path from Field and Laboratory Measurements to Global Climate Models, *Bull. Am. Meteorol. Soc.*, *88*(7), 1059–1083, doi:10.1175/BAMS-88-7-1059.

Gong, S. L. (2003), A parameterization of sea-salt aerosol source function for sub- and super-micron particles, *Global Biogeochem. Cycles*, *17*(4), n/a-n/a, doi:10.1029/2003GB002079.

Haga, D. I., R. Iannone, M. J. Wheeler, R. Mason, E. A. Polishchuk, T. Fetch, B. J. Van Der Kamp, I. G. McKendry, and A. K. Bertram (2013), Ice nucleation properties of rust and bunt fungal spores and their transport to high altitudes, where they can cause heterogeneous freezing, *J. Geophys. Res. Atmos.*, *118*(13), 7260–7272, doi:10.1002/jgrd.50556.

Haga, D. I., S. M. Burrows, R. Iannone, M. J. Wheeler, R. H. Mason, J. Chen, E. A. Polishchuk, U. Pöschl, and A. K. Bertram (2014), Ice nucleation by fungal spores from the classes *Agaricomycetes*, *Ustilaginomycetes*, and *Eurotiomycetes*, and the effect on the atmospheric transport of these spores, *Atmos. Chem. Phys.*, *14*(16), 8611–8630, doi:10.5194/acp-14-8611-2014.

HALLETT, J., and S. C. MOSSOP (1974), Production of secondary ice particles during the riming process, *Nature*, *249*(5452), 26–28, doi:10.1038/249026a0.

Harrison, A. D., T. F. Whale, M. A. . Carpenter, M. A. Holden, L. Neve, D. O'Sullivan, J. Vergara Temprado, and B. J. Murray (2016), Not all feldspar is equal: a survey of ice nucleating properties across the feldspar group of minerals, *Atmos. Chem. Phys. Discuss.*, (February), 1–26, doi:10.5194/acp-2016-136.

Hartmann, S., S. Augustin, T. Clauss, J. Voigtländer, D. Niedermeier, H. Wex, and F. Stratmann (2013), Immersion freezing of ice nucleating active protein complexes, *Atmos. Chem. Phys. Discuss.*, *12*(8), 21321–21353, doi:10.5194/acpd-12-21321-2012.

Herbert, R. J., B. J. Murray, T. F. Whale, S. J. Dobbie, and J. D. Atkinson (2014), Representing time-dependent freezing behaviour in immersion mode ice nucleation, *Atmos. Chem. Phys.*, *14*(16), 8501–8520, doi:10.5194/acp-14-8501-2014.

Herbert, R. J., B. J. Murray, S. J. Dobbie, and T. Koop (2015), Sensitivity of liquid clouds to homogenous freezing parameterizations, *Geophys. Res. Lett.*, *42*(5), 1599–1605, doi:10.1002/2014GL062729.

Hoose, C., and O. Möhler (2012), Heterogeneous ice nucleation on atmospheric aerosols: A review of results from laboratory experiments, *Atmos. Chem. Phys.*, *12*(20), 9817–9854, doi:10.5194/acp-12-9817-2012.

Hoose, C., J. E. Kristjánsson, J.-P. Chen, and A. Hazra (2010a), A Classical-Theory-Based Parameterization of Heterogeneous Ice Nucleation by Mineral Dust, Soot, and Biological Particles in a Global Climate Model, *J. Atmos. Sci.*, *67*(8), 2483–2503, doi:10.1175/2010JAS3425.1.

Hoose, C., J. E. Kristjánsson, and S. M. Burrows (2010b), How important is biological ice nucleation in clouds on a global scale?, *Environ. Res. Lett.*, *5*(2), 24009, doi:10.1088/1748-9326/5/2/024009.

Huneeus, N. et al. (2011), Global dust model intercomparison in AeroCom phase I, *Atmos. Chem. Phys.*, *11*(15), 7781–7816, doi:10.5194/acp-11-7781-2011.

Knopf, D. a., P. a. Alpert, B. Wang, and J. Y. Aller (2010), Stimulation of ice nucleation by marine diatoms, *Nat. Geosci.*, *4*(2), 88–90, doi:10.1038/ngeo1037.

Kodros, J. K., C. E. Scott, S. C. Farina, Y. H. Lee, C. L'Orange, J. Volckens, and J. R. Pierce (2015), Uncertainties in global aerosols and climate effects due to biofuel emissions, *Atmos. Chem. Phys.*, *15*(15), 8577–8596, doi:10.5194/acp-15-8577-2015.

Koehler, K. A., S. M. Kreidenweis, P. J. DeMott, M. D. Petters, A. J. Prenni, and O. Möhler (2010), Laboratory investigations of the impact of mineral dust aerosol on cold cloud formation, *Atmos. Chem. Phys.*, *10*(23), 11955–11968, doi:10.5194/acp-10-11955-2010.

Korolev, A. (2007), Limitations of the WegenerBergeronFindeisen Mechanism in the Evolution of MixedPhase Clouds, *J. Atmos. Sci.*, *64*, 3372–3375, doi:10.1175/JAS4035.1.

Lafon, S., J. L. Rajot, S. C. Alfaro, and A. Gaudichet (2004), Quantification of iron oxides in desert aerosol, *Atmos. Environ.*, *38*(8), 1211–1218, doi:10.1016/j.atmosenv.2003.11.006.

Lohmann, U., and K. Diehl (2006), Sensitivity studies of the importance of dust ice nuclei for the indirect aerosol effect on stratiform mixed-phase clouds, *J. Atmos. Sci.*, 968–982.

Maki, L. R., and K. J. Willoughby (1978), Bacteria as Biogenic Sources of Freezing Nuclei, *J. Appl. Meteorol.*, *17*(7), 1049–1053, doi:10.1175/1520-0450(1978)017<1049:BABSOF>2.0.CO;2.

Mann, G. W., K. S. Carslaw, D. V. Spracklen, D. a. Ridley, P. T. Manktelow, M. P. Chipperfield, S. J. Pickering, and C. E. Johnson (2010), Description and evaluation of GLOMAP-mode: a modal global aerosol microphysics model for the UKCA composition-climate model, *Geosci. Model Dev.*, *3*(2), 519–551, doi:10.5194/gmd-3-519-2010.

Mann, G. W. et al. (2014), Intercomparison and evaluation of global aerosol microphysical properties among AeroCom models of a range of complexity, *Atmos. Chem. Phys.*, *14*(9), 4679–4713, doi:10.5194/acp-14-4679-2014.

Marcolli, C., S. Gedamke, T. Peter, and B. Zobrist (2007), Efficiency of immersion mode ice nucleation on surrogates of mineral dust, *Atmos. Chem. Phys. Discuss.*, *7*(4), 9687–9716, doi:10.5194/acpd-7-9687-2007.

Mason, R. H. et al. (2016), Size-resolved measurements of ice-nucleating particles

at six locations in North America and one in Europe, *Atmos. Chem. Phys.*, *16*(3), 1637–1651, doi:10.5194/acp-16-1637-2016.

McCoy, D. T., D. L. Hartmann, M. D. Zelinka, P. Ceppi, and D. P. Grosvenor (2015), Mixed-phase cloud physics and Southern Ocean cloud feedback in climate models, *J. Geophys. Res. Atmos.*, *120*, 9539–9554, doi:10.1002/2015JD023603.Received.

Meyers, M. P., P. J. DeMott, and W. R. Cotton (1992), New Primary Ice-Nucleation Parameterizations in an Explicit Cloud Model, *J. Appl. Meteorol.*, *31*(7), 708–721, doi:10.1175/1520-0450(1992)031<0708:NPINPI>2.0.CO;2.

Möhler, O., D. G. Georgakopoulos, C. E. Morris, S. Benz, V. Ebert, S. Hunsmann, H. Saathoff, M. Schnaiter, and R. Wagner (2008), Heterogeneous ice nucleation activity of bacteria: new laboratory experiments at simulated cloud conditions, *Biogeosciences Discuss.*, *5*(2), 1445–1468, doi:10.5194/bgd-5-1445-2008.

Monahan, E. C., D. E. Spiel, and K. L. Davidson (1986), A Model of Marine Aerosol Generation Via Whitecaps and Wave Disruption, in *Oceanic Whitecaps: And Their Role in Air-Sea Exchange Processes*, edited by E. C. Monahan and G. Mac Niocaill, pp. 167–174, Springer Netherlands, Dordrecht.

Morris, C. E., D. C. Sands, C. Glaux, J. Samsatly, S. Asaad, A. R. Moukahel, F. L. T. Gonçalves, and E. K. Bigg (2013), Urediospores of rust fungi are ice nucleation active at 10 C and harbor ice nucleation active bacteria, *Atmos. Chem. Phys.*, *13*(8), 4223–4233, doi:10.5194/acp-13-4223-2013.

Morrison, H., G. de Boer, G. Feingold, J. Harrington, M. D. Shupe, and K. Sulia (2011), Resilience of persistent Arctic mixed-phase clouds, *Nat. Geosci.*, *5*(1), 11–17, doi:10.1038/ngeo1332.

Murphy, D. M., and T. Koop (2005), Review of the vapour pressures of ice and supercooled water for atmospheric applications, *Q. J. R. Meteorol. Soc.*, *131*(608), 1539–1565, doi:10.1256/qj.04.94.

Murray, B. J., S. L. Broadley, T. W. Wilson, J. D. Atkinson, and R. H. Wills (2011), Heterogeneous freezing of water droplets containing kaolinite particles, *Atmos. Chem. Phys.*, *11*(9), 4191–4207, doi:10.5194/acp-11-4191-2011.

Murray, B. J., D. O'Sullivan, J. D. Atkinson, and M. E. Webb (2012), Ice nucleation by particles immersed in supercooled cloud droplets, *Chem. Soc. Rev.*, *41*(19), 6519, doi:10.1039/c2cs35200a.

Nickovic, S., a. Vukovic, M. Vujadinovic, V. Djurdjevic, and G. Pejanovic (2012), Technical Note: High-resolution mineralogical database of dust-productive soils for atmospheric dust modeling, *Atmos. Chem. Phys.*, *12*(2), 845–855, doi:10.5194/acp-12-845-2012.

Niedermeier, D., R. A. Shaw, S. Hartmann, H. Wex, T. Clauss, J. Voigtländer, and F. Stratmann (2011), Heterogeneous ice nucleation: exploring the transition from stochastic to singular freezing behavior, *Atmos. Chem. Phys.*, *11*(16), 8767–8775, doi:10.5194/acp-11-8767-2011.

Niedermeier, D., S. Augustin-bauditz, S. Hartmann, H. Wex, and F. Stratmann (2015), Can we define an asymptotic value for the ice active surface site density for heterogeneous ice nucleation?, *J. Geophys. Res. Atmos.*, *120*(May), 5036–5046, doi:10.1002/2014JD022814.The.

Niemand, M. et al. (2012), A Particle-Surface-Area-Based Parameterization of Immersion Freezing on Desert Dust Particles, *J. Atmos. Sci.*, *69*(10), 3077–3092, doi:10.1175/JAS-D-11-0249.1.

O'Dowd, C. et al. (2015), Connecting marine productivity to sea-spray via nanoscale biological processes: Phytoplankton Dance or Death Disco?, *Sci. Rep.*, *5*(October), 14883, doi:10.1038/srep14883.

O'Sullivan, D., B. J. Murray, T. L. Malkin, T. F. Whale, N. S. Umo, J. D. Atkinson, H. C. Price, K. J. Baustian, J. Browse, and M. E. Webb (2014), Ice nucleation by fertile soil dusts: relative importance of mineral and biogenic components, *Atmos. Chem. Phys.*, *14*(4), 1853–1867, doi:10.5194/acp-14-1853-2014.

O'Sullivan, D., B. J. Murray, J. F. Ross, T. F. Whale, H. C. Price, J. D. Atkinson, N. S. Umo, and M. E. Webb (2015), The relevance of nanoscale biological fragments for ice nucleation in clouds, *Sci. Rep.*, *5*, 8082, doi:10.1038/srep08082.

O'Sullivan, D., B. J. Murray, J. Ross, and M. E. Webb (2016), The adsorption of fungal ice-nucleating proteins on mineral dusts: a terrestrial reservoir of atmospheric ice-nucleating particles, *Atmos. Chem. Phys. Discuss.*, (January), 1–22, doi:10.5194/acp-2015-1018.

Orellana, M. V, P. A. Matrai, C. Leck, C. D. Rauschenberg, A. M. Lee, and E. Coz (2011), Marine microgels as a source of cloud condensation nuclei in the high Arctic, *Proc. Natl. Acad. Sci.*, *108*(33), 13612–13617, doi:10.1073/pnas.1102457108.

Ovadnevaite, J., C. O'Dowd, M. Dall'Osto, D. Ceburnis, D. R. Worsnop, and H. Berresheim (2011), Detecting high contributions of primary organic matter to marine aerosol: A case study, *Geophys. Res. Lett.*, *38*(2), n/a-n/a, doi:10.1029/2010GL046083.

Partanen, a.-I. et al. (2014), Global modelling of direct and indirect effects of sea spray aerosol using a source function encapsulating wave state, *Atmos. Chem. Phys.*, *14*(21), 11731–11752, doi:10.5194/acp-14-11731-2014.

Perlwitz, J. P., C. Perez Garcia-Pando, and R. L. Miller (2015), Predicting the

mineral composition of dust aerosols Part 1: Representing key processes, *Atmos. Chem. Phys. Discuss.*, *15*(3), 3493–3575, doi:10.5194/acpd-15-3493-2015.

Pouleur, S., C. Richard, J. Martin, and H. Antoun (1992), Ice nucleation activity in Fusarium acuminatum and Fusarium avenaceum, *Appl. Environ. Microbiol.*, *58*(9), 2960–2964.

Pummer, B. G. et al. (2015), Ice nucleation by water-soluble macromolecules, *Atmos. Chem. Phys.*, *15*(8), 4077–4091, doi:10.5194/acp-15-4077-2015.

Quinn, P. K., T. S. Bates, K. S. Schulz, D. J. Coffman, a. a. Frossard, L. M. Russell, W. C. Keene, and D. J. Kieber (2014), Contribution of sea surface carbon pool to organic matter enrichment in sea spray aerosol, *Nat. Geosci.*, *7*(3), 228–232, doi:10.1038/ngeo2092.

Rap, A., C. E. Scott, D. V. Spracklen, N. Bellouin, P. M. Forster, K. S. Carslaw, A. Schmidt, and G. Mann (2013), Natural aerosol direct and indirect radiative effects, *Geophys. Res. Lett.*, *40*(12), 3297–3301, doi:10.1002/grl.50441.

Riechers, B., F. Wittbracht, A. Hütten, and T. Koop (2013), The homogeneous ice nucleation rate of water droplets produced in a microfluidic device and the role of temperature uncertainty, *Phys. Chem. Chem. Phys.*, *15*(16), 5873, doi:10.1039/c3cp42437e.

Rinaldi, M. et al. (2013), Is chlorophyll- a the best surrogate for organic matter enrichment in submicron primary marine aerosol?, *J. Geophys. Res. Atmos.*, *118*(10), 4964–4973, doi:10.1002/jgrd.50417.

Rosenfeld, D., X. Yu, G. Liu, X. Xu, Y. Zhu, Z. Yue, J. Dai, Z. Dong, Y. Dong, and Y. Peng (2011), Glaciation temperatures of convective clouds ingesting desert dust, air pollution and smoke from forest fires, *Geophys. Res. Lett.*, *38*(21), n/a-n/a, doi:10.1029/2011GL049423.

Rosinski, J., P. L. Haagenson, C. T. Nagamoto, and F. Parungo (1986), Ice-forming nuclei of maritime origin, *J. Aerosol Sci.*, *17*(1), 23–46, doi:10.1016/0021-8502(86)90004-2.

Rosinski, J., P. L. Haagenson, C. T. Nagamoto, and F. Parungo (1987), Nature of ice-forming nuclei in marine air masses, *J. Aerosol Sci.*, *18*(3), 291–309, doi:10.1016/0021-8502(87)90024-3.

Rosinski, J., P. L. Haagenson, C. T. Nagamoto, B. Quintana, F. Parungo, and S. D. Hoyt (1988), Ice-forming nuclei in air masses over the Gulf of Mexico, *J. Aerosol Sci.*, *19*(5), 539–551, doi:10.1016/0021-8502(88)90206-6.

Russell, L. M., L. N. Hawkins, A. a Frossard, P. K. Quinn, and T. S. Bates (2010), Carbohydrate-like composition of submicron atmospheric particles and their

production from ocean bubble bursting., *Proc. Natl. Acad. Sci. U. S. A.*, *107*(15), 6652–7, doi:10.1073/pnas.0908905107.

Savre, J., and a M. L. Ekman (2015), A theory-based parameterization for heterogeneous ice nucleation and implications for the simulation of ice processes in atmospheric models, *J. Geophys. Res. Atmos.*, *120*(10), 4937–4961, doi:10.1002/2014JD023000.

Schnell, R. C. (1977), Ice Nuclei in Seawater, Fog Water and Marine Air off the Coast of Nova Scotia: Summer 1975, *J. Atmos. Sci.*, *34*(8), 1299–1305, doi:10.1175/1520-0469(1977)034<1299:INISFW>2.0.CO;2.

Schnell, R. C. (1982), Airborne ice nucleus measurements around the Hawaiian Islands, *J. Geophys. Res.*, *87*(C11), 8886, doi:10.1029/JC087iC11p08886.

Schnell, R. C., and G. Vali (1975), Freezing nuclei in marine waters, *Tellus*, *27*(3), 321–323, doi:10.1111/j.2153-3490.1975.tb01682.x.

Schnell, R. C., and G. Vali (1976), Biogenic Ice Nuclei: Part I. Terrestrial and Marine Sources, *J. Atmos. Sci.*, *33*(8), 1554–1564, doi:10.1175/1520-0469(1976)033<1554:BINPIT>2.0.CO;2.

Sesartic, A., U. Lohmann, and T. Storelvmo (2012), Bacteria in the ECHAM5-HAM global climate model, *Atmos. Chem. Phys.*, *12*(18), 8645–8661, doi:10.5194/acp-12-8645-2012.

Spracklen, D. V., and C. L. Heald (2014), The contribution of fungal spores and bacteria to regional and global aerosol number and ice nucleation immersion freezing rates, *Atmos. Chem. Phys.*, *14*(17), 9051–9059, doi:10.5194/acp-14-9051-2014.

Stopelli, E., F. Conen, C. E. Morris, E. Herrmann, N. Bukowiecki, and C. Alewell (2015), Ice nucleation active particles are efficiently removed by precipitating clouds, *Sci. Rep.*, *5*, 16433, doi:10.1038/srep16433.

Sullivan, R. C., L. Miñambres, P. J. DeMott, A. J. Prenni, C. M. Carrico, E. J. T. Levin, and S. M. Kreidenweis (2010), Chemical processing does not always impair heterogeneous ice nucleation of mineral dust particles, *Geophys. Res. Lett.*, *37*(24), n/a-n/a, doi:10.1029/2010GL045540.

Tan, I., T. Storelvmo, and M. D. Zelinka (2016), Observational constraints on mixed-phase clouds imply higher climate sensitivity, *Science (80-.).*, *352*(6282), 224–227, doi:10.1126/science.aad5300.

Tobo, Y., A. J. Prenni, P. J. DeMott, J. A. Huffman, C. S. McCluskey, G. Tian, C. Pöhlker, U. Pöschl, and S. M. Kreidenweis (2013), Biological aerosol particles as a key determinant of ice nuclei populations in a forest ecosystem, *J. Geophys. Res. Atmos.*, *118*(17), 10,100-10,110, doi:10.1002/jgrd.50801.

Tobo, Y., P. J. Demott, T. C. J. Hill, A. J. Prenni, N. G. Swoboda-Colberg, G. D. Franc, and S. M. Kreidenweis (2014), Organic matter matters for ice nuclei of agricultural soil origin, *Atmos. Chem. Phys.*, *14*(16), 8521–8531, doi:10.5194/acp-14-8521-2014.

Vali, G. (2008), Repeatability and randomness in heterogeneous freezing nucleation, *Atmos. Chem. Phys. Discuss.*, *8*(1), 4059–4097, doi:10.5194/acpd-8-4059-2008.

Vali, G., and J. R. Snider (2015), Time-dependent freezing rate parcel model, *Atmos. Chem. Phys.*, *15*(4), 2071–2079, doi:10.5194/acp-15-2071-2015.

Vignati, E., M. C. Facchini, M. Rinaldi, C. Scannell, D. Ceburnis, J. Sciare, M. Kanakidou, S. Myriokefalitakis, F. Dentener, and C. D. O'Dowd (2010), Global scale emission and distribution of sea-spray aerosol: Sea-salt and organic enrichment, *Atmos. Environ.*, *44*(5), 670–677, doi:10.1016/j.atmosenv.2009.11.013.

Wang, X. et al. (2015), Microbial Control of Sea Spray Aerosol Composition: A Tale of Two Blooms, *ACS Cent. Sci.*, *1*(3), 124–131, doi:10.1021/acscentsci.5b00148.

Wang, Y., X. Liu, C. Hoose, and B. Wang (2014), Different contact angle distributions for heterogeneous ice nucleation in the Community Atmospheric Model version 5, *Atmos. Chem. Phys.*, *14*(19), 10411–10430, doi:10.5194/acp-14-10411-2014.

Westbrook, C. D., and A. J. Illingworth (2013), The formation of ice in a long-lived supercooled layer cloud, *Q. J. R. Meteorol. Soc.*, *139*(677), 2209–2221, doi:10.1002/qj.2096.

Westbrook, C. D., and a. J. Illingworth (2011), Evidence that ice forms primarily in supercooled liquid clouds at temperatures > −27°C, *Geophys. Res. Lett.*, *38*(14), n/a-n/a, doi:10.1029/2011GL048021.

Wex, H., P. J. DeMott, Y. Tobo, S. Hartmann, M. Rösch, T. Clauss, L. Tomsche, D. Niedermeier, and F. Stratmann (2014), Kaolinite particles as ice nuclei: learning from the use of different kaolinite samples and different coatings, *Atmos. Chem. Phys.*, *14*(11), 5529–5546, doi:10.5194/acp-14-5529-2014.

Whale, T. F., B. J. Murray, D. O'Sullivan, N. S. Umo, K. J. Baustian, J. D. Atkinson, and G. J. Morris (2014), A technique for quantifying heterogeneous ice nucleation in microlitre supercooled water droplets, *Atmos. Meas. Tech. Discuss.*, *7*(9), 9509–9536, doi:10.5194/amtd-7-9509-2014.

Wilson, T. W. et al. (2015), A marine biogenic source of atmospheric ice-nucleating particles, *Nature*, *525*(7568), 234–238, doi:10.1038/nature14986.

Young, K. C. (1974), A Numerical Simulation of Wintertime, Orographic Precipitation: Part I. Description of Model Microphysics and Numerical Techniques, *J. Atmos. Sci.*, *31*(7), 1735–1748.

Zeng, X., W.-K. Tao, M. Zhang, a. Y. Hou, S. Xie, S. Lang, X. Li, D. O. Starr, X. Li, and J. Simpson (2009), An indirect effect of ice nuclei on atmospheric radiation, *J. Atmos. Sci.*, *66*, 41–61, doi:10.1175/2008JAS2778.1.

Zolles, T., J. Burkart, T. Häusler, B. Pummer, R. Hitzenberger, and H. Grothe (2015), Identification of ice nucleation active sites on feldspar dust particles, *J. Phys. Chem. A*, *119*(11), 2692–2700, doi:10.1021/jp509839x.

Chapter 3 Manuscript "Is black carbon an unimportant ice-nucleating particle in mixed-phase clouds?"

Authors: **Jesús Vergara-Temprado[1]*, Mark A. Holden[1,2]*, Thomas R. Orton[1,3], Daniel O'Sullivan[1], Nsikanabasi S. Umo[1,4], Jo Browse[1,5], Carly Reddington[1], María Teresa Baeza-Romero[6], Jenny M. Jones[7], Amanda Lea-Langton[7,8], Alan Williams[7], Ken S. Carslaw[1] and Benjamin J. Murray[1]**

[1]*Institute for Climate and Atmospheric Science, School of Earth and Environment, University of Leeds, Woodhouse Lane, Leeds, LS2 9JT, UK*

[2]*School of Chemistry, University of Leeds, Woodhouse Lane, Leeds, LS2 9JT, UK*

[3]*Now at: Lloyd's of London, One Lime Street, London, EC3M 7HA, UK*

[4]*Now at: Institute for Meteorology and Climate Research - Atmospheric Aerosol Research, Karlsruhe Institute of Technology, Hermann-von-Helmholtz Platz 1, 76344 Eggenstein-Leopoldshafen, Germany*

[5]*Now at: School of Geography, University of Exeter, Penryn Campus, Treliever Road, Penryn, Cornwall, TR10 9FE, UK*

[6]*Escuela de Ingeniería Industrial de Toledo, Universidad de Castilla la Mancha, Avenida Carlos III s/n, Real Fábrica de Armas, 45071 Toledo, Spain*

[7]*School of Chemical and Process Engineering, University of Leeds, Leeds, LS2 9JT, UK*

[8]*Now at: School of Mechanical, Aerospace and Civil Engineering, University of Manchester, Oxford Road, Manchester, M13 9PL, UK*

Corresponding authors: J. Vergara-Temprado (eejvt@leeds.ac.uk) and M. A. Holden

Abstract

It has been hypothesized that Black Carbon (BC) influences mixed-phase clouds by acting as an ice-nucleating particle (INP). However, the literature data for ice nucleation by BC immersed in supercooled water is extremely varied, with some studies reporting that BC is very effective at nucleating ice, whereas others report no ice-nucleating ability. Here we present new experimental results for immersion mode ice nucleation by BC from two contrasting sources. We observe no significant heterogeneous nucleation by either sample. Using a global aerosol model, we quantify the maximum relative importance of BC for ice-nucleation when compared with feldspar and marine organic aerosol acting as INP. Based on the upper limit from our laboratory data, we show that BC contributes at least several orders of magnitude less INP than feldspar and marine organic aerosol. Representations of its atmospheric ice-nucleating ability based on older laboratory data produce unrealistic results when compared against ambient observations of INP. Since BC is a complex material, it cannot be unambiguously ruled out as an important INP species in all locations at all times. Therefore, we use our model to estimate a range of values for the density of active sites that BC particles must have to be relevant for ice nucleation in the atmosphere. The estimated values will guide future work on BC, defining the required sensitivity of future experimental studies.

1. Introduction

Black carbon particles (BC), emitted from both anthropogenic and natural combustion processes, are ubiquitous in the present-day atmosphere with an estimated total emission rate of 7.5 Tg yr^{-1} [*Bond et al.*, 2013]. It is estimated that the anthropogenic emissions of BC have increased from ~1 Tg yr^{-1} in 1850 to ~5 Tg yr^{-1} in 2000 [*Lee et al.*, 2013], which is thought to have led to a significant impact on climate [*Bond et al.*, 2013]. BC has a strong warming effect through the absorption of solar and infrared radiation, and it has been suggested that reduction in black carbon emissions might go some way to mitigating global warming [*Bond et al.*, 2013]. However, to accurately assess the efficacy of reducing BC emissions it is important to quantify the impacts of BC aerosol on clouds. It is estimated that BC particles contribute substantially to global cloud condensation nuclei (CCN)

concentrations and they are an important CCN in industrial regions [*Spracklen et al.*, 2011]. BC therefore influences the albedo and lifetime of clouds through nucleating cloud droplets. If these immersed particles could also nucleate ice effectively then the lifetime and albedo of supercooled clouds would be affected. This 'glaciation indirect effect', which would most likely enhance precipitation and reduce cloud lifetime, could potentially offset the aerosol effects on liquid clouds [*Lohmann*, 2002, 2017]. However, the ice-nucleating ability of BC under conditions pertinent to supercooled clouds remains very uncertain.

While it has been shown in laboratory studies that BC nucleates ice under conditions relevant for cirrus clouds [*Möhler*, 2005; *Koehler et al.*, 2009; *Kanji et al.*, 2011; *Hoose and Möhler*, 2012; *Ullrich et al.*, 2017], there are divergent results from laboratory and field studies of the ability of BC to nucleate ice under water-saturated conditions, which are relevant for mixed-phase clouds [*DeMott*, 1990; *Diehl and Mitra*, 1998; *Hoose and Möhler*, 2012; *Schill et al.*, 2016; *Ullrich et al.*, 2017]. For example, a strong correlation between BC and the ice crystal concentration in a mixed-phase orographic mountain wave cloud suggested BC might nucleate ice [*Twohy et al.*, 2010]. However, in the same field campaign BC was not enhanced significantly in the ice crystal residues over the background air [*Pratt et al.*, 2009]. In one study of mixed-phase clouds at a high-altitude observatory in the Alps, soot particles only made up 5% of the background aerosol, but 27% of ice crystal residues [*Cozic et al.*, 2008]. In contrast, several studies found that BC accounted for only a minor fraction of ice crystal residues, but mineral dust was clearly enhanced [*Kamphus et al.*, 2010; *Baustian et al.*, 2012; *Kupiszewski et al.*, 2016; *Schmidt et al.*, 2017]. More recently, analysis of INP chemical composition in air influenced by biomass burning events using electron microscopy showed that between 0% to 64% of INPs were BC particles and suggested that biomass burning particles could be an important regional source of INP, especially during periods when other INPs such as desert dust are absent [*Mccluskey et al.*, 2014]. Measurements of the ice-nucleating efficiencies of BC particles from diesel engines [*Schill et al.*, 2016], found that fresh and photochemically aged BC particles did not nucleate ice effectively above their limit of detection. Overall, the field results do not clarify whether BC particles are consistently playing a role as INPs in the atmosphere, and

they suggest that BC (or compounds generated and transported along with BC) might be playing a sporadic role in nucleating ice under certain atmospheric conditions.

The available data from laboratory studies also leave open the question of whether or not BC is an efficient INP. Some studies show evidence that BC can nucleate ice in supercooled droplets [*DeMott*, 1990; *Diehl and Mitra*, 1998; *Gorbunov et al.*, 2001; *Popovicheva et al.*, 2008; *Wright et al.*, 2013; *Brooks et al.*, 2014]. Based on the available literature data [*DeMott*, 1990; *Diehl and Mitra*, 1998], a parameterization of the density of ice-nucleating active sites (n_s) was derived and in combination with BC concentrations in the atmosphere it was suggested that BC is a very important INP type [*Murray et al.,* 2012]. However, more recent studies could not reproduce similar values of n_s for BC, and the upper limits estimated from the limits of detection of the instruments were orders of magnitude lower [*Schill et al.*, 2016; *Ullrich et al.*, 2017]. The large variation in BC ice nucleation activity reported in these studies means that the contribution of BC to a possible anthropogenic glaciation effect has remained poorly quantified, since modelling results will depend strongly on the represented ability of BC for nucleating ice under mixed-phase conditions [*Hoose et al.*, 2010a, 2010b; *Savre and Ekman*, 2015].

2. Laboratory study of ice nucleation by soot samples

Given the large variation in ice-nucleating activities reported for the relatively few experimental studies of the ice-nucleating ability of BC, we have made new laboratory measurements. We have taken great care in these experiments to characterize the background INP which inevitably contaminate experiments such as these, but which can lead to a false ice nucleation signal. We have also taken care to generate BC samples in a reproducible and well-characterized way.

For these experiments, we have generated BC particles from the incomplete combustion of liquid fuels. By definition [*Petzold et al.*, 2013], these laboratory generated BC samples should be referred to as soot. Much of the BC in the atmosphere originates from incomplete combustion, but on transport through the atmosphere it is expected to evolve through the adsorption of other chemical

species, reactions with gas phase constituents, and aggregation with other aerosol particles, hence this atmospheric material is then generally termed as BC. In these experiments, we consider fresh soot particles generated in our laboratory as a proxy for atmospheric BC.

The fuels used to generate the soots for this study were a proxy for hydrocarbon combustion (*n*-decane, $C_{10}H_{22}$), and a proxy for biomass burning (eugenol, $C_{10}H_{12}O_2$). Eugenol is used as a proxy for the combustion of lignin, which constitutes 20 % of pine wood [*Fitzpatrick et al.*, 2008]. Lignin has previously been shown to contribute to soot production in biomass burning, alongside cellulose [*Fitzpatrick et al.*, 2008; *Wilson et al.*, 2013]. Consequently, soot from eugenol is similar in composition to that from pine combustion [*Baeza-Romero et al.*, 2010]. We used the same methods to produce soot from *n*-decane and eugenol, a wick diffusion burner in filtered air, as described in previous studies where the soot was characterized by mass spectrometry [*Baeza-Romero et al.*, 2010; *Wilson et al.*, 2013] (the methodology is described in detail in supplementary S1). For our experiments, soot was collected on glass slides at the top of a glass chimney and both fuels led to soot spherules with the classic fractal soot morphology (see TEM images, Figure 1). Whilst they are morphologically similar, the soot from these fuels differ in several ways. For example, soot from eugenol contains larger oxygenated polyaromatic hydrocarbons (PAHs), has a greater oxygen content and has a lower elemental carbon:total carbon ratio than soot from *n*-decane [*Fitzpatrick et al.*, 2008; *Baeza-Romero et al.*, 2010]. Hence, we produced two contrasting examples of soot, both of which are thought to be relevant for the atmosphere.

Water suspensions of soot were prepared at 10^{-3} wt%. This is a lower mass ratio compared to similar microlitre experiments performed on mineral dusts, and was selected to avoid significant aggregation of the soot, since this would lead to poor dispersion in suspension, and introduce additional uncertainties into the ice nucleation measurements. Laser diffraction was used to evaluate the particle size distributions and aggregation, the results of which are shown in the supplementary information. At 10^{-1} wt%, about 50 % of the soot surface area is associated with

particles >1 μm in diameter, compared with 0 - 20 % of the surface area at the concentrations used in this study. For even more hydrophobic soots, such as acetylene burner soot, it was not possible to produce suspensions. Microlitre droplets of these suspensions were cooled down to test their ice-nucleating efficiency following the method presented in *Whale et al.*, [2014]. Here, the active site density is used [*Connolly et al.*, 2009], which is a singular time-independent description of ice nucleation, and is calculated as:

$$\frac{n(T)}{N} = 1 - \exp(-n_s(T)A) \quad (1)$$

where $n(T)$ is the number of droplets frozen at temperature T, N is the total number of droplets in the experiment and A is the surface area of BC particles per droplet. The size distribution of BC particles in the suspensions was measured using laser diffraction, which also demonstrated that the BC particles were not significantly aggregated. For one batch of soot, the Brunauer–Emmett–Teller (BET) specific surface area was also measured. For eugenol, the specific surface area was 49.43 ± 0.89 m^2/g, whilst for *n*-decane soot it was 65.47 ± 0.81 m^2/g. The surface areas measured using laser diffraction and BET were similar, and therefore gave similar values of $n_s(T)$.

The resulting fraction of droplets frozen as a function of temperature are shown in Figure 2a for experiments with and without soot in the droplets. In all the experiments conducted, we did not measure any significant increase in ice nucleation activity above the handling blanks when soot particles were present. In these experiments, the handling blanks did not freeze at the homogeneous limit, but instead froze heterogeneously. This is caused by the contact between the water and the hydrophobic glass slides, or by trace contaminants. The handling blanks were MilliQ water samples run alongside the soot suspensions, reproducing every process, including sonication and stirring, that the soot suspensions were exposed to. These handling blanks froze over a broader range than standard MilliQ blanks, and included freezing at warmer temperatures caused by the introduction of impurities.

Given that there is no significant difference in freezing temperatures between the soot samples and handling blanks, it is not possible to ascribe the freezing temperatures measured to the influence of soot alone; instead, the freezing could either be entirely unrelated to the soot or a convolution of the soot and other contaminants acting as INPs. These results are similar to the observations of *Schill et al.* [2016] and *Ullrich et al.* [2017], where no significant ice nucleation ability of BC was observed. However, whilst no significant activity of these soots has been measured, they do define a limiting freezing efficiency which we can use to draw conclusions about the potential of BC to contribute to the population of atmospheric INP.

From our fraction frozen results, we can estimate the upper limit of the density of active ice-nucleating sites for our soot samples (see Figure 2b). This is done using equation (1) and a simple parameterization of this upper limit is given in the figure caption. The upper limit defined here (NEW-UPL) gives smaller values of the upper limits of n_s than previously reported by *Ullrich et al.*, [2017], but similar to that defined by *Schill et al.*, [2016]. All three of the recent upper limit parameterizations (this study, *Ullrich et al.*, [2017] and *Schill et al.*, [2016]) are at least three orders of magnitude smaller than the old parameterization defined by *Murray et al.* [2012] on the basis of literature data from *DeMott* [1990] and *Diehl and Mitra* [1998]. *DeMott* [1990] used an expansion chamber to study the ice-nucleating ability of soots generated by a acetylene burner whereas *Diehl and Mitra* [1998] froze droplets containing soot particles from kerosene-burner exhaust by injecting them into a wind tunnel at various temperatures.

Given the discrepancy in the observed values of n_s from different studies (Figure 2b), one cannot readily conclude what the typical ice-nucleating activity of BC particles is in the atmosphere. These observed differences in BC n_s could be due to structural differences in various types of BC from different fuels or be related to processes affecting the BC ice-nucleating ability such as other materials being adsorbed to the soot during production, such as organic carbon species / PAHs or

during atmospheric ageing. Therefore, soot particles might have different ice-nucleating abilities depending on their properties and sources, so assuming a single distribution of n_s values at all times and locations might misrepresent its ability as an INP in the atmosphere. However, an exploratory study of its atmospheric potential as INP can be done by comparing its potential contribution to global INP concentrations with that of other well-characterized INP species.

3. Modelling the contribution of BC to the global atmospheric burden on INP

To estimate the possible contribution of BC particles to the global distribution of INP, we use the global aerosol model GLOMAP-mode, as used in *Vergara-Temprado et al.*, [2017] (hereafter VT17). We estimate the concentrations in the atmosphere of two well-known ice-nucleating aerosol species, K-feldspar [*Atkinson et al.*, 2013] and marine organic aerosols [*Wilson et al.*, 2015] and compare these to the predicted contribution of BC INP. We can consider that for any aerosol species to be relevant in the atmosphere as an INP, it will have to produce similar or greater concentrations to the simulated INP concentrations of K-feldspar and marine organics (Figure 3). Below these concentrations, it is unlikely to be an important INP globally, however, higher concentrations would only indicate that this is more important than the two species modelled (in some locations other INP types may also be important). In our model, BC is emitted from wildfires that vary seasonally [*Van der Werf et al.*, 2003], fossil fuel, and biofuel emissions as described in *Mann et al.*, [2010]. The annual-mean fluxes are defined by *Bond*, [2004]. BC is emitted internally-mixed with organic carbon into the insoluble Aitken mode and then it is moved to the soluble modes by atmospheric ageing. The transport, mixing and scavenging of BC particles is driven by the meteorology of the year 2001 as used in VT17. A more detailed description of the model and its evaluation against atmospheric BC measurements is given in the supplementary information (see S2).

With the BC concentrations simulated, we can calculate the BC INP concentration for a given $n_s(T)$ following the method shown in VT17. As the reported values of n_s range by several orders of magnitude, we define two limiting parameterizations, one using the upper limit presented in this study (NEW-UPL) and another using the

maximum observed values reported in literature data corresponding to the parameterization shown in *Murray et al.* [2012] (OLD) (Figure 2), which was based on data from *DeMott* [1990] and *Diehl and Mitra* [1998].

The INP distribution at the Earth's surface is shown at an activation temperature of -25 ^{o}C (i.e. $[INP]_{-25}$; where square brackets indicate concentration); that is, the number of particles that would nucleate ice if exposed to this temperature in a mixed-phase cloud (Figure 3). These surface-level plots are useful for assessing the distribution and make-up of the INP population around the globe, but they do not tell us where INPs can nucleate ice and influence clouds. To show this, we calculated the INP concentration throughout the atmosphere using local ambient temperatures and particle concentrations. The annual mean $[INP]_{ambient}$ plotted in Figure 4 was calculated by averaging the daily $[INP]_{ambient}$ values as the daily variations in temperature can substantially affect the simulated mean concentrations. At temperatures below the minimum temperature limit of each parameterization, we use the value of n_s for the lowest experimental temperature reported to avoid extrapolating the parameterizations.

In both the $[INP]_{-25}$ (Figure 3) and $[INP]_{ambient}$ plots (Figure 4), when the NEW-UPL n_s values are used the concentrations of INP from BC are several orders of magnitude smaller than simulated assuming K-feldspar and marine organic aerosols, which suggests that BC is unlikely to play an influential role as an ice-nucleating particle on global and regional scales if the soot we generated is representative of atmospheric BC. However, when the OLD parameterization for n_s is used, BC completely dominates the global INP distribution both for $[INP]_{ambient}$ and $[INP]_{-25}$.

Given this large difference, we estimate the n_s values required for BC to be an important INP type given present-day BC emissions by calculating the percentage of surface gridboxes that would be dominated by BC particles if they were to have a particular n_s value (Figure 5). This is done by calculating BC [INP] from the simulated surface area distribution of BC for a range of n_s values (from 10^{-5} to 10^{9} cm^{-2}). We then calculate at each temperature the fraction of surface grid-boxes in

our model where the BC [INP] exceeds INP concentrations simulated by VT17, weighting each grid-box by the geographic surface area that it represents. This approach helps us to place the other literature data for ice nucleation by BC in context and will similarly help place any future measurements of the ice nucleation ability of BC in context. The OLD parameterization falls in the range of values where BC would dominate the surface INP concentrations by orders of magnitude and the NEW-UPL produces values that are orders of magnitude lower than the minimum required to influence surface concentrations. Previously reported upper limits are also lower than the required n_s values necessary to influence surface concentrations.

We then test the realism of the OLD and NEW-UPL parameterizations against ambient INP observations by evaluating the simulated INP concentrations against two contrasting atmospheric INP datasets, one based on remote marine locations in the Southern Ocean [*Bigg*, 1973] and another in a relatively higher BC loaded environment from several places in China [*Yin et al.*, 2012] (Figure 6a and 6b). When the NEW-UPL is used, BC alone cannot explain the observed INP concentrations and under-represents the atmospheric concentrations by more than an order of magnitude, suggesting that other species are responsible for producing these INP concentrations. On the other hand, when the OLD parameterization is used, the measured concentrations in both environments are overestimated by more than two orders of magnitude, suggesting that, if we consider all atmospheric BC particles to act with this efficiency in the atmosphere, we will likely overestimate their influence as INPs. This conclusion is in agreement with many field observations, which suggest that mineral dust is the dominant aerosol found in ice crystals residues [*Pratt et al.*, 2009; *Kamphus et al.*, 2010; *Baustian et al.*, 2012; *Schmidt et al.*, 2017] although others did show that BC aerosols might contribute to the observed INP concentration [*Cozic et al.*, 2008; *Mccluskey et al.*, 2014]. K-feldspar and marine organic aerosols can explain these atmospheric concentrations within an order of magnitude, as shown previously in *Vergara-Temprado et al.* [2017]. Hence, we conclude that the OLD parameterization is probably unrealistic and that it is not possible that all atmospheric BC has such a high ice-nucleating efficiency. This conclusion has important implications for modelling studies that have previously

treated BC as INP in the immersion mode [*Philips et al.*, 2007; *Hoose et al.*, 2010a, 2010b; *Fan et al.*, 2012; *Yun and Penner*, 2012; *Wang et al.*, 2014; *Savre and Ekman*, 2015]. However, we cannot completely dismiss the potential influence that BC produced from different fuels, or exposed to different conditions, might have on INPs regionally, or during exceptional events such as large biomass burning events.

4. Conclusions

Our modelling estimates suggest that if all BC particles in the atmosphere behave as reported in this study, and by several other recent studies [*Schill et al.*, 2016; *Ullrich et al.*, 2017], BC is unlikely to play a substantial atmospheric role as ice-nucleating particles through the immersion mode. We also conclude that a representation of BC INPs from *Murray et al.* [2012], which was based on the studies of *DeMott*, [1990] and *Diehl and Mitra*, [1998], results in an overestimation of surface-level concentrations of INPs in remote and polluted environments by more than two orders of magnitude compared to observations.

The question of whether the ice-nucleating ability of these studied BC particles is representative of the ice-nucleating ability of atmospheric BC particles globally at all times remains open, since the discrepancies between various studies cannot be currently explained. Furthermore, we cannot rule out that atmospheric BC particles could be affected by processes enhancing their ice-nucleating ability to levels that could make them relevant regionally or sporadically. Hence, we suggest that more studies to clarify the sources of discrepancies in the laboratory datasets are necessary to either quantify the effect of BC as INPs in the atmosphere or rule out its relevance completely. Specifically, experiments with contemporary techniques where special attention is paid to characterizing and controlling impurities need to be done with the specific BC types used in previous studies where soot was found to be an effective ice-nucleating material. Nevertheless, we recommend that the old parameterisations, such the reported in *Murray et al.* [2012], should not be used to describe the ice-nucleating ability of all soot in the atmosphere. Overall, the available evidence suggests that BC is at most, of second-order importance when

compared to other ice-nucleating aerosol types such as mineral dust or marine organics.

Acknowledgments, Samples, and Data

This study has been funded by the European Union' Seventh Framework Programme (FP7/2007-797 2013) under grant agreement no. 603445 (BACCHUS), the European Research Council (ERC, 240449 ICE and 648661 MarineIce) and the Engineering and Physical Sciences Research Council (EPSRC, EP/M003027/1). The global model simulations were performed on the ARCHER UK National Supercomputing Service. Ken S. Carslaw is a Royal Society Wolfson Merit Award holder. Nsikanabasi Umo acknowledges funding from the Niger Delta Development Commission (NDDC) in Nigeria (NDDC/DEHSS/ 2010PGFS/AK/011) and the Alexander von Humboldt Foundation, Germany (1188375). All the data used in this manuscript can be accessed by contacting the authors.

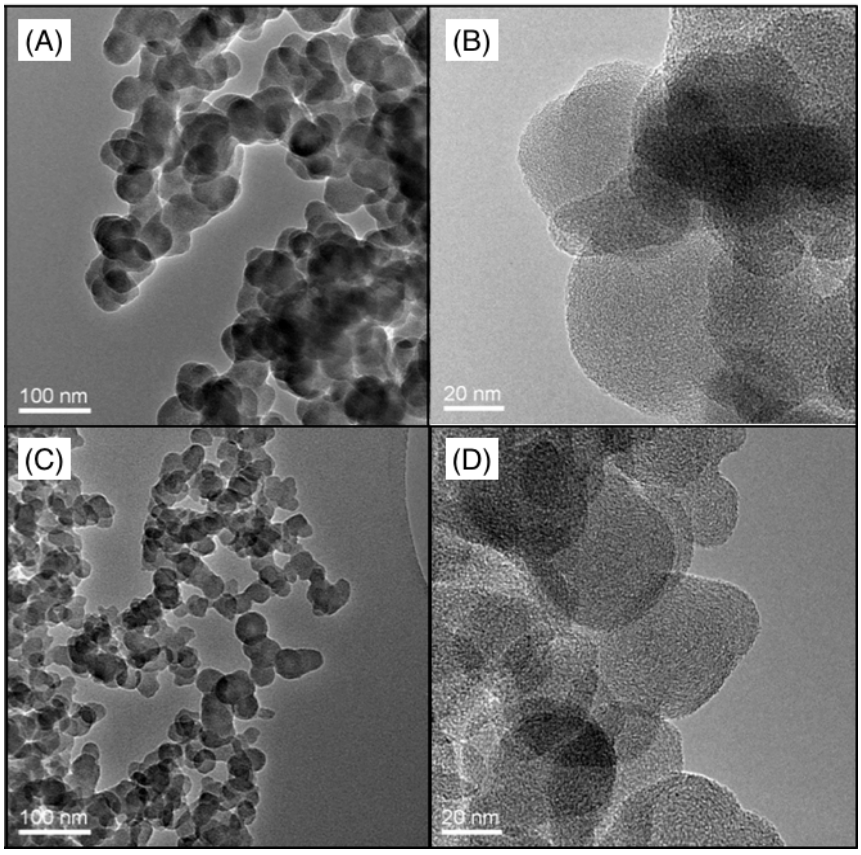

Figure 1 Transmission Electron Microscopy (TEM) images of eugenol and *n*-decane soot that were generated in the laboratory for this study. Eugenol soot images are shown on the top plates [(A) and (B)] while the plates below [(C) and (D)] are *n*-decane soot images. The magnification of each image is labelled at the bottom left hand corner of the image.

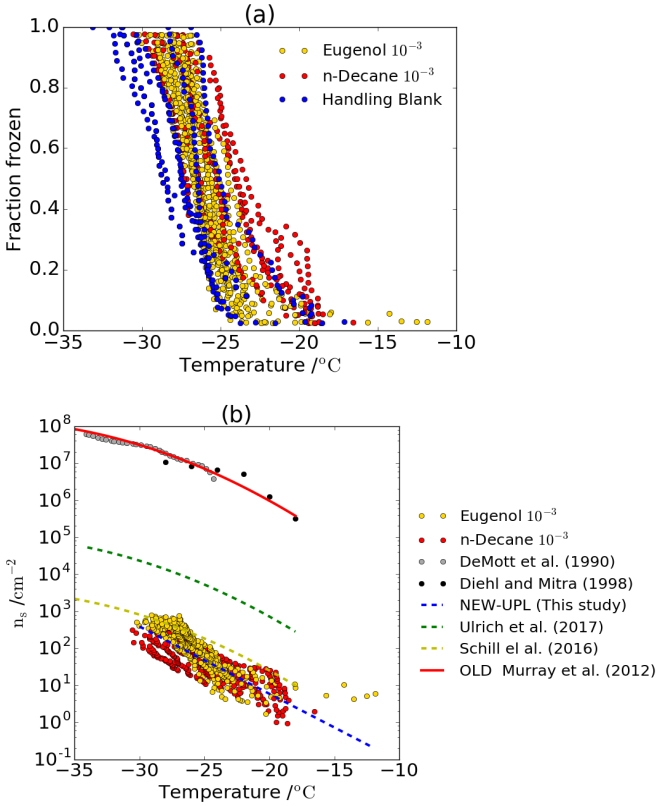

Figure 2 (a) Fraction frozen curves of our experiments for the two different BC generated from eugenol and *n*-decane with the baseline of our experiments defined by the representative handling blanks (blue). (b) Upper limit of density of active sites that the studied BC particles can have. Other parameterizations from the literature are shown for comparison. The upper limit is parameterized with the following equation: $\boldsymbol{n_s\ (cm^{-2}) = exp(-6.608 - 0.419 \cdot T(\ ^oC))}$ valid in the temperature range -30ºC to -12ºC.

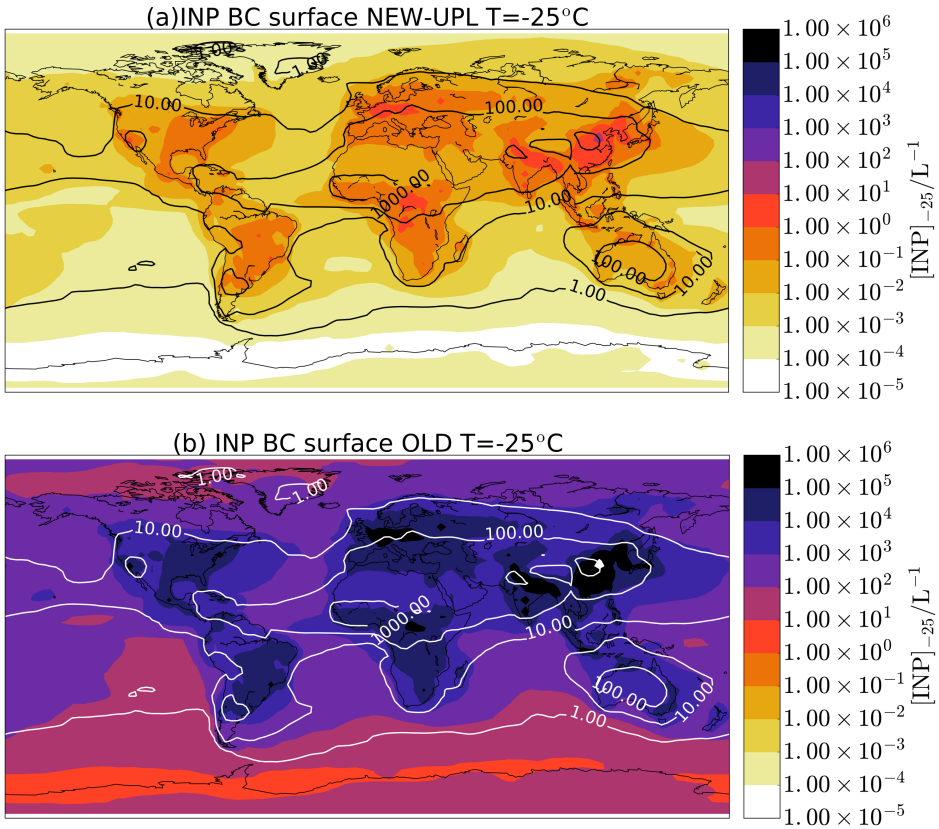

Figure 3 Ice-nucleating particles concentrations from BC particles and the simulated concentrations in VT17 (using feldspar and marine organic aerosols). The contour lines show $[INP]_{-25}$ from VT17 and the colour maps show the same values simulated when using BC INP calculated with (a) NEW-UPL and (b) OLD.

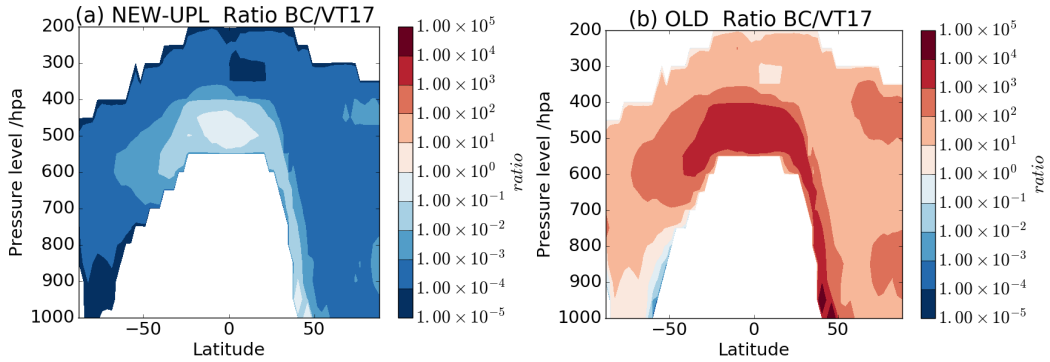

Figure 4 Zonal mean profiles of the ratio between the number of BC ice-nucleating particles at local ambient temperature ($[INP]_{ambient}$) and the concentrations as simulated in VT17 for marine organics and K-feldspar. (a) Using NEW-UPL for calculating BC $[INP]_{ambient}$ and (b) using OLD.

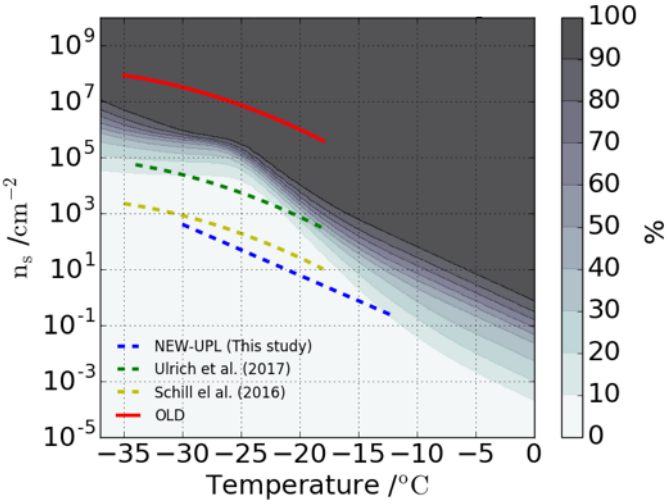

Figure 5 Percentage of the globe surface area that would be dominated by BC particles at each temperature as a function of BC n_s, when compared with the sum of INP produced from marine organics and K-feldspar (from VT17).

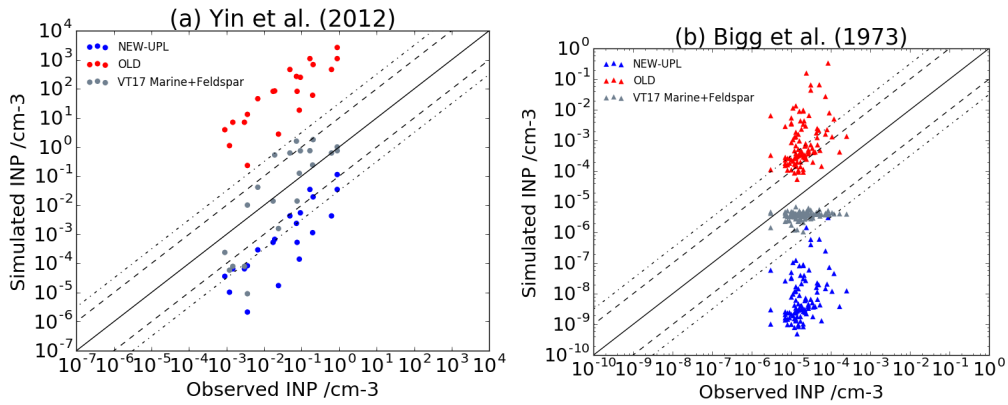

Figure 6 (a) Comparison between the simulated values of BC INPs when using NEW-UPL and OLD parameterization, and observed INP concentrations from different places in China [*Yin et al.*, 2012] (b) Same as (a) but for the Southern Ocean [*Bigg*, 1973]. The comparison with the sum of marine organics and K-feldspar (from VT17) is also shown for comparison in both panels.

References:

Atiku, F. A., E. J. S. Mitchell, A. R. Lea-Langton, J. M. Jones, A. Williams, and K. D. Bartle (2016), The Impact of Fuel Properties on the Composition of Soot Produced by the Combustion of Residential Solid Fuels in a Domestic Stove, *Fuel Process. Technol.*, *151*, 117–125, doi:10.1016/j.fuproc.2016.05.032.

Atkinson, J. D., B. J. Murray, M. T. Woodhouse, T. F. Whale, K. J. Baustian, K. S. Carslaw, S. Dobbie, D. O'Sullivan, and T. L. Malkin (2013), The importance of feldspar for ice nucleation by mineral dust in mixed-phase clouds., *Nature*, *498*(7454), 355–8, doi:10.1038/nature12278.

Baeza-Romero, M. T., J. M. Wilson, E. M. Fitzpatrick, J. M. Jones, and A. Williams (2010), In Situ Study of Soot from the Combustion of a Biomass Pyrolysis Intermediate—Eugenol—and n-Decane Using Aerosol Time of Flight Mass Spectrometry, *Energy & Fuels*, *24*(1), 439–445, doi:10.1021/ef9008746.

Baustian, K. J., D. J. Cziczo, M. E. Wise, K. A. Pratt, G. Kulkarni, A. G. Hallar, and M. A. Tolbert (2012), Importance of aerosol composition, mixing state, and morphology for heterogeneous ice nucleation: A combined field and laboratory approach, *J. Geophys. Res. Atmos.*, *117*(D6), n/a-n/a, doi:10.1029/2011JD016784.

Bigg, E. K. (1973), Ice Nucleus Concentrations in Remote Areas, *J. Atmos. Sci.*, *30*(6), 1153–1157, doi:10.1175/1520-0469(1973)030<1153:INCIRA>2.0.CO;2.

Bond, T. C. (2004), A technology-based global inventory of black and organic carbon emissions from combustion, *J. Geophys. Res.*, *109*(D14), D14203, doi:10.1029/2003JD003697.

Bond, T. C. et al. (2013), Bounding the role of black carbon in the climate system: A scientific assessment, *J. Geophys. Res. Atmos.*, *118*(11), 5380–5552, doi:10.1002/jgrd.50171.

Brooks, S. D., K. Suter, and L. Olivarez (2014), Effects of chemical aging on the ice nucleation activity of soot and polycyclic aromatic hydrocarbon aerosols, *J. Phys. Chem. A*, *118*(43), 10036–10047, doi:10.1021/jp508809y.

Connolly, P. J., O. Möhler, P. R. Field, H. Saathoff, R. Burgess, T. Choularton, and M. Gallagher (2009), Studies of heterogeneous freezing by three different desert dust samples, *Atmos. Chem. Phys.*, *9*(8), 2805–2824, doi:10.5194/acp-9-2805-2009.

Cozic, J., S. Mertes, B. Verheggen, D. J. Cziczo, S. J. Gallavardin, S. Walter, U. Baltensperger, and E. Weingartner (2008), Black carbon enrichment in atmospheric ice particle residuals observed in lower tropospheric mixed phase

clouds, *J. Geophys. Res. Atmos.*, *113*(15), 1–11, doi:10.1029/2007JD009266.

DeMott, P. J. (1990), An Exploratory Study of Ice Nucleation by Soot Aerosols, *J. Appl. Meteorol.*, *29*, 1072–1079, doi:10.1175/1520-0450(1990)029<1072:AESOIN>2.0.CO;2.

Diehl, K., and S. K. Mitra (1998), A laboratory study of the effects of a kerosene-burner exhaust on ice nucleation and the evaporation rate of ice crystals, *Atmos. Environ.*, *32*(18), 3145–3151, doi:10.1016/S1352-2310(97)00467-6.

Fan, S. M., J. P. Schwarz, J. Liu, D. W. Fahey, P. Ginoux, L. W. Horowitz, H. Levy, Y. Ming, and J. R. Spackman (2012), Inferring ice formation processes from global-scale black carbon profiles observed in the remote atmosphere and model simulations, *J. Geophys. Res. Atmos.*, *117*(23), 1–12, doi:10.1029/2012JD018126.

Fitzpatrick, E. M., J.A Jones, M. Pourkashanian, A.B. Ross, A. Williams, and K. D. Bartle (2008), Mechanistic Aspects of Soot Formation from the Combustion of Pine Wood, *Energy & Fuels*, *22*(6), 3771–3778, doi:10.1021/ef800456k.

Gorbunov, B., A. Baklanov, N. Kakutkina, H. Windsor, and R. Toumi (2001), Ice nucleation on soot particles, *J. Aerosol Sci.*, *32*(2), 199–215, doi:10.1016/S0021-8502(00)00077-X.

Hoose, C., and O. Möhler (2012), Heterogeneous ice nucleation on atmospheric aerosols: A review of results from laboratory experiments, *Atmos. Chem. Phys.*, *12*(20), 9817–9854, doi:10.5194/acp-12-9817-2012.

Hoose, C., J. E. Kristjánsson, J.-P. Chen, and A. Hazra (2010a), A Classical-Theory-Based Parameterization of Heterogeneous Ice Nucleation by Mineral Dust, Soot, and Biological Particles in a Global Climate Model, *J. Atmos. Sci.*, *67*(8), 2483–2503, doi:10.1175/2010JAS3425.1.

Hoose, C., J. E. Kristjánsson, and S. M. Burrows (2010b), How important is biological ice nucleation in clouds on a global scale?, *Environ. Res. Lett.*, *5*(2), 24009, doi:10.1088/1748-9326/5/2/024009.

Kamphus, M., M. Ettner-Mahl, T. Klimach, F. Drewnick, L. Keller, D. J. Cziczo, S. Mertes, S. Borrmann, and J. Curtius (2010), Chemical composition of ambient aerosol, ice residues and cloud droplet residues in mixed-phase clouds: Single particle analysis during the cloud and aerosol characterization experiment (CLACE 6), *Atmos. Chem. Phys.*, *10*(16), 8077–8095, doi:10.5194/acp-10-8077-2010.

Kanji, Z. A., P. J. DeMott, O. Möhler, and J. P. D. Abbatt (2011), Results from the University of Toronto continuous flow diffusion chamber at ICIS 2007: instrument intercomparison and ice onsets for different aerosol types, *Atmos. Chem. Phys.*, *11*(1), 31–41, doi:10.5194/acp-11-31-2011.

Koehler, K. A., P. J. DeMott, S. M. Kreidenweis, O. B. Popovicheva, M. D. Petters, C. M. Carrico, E. D. Kireeva, T. D. Khokhlova, and N. K. Shonija (2009), Cloud condensation nuclei and ice nucleation activity of hydrophobic and hydrophilic soot particles, *Phys. Chem. Chem. Phys.*, 7906, doi:10.1039/b905334b.

Kupiszewski, P. et al. (2016), Ice residual properties in mixed-phase clouds at the high-alpine Jungfraujoch site, *J. Geophys. Res. Atmos.*, *121*(20), 12,343-12,362, doi:10.1002/2016JD024894.

Lee, Y. H. et al. (2013), Evaluation of preindustrial to present-day black carbon and its albedo forcing from Atmospheric Chemistry and Climate Model Intercomparison Project (ACCMIP), *Atmos. Chem. Phys.*, *13*(5), 2607–2634, doi:10.5194/acp-13-2607-2013.

Lohmann, U. (2002), A glaciation indirect aerosol effect caused by soot aerosols, *Geophys. Res. Lett.*, *29*(4), 1052, doi:10.1029/2001GL014357.

Lohmann, U. (2017), Anthropogenic Aerosol Influences on Mixed-Phase Clouds, *Curr. Clim. Chang. Reports*, doi:10.1007/s40641-017-0059-9.

Mann, G. W., K. S. Carslaw, D. V. Spracklen, D. a. Ridley, P. T. Manktelow, M. P. Chipperfield, S. J. Pickering, and C. E. Johnson (2010), Description and evaluation of GLOMAP-mode: a modal global aerosol microphysics model for the UKCA composition-climate model, *Geosci. Model Dev.*, *3*(2), 519–551, doi:10.5194/gmd-3-519-2010.

Mccluskey, C. S., P. J. Demott, A. J. Prenni, E. J. T. Levin, G. R. Mcmeeking, A. P. Sullivan, T. C. J. Hill, S. Nakao, C. M. Carrico, and S. M. Kreidenweis (2014), Characteristics of atmospheric ice nucleating particles associated with biomass burning in the US: Prescribed burns and wildfire, *J. Geophys. Res. Atmos.*, 458–470, doi:10.1002/2014JD021980

Möhler, O. (2005), Effect of sulfuric acid coating on heterogeneous ice nucleation by soot aerosol particles, *J. Geophys. Res.*, *110*(D11), D11210, doi:10.1029/2004JD005169.

Murray, B. J., D. O'Sullivan, J. D. Atkinson, and M. E. Webb (2012), Ice nucleation by particles immersed in supercooled cloud droplets, *Chem. Soc. Rev.*, *41*(19), 6519, doi:10.1039/c2cs35200a.

Philips, V. T. J., L. J. Donner, and S. T. Garner (2007), Nucleation Processes in Deep Convection Simulated by a Cloud-System-Resolving Model with Double-Moment Bulk Microphysics, *J. Atmos. Sci.*, *64*, 738–761, doi:10.1175/JAS3869.1.

Popovicheva, O., E. Kireeva, N. Persiantseva, T. Khokhlova, N. Shonija, V. Tishkova, and B. Demirdjian (2008), Effect of soot on immersion freezing of

water and possible atmospheric implications, *Atmos. Res.*, *90*(2–4), 326–337, doi:10.1016/j.atmosres.2008.08.004.

Pratt, K. a., P. J. DeMott, J. R. French, Z. Wang, D. L. Westphal, A. J. Heymsfield, C. H. Twohy, A. J. Prenni, and K. a. Prather (2009), In situ detection of biological particles in cloud ice-crystals, *Nat. Geosci.*, *2*(6), 398–401, doi:10.1038/ngeo521.

Savre, J., and A M. L. Ekman (2015), A theory-based parameterization for heterogeneous ice nucleation and implications for the simulation of ice processes in atmospheric models, *J. Geophys. Res. Atmos.*, *120*(10), 4937–4961, doi:10.1002/2014JD023000.

Schill, G. P. et al. (2016), Ice nucleating particle emissions from photochemically-aged diesel and biodiesel exhaust, *Geophys. Res. Lett.*, 1–8, doi:10.1002/2016GL069529.

Schmidt, S., J. Schneider, T. Klimach, S. Mertes, L. P. Schenk, P. Kupiszewski, J. Curtius, and S. Borrmann (2017), Online single particle analysis of ice particle residuals from mountain-top mixed-phase clouds using laboratory derived particle type assignment, *Atmos. Chem. Phys.*, *17*(1), 575–594, doi:10.5194/acp-17-575-2017.

Spracklen, D. V., K. S. Carslaw, U. Pöschl, A. Rap, and P. M. Forster (2011), Global cloud condensation nuclei influenced by carbonaceous combustion aerosol, *Atmos. Chem. Phys.*, *11*(17), 9067–9087, doi:10.5194/acp-11-9067-2011.

Twohy, C. H. et al. (2010), Relationships of Biomass-Burning Aerosols to Ice in Orographic Wave Clouds, *J. Atmos. Sci.*, *67*(8), 2437–2450, doi:10.1175/2010JAS3310.1.

Ullrich, R., C. Hoose, O. Möhler, M. Niemand, R. Wagner, K. Höhler, N. Hiranuma, H. Saathoff, and T. Leisner (2017), A New Ice Nucleation Active Site Parameterization for Desert Dust and Soot, *J. Atmos. Sci.*, *74*(3), 699–717, doi:10.1175/JAS-D-16-0074.1.

Vergara-Temprado, J. et al. (2017), Contribution of feldspar and marine organic aerosols to global ice nucleating particle concentrations, *Atmos. Chem. Phys.*, *17*(5), 3637–3658, doi:10.5194/acp-17-3637-2017.

Wang, Y., X. Liu, C. Hoose, and B. Wang (2014), Different contact angle distributions for heterogeneous ice nucleation in the Community Atmospheric Model version 5, *Atmos. Chem. Phys.*, *14*(19), 10411–10430, doi:10.5194/acp-14-10411-2014.

Van der Werf, G. R., J. T. Randerson, G. J. Collatz, and L. Giglio (2003), Carbon emissions from fires in tropical and subtropical ecosystems, *Glob. Chang.*

Biol., *9*(4), 547–562, doi:10.1046/j.1365-2486.2003.00604.x.

Whale, T. F., B. J. Murray, D. O'Sullivan, N. S. Umo, K. J. Baustian, J. D. Atkinson, and G. J. Morris (2014), A technique for quantifying heterogeneous ice nucleation in microlitre supercooled water droplets, *Atmos. Meas. Tech. Discuss.*, *7*(9), 9509–9536, doi:10.5194/amtd-7-9509-2014.

Wilson, J. M., M. T. Baeza-Romero, J. M. Jones, M. Pourkashanian, A. Williams, A. R. Lea-Langton, A. B. Ross, and K. D. Bartle (2013), Soot Formation from the Combustion of Biomass Pyrolysis Products and a Hydrocarbon Fuel, n - Decane: An Aerosol Time Of Flight Mass Spectrometer (ATOFMS) Study, *Energy & Fuels*, *27*(3), 1668–1678, doi:10.1021/ef3019386.

Wilson, T. W. et al. (2015), A marine biogenic source of atmospheric ice-nucleating particles, *Nature*, *525*(7568), 234–238, doi:10.1038/nature14986.

Wright, T. P., M. D. Petters, J. D. Hader, T. Morton, and A. L. Holder (2013), Minimal cooling rate dependence of ice nuclei activity in the immersion mode, *J. Geophys. Res. Atmos.*, *118*(18), 10,535-10,543, doi:10.1002/jgrd.50810.

Yin, J., D. Wang, and G. Zhai (2012), An evaluation of ice nuclei characteristics from the long-term measurement data over North China, *Asia-Pacific J. Atmos. Sci.*, *48*(2), 197–204, doi:10.1007/s13143-012-0020-8.

Yun, Y., and J. E. Penner (2012), Global model comparison of heterogeneous ice nucleation parameterizations in mixed phase clouds, *J. Geophys. Res. Atmos.*, *117*(7), 1–23, doi:10.1029/2011JD016506.

Chapter 4 Manuscript "Strong control of Southern Ocean cloud reflectivity by ice-nucleating particles"

Authors: Jesús Vergara-Temprado[1], Annette Miltenberger[1], Kalli Furtado[2], Daniel Grosvenor[1], Ben J. Shipway[2], Adrian A. Hill[2], Jonathan M. Wilkinson[2], Paul R. Field[1,2], Benjamin J. Murray[1] and Ken S. Carslaw[1]

[1] Institute for Climate and Atmospheric science, School of Earth and Environment, University of Leeds, Leeds, LS2 9JT, UK

[2]Met Office, Exeter, UK

Correspondence: Jesús Vergara-Temprado (eejvt@leeds.ac.uk)

Abstract

Large biases in climate model simulations of cloud radiative properties over the Southern Ocean cause large errors in modelled sea-surface temperatures [*Wang et al.*, 2014] and atmospheric circulation [*Hwang and Frierson*, 2013]. Here we combine cloud-resolving model simulations with new estimates of the concentration of ice-nucleating particles in this region to show that our simulated Southern Ocean clouds reflect far more radiation than predicted by global models, in agreement with satellite observations. Specifically, we show that the clouds which are most sensitive to the concentration of ice-nucleating particles are low-level mixed-phase clouds in the cold sectors of extra-tropical cyclones, which have previously been identified as a main contributor to the Southern Ocean radiation bias [*Bodas-Salcedo et al.*, 2014]. The very low ice-nucleating particle concentrations that prevail over the Southern Ocean strongly suppress cloud droplet freezing, reduce precipitation and enhance cloud reflectivity. The results help explain why a strong radiation bias occurs mainly in this remote region away from major sources of ice-nucleating particles. The results present a substantial challenge to climate models to be able to simulate realistic ice-nucleating particle concentrations and their effects under specific meteorological conditions.

1. Main text

Comparisons between climate models and satellite observations over the Southern Ocean (SO) show that models generally simulate "10s" Wm-2 too little reflection of shortwave (SW) radiation [Trenberth and Fasullo, 2010; Bodas-Salcedo et al., 2014]. Excess SW absorption at the surface causes an error of about 2 ^{o}K of warming in the SO annual mean sea surface temperature [Wang et al., 2014]. This error has significant consequences for the ability of models to simulate sea ice, the jet stream and storm track location [Ceppi et al., 2012], and it has been linked to the double-ITCZ problem [Hwang and Frierson, 2013]. Most of the simulated radiative biases are associated with low and mid-level clouds containing supercooled droplets and ice (mixed-phase clouds) [Williams et al., 2013; Bodas-Salcedo et al., 2014] which dominate cloud radiative effects over the SO [Haynes et al., 2011; Bodas-Salcedo et al., 2016a].

Several potential causes of radiative bias over the SO have been explored in global models, such as the representation of aerosols (which act as cloud condensation nuclei and affect droplet concentrations [*McCoy et al.*, 2015b]); issues with the model boundary layer physics[*Bodas-Salcedo et al.*, 2012]; or treatment of the effects of small-scale turbulence in mixed-phase conditions that can enhance the generation of liquid water [*Korolev and Field*, 2008; *Furtado et al.*, 2015], increasing slightly the amount of reflected radiation. It is known that mixed-phase clouds are a source of large uncertainty in climate model simulations, with important consequences for cloud feedbacks and climate sensitivity [*McCoy et al.*, 2015a; *Tan et al.*, 2016]. Examination of mixed-phase cloud properties in high-resolution models show that the reflected SW radiation could be increased by 15% [*Furtado and Field*, 2017] through changes in the sub-grid distributions of relative humidity used for the depositional growth of ice particles and through changes in the riming efficiency of ice crystals. These studies managed to increase the simulated amounts of cloud liquid water, making the clouds more reflective, but the bias problem has not been solved [*Tan and Storelvmo*, 2016].

The introduction of ice in clouds leads to the depletion of supercooled liquid water via several microphysical pathways. Mixtures of supercooled liquid water and ice are thermodynamically unstable due to the lower saturation vapour pressure of ice, which leads to quick ice grow at the expense of the liquid water in what is known as the Wegener-Bergeron-Findeisen process. The larger ice crystals then precipitate while collecting smaller water droplets (riming process) which additionally depletes the liquid in the cloud. These changes in the composition of the cloud strongly affects its radiative properties. The top-of-atmosphere SW flux is therefore affected on a global scale by the concentration of ice-nucleating particles (INPs) [*DeMott et al.*, 2010; *Yun and Penner*, 2012; *Tan et al.*, 2016; *Sagoo and Storelvmo*, 2017]. However, it has not been established whether INPs over the SO are quantitatively consistent with the behaviour and radiative properties of the specific clouds that are known to be associated with the model-observation bias [*Bodas-Salcedo et al.*, 2014].

Here we use new information about INP concentrations and properties combined with a high-resolution numerical weather prediction model with a state-of-the-art double-moment bulk microphysics scheme to explore ice formation and the impact on the radiative properties of cyclonic systems over the SO. The model is convection-permitting and should be able represent the small-scale partitioning between ice and liquid water, which typically occurs over a few kilometres in mid-latitude mixed-phase clouds [*Field et al.*, 2004] and has to be parametrized in low-resolution global models. We therefore reduce the effect of the sub-grid assumptions regarding the ice-water partitioning [*Furtado and Field*, 2017], which is a major cause of uncertainty in global models [*Forbes and Ahlgrimm*, 2014; *Tan and Storelvmo*, 2016].

Figure 1a shows concentrations of INP over the South Atlantic simulated by a global aerosol model [*Vergara-Temprado et al.*, 2017] (VT17). We define the range of possible INP concentrations affecting SO cyclones as the daily variability of the simulated concentrations in a South Atlantic transect (40-70S, 20W) (Figure 1a).

The simulated INP range of 2-3 orders of magnitude agrees well with measurements over marine regions (Figure 1a). Simulated concentrations over the remote SO are several orders of magnitude lower than over continental regions close to dust sources (Figure 1b), which is corroborated by measurements of very low ice concentrations in the SO region [*Grosvenor et al.*, 2012; *Chubb et al.*, 2013]. The SO INP concentrations are also a factor 5-10 lower than over the North Pacific and North Atlantic, which are the other main regions of the planet affected by post-frontal mixed-phase clouds (Figure 1b). We also test several earlier parameterizations of INP. *DeMott et al.*, [2010] (DM10) uses the simulated concentration of aerosols larger than 0.5 μm from all aerosol species apart from sea-salt and *DeMott et al.*, [2015] (DM15) is based on the concentration of dust particles. We also use a commonly used parameterization of INP based on temperature only [*Meyers et al.*, 1992] (M92). Both DM10 and M92 parameterizations have been shown to overestimate measured ambient INP concentrations over remote marine regions, whereas DM15 and the range of values given by the aerosol model (VT17) agree much better with the measurements in similar remote marine environments [*Vergara-Temprado et al.*, 2017].

We simulate three cyclonic cloud systems, each containing extensive regions of stratocumulus and cumulus mixed-phase clouds. The cyclones occurred over the South Atlantic during the austral summer when the largest radiative biases occur [*Bodas-Salcedo et al.*, 2016a]. Two of the cloud systems (cases 1 and 2) have moderately cold cloud tops of around -15 ^{o}C and case 3 was chosen to have a much smaller supercooling, with an average cloud top temperature of around -7^{o}C. The simulations were made using the UK Met Office global Unified Model with a horizontal grid spacing of ~25 km with an embedded ~1000 km domain with a grid-spacing of 0.02^{o}, or about 2.2km (Figure 2e-h), see Methods. An extra set of simulations was performed with a coarser grid-spacing of 7 km for a larger area to test the effects of the ice nucleation scheme on other parts of the cyclone (Figure 2a-c). Within the high-resolution domain cloud microphysics processes are simulated using the Cloud-AeroSol Interactive Microphysics (CASIM) scheme [*Grosvenor et al.*, 2017; *Miltenberger et al.*, 2017] which represents the mass and number concentration of hydrometeors (see Methods). The global model, in common with

most climate models [*McCoy et al.*, 2015a], does not have a representation of INP, but instead calculates cloud glaciation as a function of temperature and has single-moment microphysics [*Wilson and Ballard*, 1999; *Walters et al.*, 2017].

Figures 2 and 3 show that the liquid water path (column-integrated water per unit area) and the reflected SW radiation of the cloud systems are strongly affected by the INP parameterization (Extended Data Figures 1-4 show additional results for cloud-top temperature, cloud droplet concentrations and cloud-top phase). However, changing the representation of INP has very little effect on parts of the cyclone that are already simulated well by the global model, such as the frontal cloud (Figure 2a-d). In cases C1 and C2 with cold cloud-top temperatures the domain-mean SW flux is simulated within -7 to +12% of the observations from the NASA Clouds and the Earth's Radiant Energy System (CERES) [*Kratz et al.*, 2014] satellite instrument (see Methods) when either the VT17 or DM15 parameterisation is used. The range of INP concentrations in VT17 results in a range of simulated SW fluxes that spans the observations (slightly higher (lower) when INP concentrations are assumed to be at the low (high) end of the VT17 range). The same is true for the simulated liquid water path, which is higher than observed with low INP and is about right or slightly low with the highest model-derived INP concentrations. In contrast, M92, which predicts unrealistically high INP concentrations over the SO, simulates SW fluxes that are 28-36% too low and liquid water paths that are a factor 7 too low.

The frequency distribution of reflected SW fluxes improves greatly with the more realistic representations of INP (Figure 3c-e and Extended Data Figure 1). The correlation of the satellite-derived SW distribution with the simulated distribution based on the INP model is 0.8 - 0.92, but is only 0.03 for the global model and 0.03 for the high-resolution model with the M92 parameterization. For cloud systems C1 and C2, the M92 INP parameterisation rarely predicts regions of SW fluxes higher than 400 W m^{-2}, while the model with realistic INP concentrations predicts the peak frequency to occur above this value, in good agreement with the measurements.

The cloud system with warmer cloud tops (case 3) is also poorly simulated by the global model (Figure 3). The low INP parameterisations simulate the frequency distribution of the reflected SW radiation much better than the high INP parameterisations (Figure 3e). However, the absolute liquid water path (Figure 3b) is over-predicted by the low INP parameterisations, which might imply that we are missing a secondary ice production processes [*Field et al.*, 2016] (although switching on and off the Hallet-Mossop process did not affect the simulated cloud significantly).

To determine the relationship between INP concentration and cloud properties in the high-resolution runs, we calculated the domain-median concentrations of in-cloud INPs that were active at local temperatures for each simulation (Figure 4) (see Methods). There is a clear inverse relationship between the mean reflected SW radiative flux and the INP concentration; as also seen in previous studies using global model simulations [*Yun and Penner*, 2012; *Tan and Storelvmo*, 2016; *Sagoo and Storelvmo*, 2017]. We find this relationship to be linear with the logarithm of the INP concentration up to about 0.1 to 1 L^{-1}, above which the reflected SW radiation drops sharply as the ice processes become efficient enough to deplete most of the liquid water. The slope is about 15 W m^{-2} per decade change in INP for the cold cloud cases but about 6 W m^{-2} per decade increase in INP for the warmer cloud.

While adjustments to model microphysical processes lead to changes in cloud reflectance [*Storelvmo et al.*, 2011; *Tan and Storelvmo*, 2016; *Frey and Kay*, 2017; *Furtado and Field*, 2017], such changes are likely to have broadly uniform effects in different global regions. Therefore model tuning will not account for important regional and temporal variations [*McCoy et al.*, 2016] caused by large variations in INP concentrations (Figure 1b). Combining the previously computed sensitivities for the cloud systems simulated with the expected variability in INP concentrations in the SO (~ 4 orders of magnitude, Figure 1b) we estimate that INP could modulate the radiative properties of similar cloud systems by 24 to 60 Wm^{-2}. Globally, the variability in INP concentrations is about 7 orders of magnitude. For similar clouds (and dependent on the incoming SW flux) INP variations could modulate the

radiative properties by between 42 and 105 Wm^{-2}, although increases above $0.1L^{-1}$ could potentially deplete most liquid water affecting strongly its radiative properties. We therefore argue that to accurately represent ice processes in models, cloud glaciation needs to be linked to realistic INP concentrations.

Our results suggest that the low INP concentrations over the remote SO are a major factor in causing mixed-phase clouds to persist in a supercooled state for longer than similar clouds in high INP environments and that this is likely to be an important factor explaining model biases in reflected SW radiation. Effectively, our findings suggest that ice formation processes in global models are causing the SO clouds to behave as if they had higher INP concentrations than in reality. The important role of INP is a complicating factor for climate models, most of which do not currently simulate the microphysical processes required to link INPs to changes in cloud properties in a realistic way. Adjustments to the freezing temperature as a proxy for the proper representation of INP concentrations appears not to have the same effect on cloud properties [*Bodas-Salcedo et al.*, 2016b; *Furtado and Field*, 2017] and can lead to unphysical relations between cloud cover and cloud glaciation temperature [*McCoy et al.*, 2016]. Hence, a representation of cloud microphysical processes that considers the spatial and temporal differences in INP concentrations is crucial to correctly represent mixed-phase clouds in the present climate and the way that they affect past climates [*Sagoo and Storelvmo*, 2017]. Changes in the atmospheric INP concentrations due to natural or human-induced effects on aerosol emissions could also affect climate by modifying the properties of these clouds.

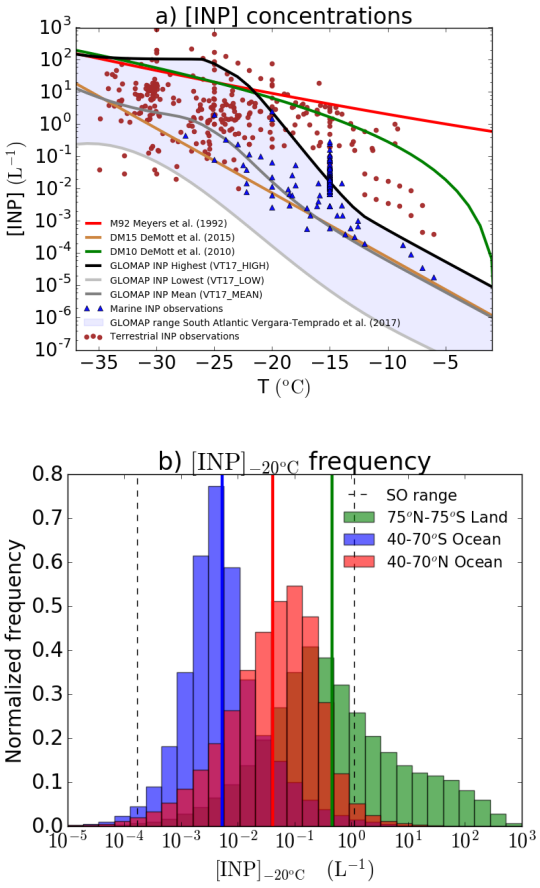

Figure 1. Ice-nucleating particle concentrations. a) Various parameterizations used in our simulations (see legend). The dataset used in Vergara-Temprado et al. (2017) is shown for comparison. The points are divided between marine and terrestrial locations. b) Frequency distribution of daily averaged INP concentrations at an activation temperature of -20ºC for mid-to-high latitudes for ocean regions in the Norther and Southern hemispheres between 850 and 600 hpa. INP concentrations over land (whole globe from 75ºN to 75ºS at the same altitudes) are also shown for comparison. The vertical lines show the median values of the distributions. Note that the INP model is subject to low biases over continental regions [Vergara-Temprado et al., 2017], so the actual values over land are probably higher.

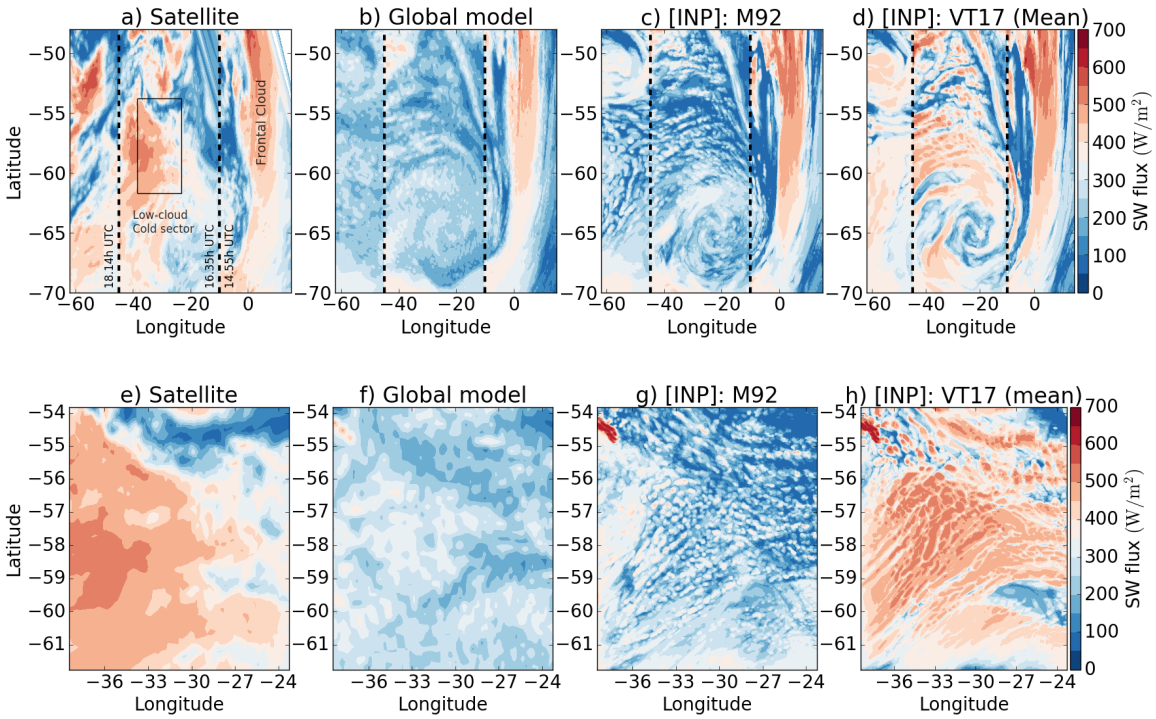

Figure 2. Top-of-atmosphere outgoing shortwave radiation for the observed and simulated cloud. Results show the first cloud system C1 with different representations of INP. Cloud top temperatures are shown in Extended data figure 8. The first row shows the 0.07° grid-spacing simulations of the whole cyclone collocated with the satellite observations (a). The image is divided by two black dashed lines in 3 areas, each corresponding to a different satellite retrieval. A box in drawn in the satellite image to show the position of the 2.2km resolution domains (panels e-h). The first column corresponds to the satellite data (CERES). The second column corresponds shows the output of the global model and the successive columns are for the high-resolution runs using the M92 INP scheme and the mean INP values simulated from VT17. A figure with all the cases studied is given in the supplementary information (Figure S7).

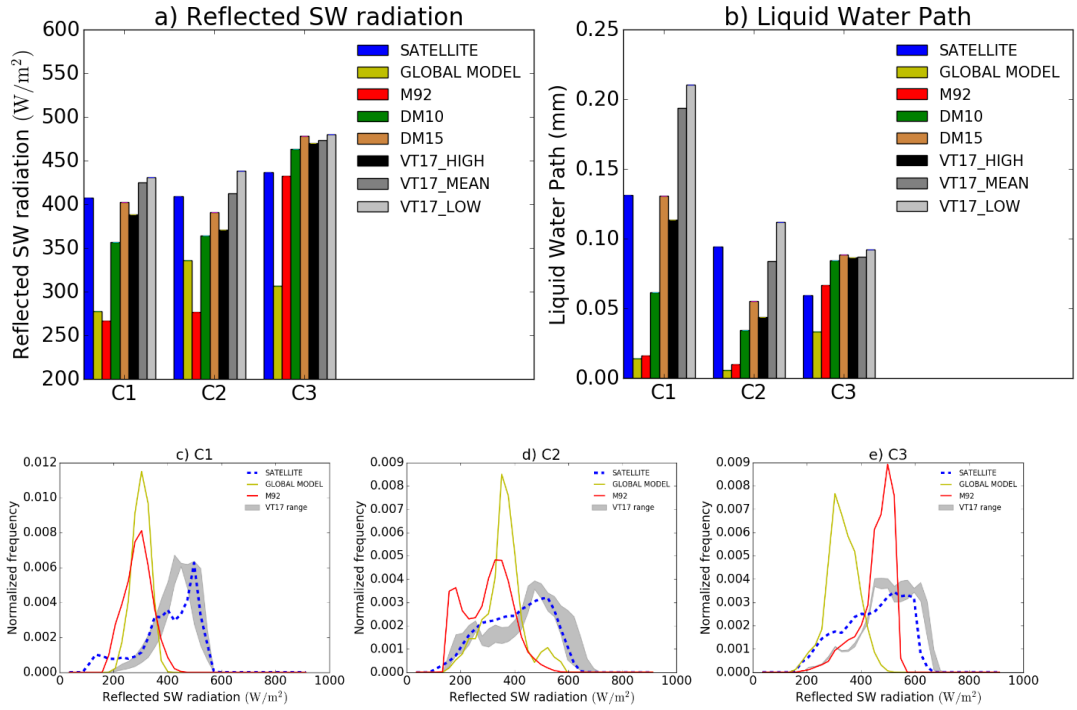

Figure 3 Top-of-atmosphere outgoing shortwave radiation and cloud liquid water path for all studied cloud systems. (a,b) Show the domain mean value of reflected SW radiation (a) and LWP (b). The bottom three panels (d,e,f) show the distribution of low and mid-cloud reflected SW radiation fluxes for the three clouds studied (C1,C2,C3) for the simulations with the global model and the high-resolution simulations with M92 and the VT17 range of INP values. More detailed versions of these plots are given in Extended Data Figure 1). Model grid-boxes with a cloud top temperature less than -35^{o}C and columns with a LWP less than 0.001 mm were removed from the calculations to exclude the effect of high clouds and cloud-free areas.

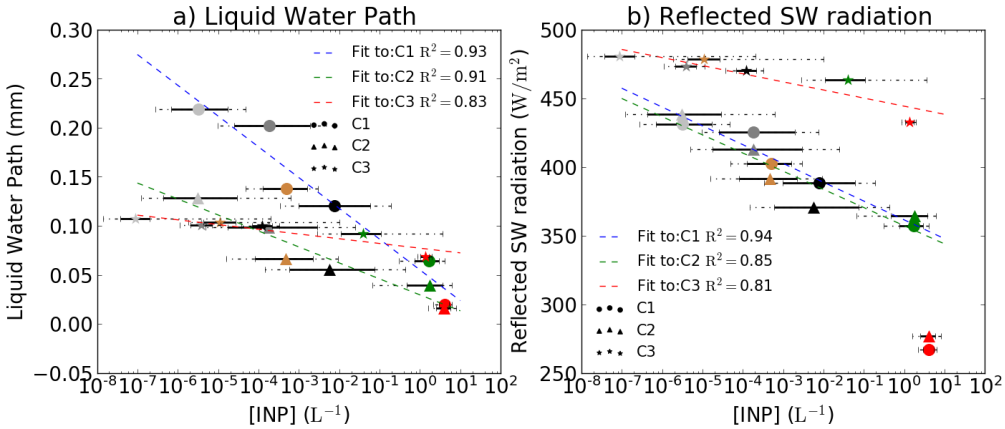

Figure 4. Relationship between cloud properties and ice-nucleating particle concentrations. a) Median modelled in-cloud activated INP versus LWP, (b) INP versus reflected SW flux. The solid-line error bars on the INP axis correspond to the 66% confidence interval of the distribution of in-cloud activated INPs and the dashed line error bars correspond to the 95% interval. The colours of the points correspond to the different INP parameterizations and they follow the legend shown in Figure 3. A linear fit to the data points corresponding to each cloud is also shown with its corresponding coefficient of determination (R2). The linear regime ends for concentrations higher than about 1 to 5 L-1 so, runs with higher values were not included in the linear fit.

References:

Bodas-Salcedo, A., K. D. Williams, P. R. Field, and A. P. Lock (2012), The surface downwelling solar radiation surplus over the Southern Ocean in the met office model: The role of midlatitude cyclone clouds, *J. Clim.*, *25*(21), 7467–7486, doi:10.1175/JCLI-D-11-00702.1.

Bodas-Salcedo, A., K. D. Williams, M. A. Ringer, I. Beau, J. N. S. Cole, J.-L. Dufresne, T. Koshiro, B. Stevens, Z. Wang, and T. Yokohata (2014), Origins of the Solar Radiation Biases over the Southern Ocean in CFMIP2 Models*, *J. Clim.*, *27*(1), 41–56, doi:10.1175/JCLI-D-13-00169.1.

Bodas-Salcedo, A., T. Andrews, A. V. Karmalkar, and M. A. Ringer (2016a), Cloud liquid water path and radiative feedbacks over the Southern Ocean, *Geophys. Res. Lett.*, *43*(20), 10,938-10,946, doi:10.1002/2016GL070770.

Bodas-Salcedo, A., P. G. Hill, K. Furtado, K. D. Williams, P. R. Field, J. C. Manners, P. Hyder, and S. Kato (2016b), Large contribution of supercooled liquid clouds to the solar radiation budget of the Southern Ocean, *J. Clim.*, *29*(11), 4213–4228, doi:10.1175/JCLI-D-15-0564.1.

Ceppi, P., Y. T. Hwang, D. M. W. Frierson, and D. L. Hartmann (2012), Southern Hemisphere jet latitude biases in CMIP5 models linked to shortwave cloud forcing, *Geophys. Res. Lett.*, *39*(19), 1–5, doi:10.1029/2012GL053115.

Chubb, T. H., J. B. Jensen, S. T. Siems, and M. J. Manton (2013), In situ observations of supercooled liquid clouds over the Southern Ocean during the HIAPER Pole-to-Pole Observation campaigns, *Geophys. Res. Lett.*, *40*(19), 5280–5285, doi:10.1002/grl.50986.

DeMott, P. J., a J. Prenni, X. Liu, S. M. Kreidenweis, M. D. Petters, C. H. Twohy, M. S. Richardson, T. Eidhammer, and D. C. Rogers (2010), Predicting global atmospheric ice nuclei distributions and their impacts on climate., *Proc. Natl. Acad. Sci. U. S. A.*, *107*(25), 11217–11222, doi:10.1073/pnas.0910818107.

DeMott, P. J. et al. (2015), Integrating laboratory and field data to quantify the immersion freezing ice nucleation activity of mineral dust particles, *Atmos. Chem. Phys.*, *15*(1), 393–409, doi:10.5194/acp-15-393-2015.

Field, P. R., R. J. Hogan, P. R. A. Brown, A. J. Illingworth, T. W. Choularton, P. H. Kaye, E. Hirst, and R. Greenaway (2004), Simultaneous radar and aircraft observations of mixed-phase cloud at the 100 m scale, *Q. J. R. Meteorol. Soc.*, *130*(600), 1877–1904, doi:10.1256/qj.03.102.

Field, P. R. et al. (2016), Chapter 7. Secondary Ice Production - current state of the science and recommendations for the future, *Meteorol. Monogr.*, AMSMONOGRAPHS-D-16-0014.1, doi:10.1175/AMSMONOGRAPHS-D-

16-0014.1.

Forbes, R. M., and M. Ahlgrimm (2014), On the Representation of High-Latitude Boundary Layer Mixed-Phase Cloud in the ECMWF Global Model, *Mon. Weather Rev.*, *142*(9), 3425–3445, doi:10.1175/MWR-D-13-00325.1.

Frey, W. R., and J. E. Kay (2017), The influence of extratropical cloud phase and amount feedbacks on climate sensitivity, *Clim. Dyn.*, *0*(0), 0, doi:10.1007/s00382-017-3796-5.

Furtado, K., and P. Field (2017), The role of ice-microphysics parametrizations in determining the prevalence of supercooled liquid water in high-resolution simulations of a Southern Ocean midlatitude cyclone, *J. Atmos. Sci.*, JAS-D-16-0165.1, doi:10.1175/JAS-D-16-0165.1.

Furtado, K., P. R. Field, I. A. Boutle, C. J. Morcrette, and J. M. Wilkinson (2015), A Physically-based, Subgrid Parametrization for the Production and Maintenance of Mixed-phase Clouds in a General Circulation Model, *J. Atmos. Sci.*, 150930161939004, doi:10.1175/JAS-D-15-0021.1.

Grosvenor, D. P., T. W. Choularton, T. Lachlan-Cope, M. W. Gallagher, J. Crosier, K. N. Bower, R. S. Ladkin, and J. R. Dorsey (2012), In-situ aircraft observations of ice concentrations within clouds over the Antarctic Peninsula and Larsen Ice Shelf, *Atmos. Chem. Phys.*, *12*(23), 11275–11294, doi:10.5194/acp-12-11275-2012.

Grosvenor, D. P., P. R. Field, A. A. Hill, and B. J. Shipway (2017), The relative importance of macrophysical and cloud albedo changes for aerosol-induced radiative effects in closed-cell stratocumulus: Insight from the modelling of a case study, *Atmos. Chem. Phys.*, *17*(8), 5155–5183, doi:10.5194/acp-17-5155-2017.

Haynes, J. M., C. Jakob, W. B. Rossow, G. Tselioudis, and J. B. Brown (2011), Major characteristics of Southern Ocean cloud regimes and their effects on the energy budget, *J. Clim.*, *24*(19), 5061–5080, doi:10.1175/2011JCLI4052.1.

Hwang, Y.-T., and D. M. W. Frierson (2013), Link between the double-Intertropical Convergence Zone problem and cloud biases over the Southern Ocean., *Proc. Natl. Acad. Sci. U. S. A.*, *110*(13), 4935–40, doi:10.1073/pnas.1213302110.

Korolev, A., and P. R. Field (2008), The Effect of Dynamics on Mixed-Phase Clouds: Theoretical Considerations, *J. Atmos. Sci.*, *65*(1), 66–86, doi:10.1175/2007JAS2355.1.

Kratz, D. P., P. W. Stackhouse, S. K. Gupta, A. C. Wilber, P. Sawaengphokhai, and G. R. McGarragh (2014), The fast longwave and shortwave flux (FLASHFlux) data product: Single-scanner footprint fluxes, *J. Appl. Meteorol. Climatol.*, *53*(4), 1059–1079, doi:10.1175/JAMC-D-13-061.1.

McCoy, D. T., D. L. Hartmann, M. D. Zelinka, P. Ceppi, and D. P. Grosvenor (2015a), Mixed-phase cloud physics and Southern Ocean cloud feedback in climate models, *J. Geophys. Res. Atmos.*, *120*, 9539–9554, doi:10.1002/2015JD023603.Received.

McCoy, D. T., S. M. Burrows, R. Wood, D. P. Grosvenor, S. M. Elliott, P.-L. Ma, P. J. Rasch, and D. L. Hartmann (2015b), Natural aerosols explain seasonal and spatial patterns of Southern Ocean cloud albedo, *Sci. Adv.*, *1*(6), e1500157–e1500157, doi:10.1126/sciadv.1500157.

McCoy, D. T., I. Tan, D. L. Hartmann, M. D. Zelinka, and T. Storelvmo (2016), On the relationships among cloud cover, mixed-phase partitioning, and planetary albedo in GCMs, *J. Adv. Model. Earth Syst.*, *8*(2), 650–668, doi:10.1002/2015MS000589.

Meyers, M. P., P. J. DeMott, and W. R. Cotton (1992), New Primary Ice-Nucleation Parameterizations in an Explicit Cloud Model, *J. Appl. Meteorol.*, *31*(7), 708–721, doi:10.1175/1520-0450(1992)031<0708:NPINPI>2.0.CO;2.

Miltenberger, A. K., P. R. Field, A. A. Hill, P. Rosenberg, B. J. Shipway, J. M. Wilkinson, R. Scovell, and A. M. Blyth (2017), Aerosol-cloud interactions in mixed-phase convective clouds. Part 1: Aerosol perturbations, *Atmos. Chem. Phys. Discuss.*, (September), 1–45, doi:10.5194/acp-2017-788.

Sagoo, N., and T. Storelvmo (2017), Testing the sensitivity of past climates to the indirect effects of dust, *Geophys. Res. Lett.*, *44*(11), 5807–5817, doi:10.1002/2017GL072584.

Storelvmo, T., C. Hoose, and P. Eriksson (2011), Global modeling of mixed-phase clouds: The albedo and lifetime effects of aerosols, *J. Geophys. Res.*, *116*(D5), D05207, doi:10.1029/2010JD014724.

Tan, I., and T. Storelvmo (2016), Sensitivity Study on the Influence of Cloud Microphysical Parameters on Mixed-Phase Cloud Thermodynamic Phase Partitioning in CAM5, *J. Atmos. Sci.*, *73*(2), 709–728, doi:10.1175/JAS-D-15-0152.1.

Tan, I., T. Storelvmo, and M. D. Zelinka (2016), Observational constraints on mixed-phase clouds imply higher climate sensitivity, *Science (80-.).*, *352*(6282), 224–227, doi:10.1126/science.aad5300.

Trenberth, K. E., and J. T. Fasullo (2010), Simulation of Present-Day and Twenty-First-Century Energy Budgets of the Southern Oceans, *J. Clim.*, *23*(2), 440–454, doi:10.1175/2009JCLI3152.1.

Vergara-Temprado, J. et al. (2017), Contribution of feldspar and marine organic aerosols to global ice nucleating particle concentrations, *Atmos. Chem. Phys.*, *17*(5), 3637–3658, doi:10.5194/acp-17-3637-2017.

Walters, D. et al. (2017), The Met Office Unified Model Global Atmosphere 6.0/6.1 and JULES Global Land 6.0/6.1 configurations, *Geosci. Model Dev.*, *10*(4), 1487–1520, doi:10.5194/gmd-10-1487-2017.

Wang, C., L. Zhang, S.-K. Lee, L. Wu, and C. R. Mechoso (2014), A global perspective on CMIP5 climate model biases, *Nat. Clim. Chang.*, *4*(3), 201–205, doi:10.1038/nclimate2118.

Williams, K. D., A. Bodas-Salcedo, M. Déqué, S. Fermepin, B. Medeiros, M. Watanabe, C. Jakob, S. A. Klein, C. A. Senior, and D. L. Williamson (2013), The Transpose-AMIP II Experiment and Its Application to the Understanding of Southern Ocean Cloud Biases in Climate Models, *J. Clim.*, *26*(10), 3258–3274, doi:10.1175/JCLI-D-12-00429.1.

Wilson, D. R., and S. P. Ballard (1999), A microphysically based precipitation scheme for the UK meteorological office unified model, *Q. J. R. Meteorol. Soc.*, *125*(557), 1607–1636, doi:10.1002/qj.49712555707.

Yun, Y., and J. E. Penner (2012), Global model comparison of heterogeneous ice nucleation parameterizations in mixed phase clouds, *J. Geophys. Res. Atmos.*, *117*(7), 1–23, doi:10.1029/2011JD016506.

Chapter 5 Conclusions

Our understanding of the process of ice nucleation and its representation in climate models has several fundamental and large uncertainties. I have contributed to advancing knowledge of ice nucleation through the three manuscripts presented in this thesis. Each manuscript has worked towards improving our understanding of a scientific questions presented in the introduction.

The first question related to the relative contribution of marine organic aerosols and K-feldspar to global ice-nucleating particle (INP) concentrations and has been tackled by improving the model representation of ice-nucleating particles based on new laboratory measurements. The second question related to the importance of black carbon particles to nucleate ice, which has been addressed through global model simulations with new estimates of the BC ice-nucleating ability. And finally, in relation to the third question on the role of ice-nucleating particles on radiative properties of Southern Ocean cyclones, I studied how the low concentrations of ice-nucleating particles in remote marine environments affect cloud reflectivity and whether they can help to understand model radiative biases.

The conclusions of this thesis are as follows:

1. **The relative contribution of feldspar and marine organic aerosols to global INP concentrations has been quantified and evaluated.**
    a. The global modelling results suggest that mineral dust particles, whose ice-nucleating ability is considered to be dominated by potassium feldspar [*Atkinson et al.*, 2013], are a dominant source of atmospheric ice nucleation in the mixed-phase temperature range. The model results are consistent with several field studies looking at the composition of ice-nucleating particles in the atmosphere [*Kamphus et al.*, 2010; *Baustian et al.*, 2012; *Kupiszewski et al.*, 2016; *Schmidt et al.*, 2017] and previous modelling studies [*Hoose et al.*, 2010; *Niemand et al.*, 2012; *Atkinson et al.*, 2013; *Spracklen and Heald*, 2014].Desert dust is a very efficient ice nucleator; however, the sporadic nature of dust plumes makes its atmospheric relevance as an ice-nucleating particle also very variable. On seasonal mean

timescales feldspar dominates the INP concentration in the Northern Hemisphere and several areas of the Southern Hemisphere. However, on a daily basis the contribution of marine organic aerosols [*Wilson et al.*, 2015] to INP concentrations exceeds that of feldspar up to 30% of the days in the Northern Hemisphere and almost always over the remote marine Southern Hemisphere.

b. The model representation of INP based of marine organics and feldspar produces better agreement with atmospheric observations of INP than some of the previously used parametrizations [*Meyers et al.*, 1992; *DeMott et al.*, 2010; *Niemand et al.*, 2012]. Overall, the model can reproduce about 60% of the points from our dataset of 459 datapoints within an order of magnitude and up to 78% within 1.5 orders of magnitude. The agreement is much better for marine regions, with 80% of the measured values simulated within an order of magnitude. This result shows how linking ice nucleation to the aerosol concentrations can improve the predictive capability of models.

c. There are two main biases found in the simulations with respect to measured INP concentrations. First, our model tends to produce concentrations in terrestrial regions at high temperatures that are a few orders of magnitude lower than measured. This might be indicative of a missing source of INP not represented in the model acting at temperatures higher than -15 ^{o}C. The second bias is an overestimation by the model at low temperatures in the North American region. Some possible explanations of why this bias appears include the effect of sulphur coatings deactivating the ice-nucleating ability of feldspar [*Augustin-Bauditz et al.*, 2014], the parameterization for the density of active sites in feldspar particles being too efficient at low temperatures [*Niedermeier et al.*, 2015; *Peckhaus et al.*, 2016] or uncertainties related to the removal and transport processes of dust particles.

Recommendations for future studies:

a. Identifying the possible source of terrestrial high-temperature INP. Possible candidates include soil dust particles whose ice-nucleating ability could be enhanced by organic fragments attached to their surface [*O'Sullivan et al.*, 2016] or anthropogenic emitted aerosols such as lead particles[*Cziczo et al.*, 2009]. The effect that different chemical solutes can have on the ice-nucleating ability of feldspar particles should also be considered. If any enhancement in the ability to nucleate ice due to anthropogenic emissions on nitrates could occur in the atmosphere efficiently enough to modify substantially the number of nucleation events, it would lead to an anthropogenic change in cloud properties that currently has not been considered or studied.
b. Improving and constraining the microphysical processes of aerosol models is crucial to be able to determine more accurately the importance of the different aerosol species for ice nucleation. More specifically, the microphysical processes affecting the surface area concentration of dust particles in remote places is a very model-dependant quantity which is currently very poorly constrained. Uncertainties related to the transport, emissions and removal of dust particles can strongly affect the simulated size distribution in remote marine regions, affecting substantially the simulated INP concentration. Efforts towards constraining these processes and evaluating the dust size distributions in remote areas will help to reduce the uncertainties associated with simulations of INP concentrations by dust aerosols.

2. The role of BC particle to nucleate ice under mixed-phase conditions based on various laboratory estimates of its density of active sites has been assessed.

a. Several previous modelling studies concluded that BC particles are efficient INPs in the immersion mode based on experiments from *DeMott* [1990] and *Diehl and Mitra* [1998]. The efficiency at which BC particles were nucleating ice in these experiments has not been reproduced in recent studies. Our new experimental estimates suggest

that BC is not efficient enough to nucleate ice above the limit of detection of modern instruments. The upper limits of the density of active sites for the soot particles generated in the laboratory are much lower than its previously reported n_s values.

b. The BC concentrations produced by the GLOMAP model were compared with several campaigns from the GASSP dataset [*Reddington et al.*, 2017] finding a reasonable agreement with most campaigns. This makes our model suitable for assessing the potential importance of BC particles as INP in the atmosphere.

c. The simulated INP concentrations obtained when using previous estimates of the ice-nucleating ability of BC particles are several orders of magnitude higher than field observations. Furthermore, if all the BC particles in the atmosphere would have such efficiency, they would dominate the global INP concentrations by several orders of magnitude when compared with feldspar and marine organic aerosols. This possibility is not consistent with a number of field studies where dust particles have been observed to be the principal component for ice nucleation under mixed-phase conditions [*Kamphus et al.*, 2010; *Baustian et al.*, 2012; *Kupiszewski et al.*, 2016; *Schmidt et al.*, 2017] . Hence, I conclude that assuming all BC particles nucleate ice with previously reported efficiencies at all times is unrealistic.

d. Using new estimates of the upper limit of the density of active sites that BC particles can have based on laboratory studies, I estimate that BC does not play a major role as an INP in the atmosphere under mixed-phase conditions.

e. We estimated how efficient BC particles need to be in order to produce higher INP concentrations than marine organic and feldspar aerosols. These estimates will provide future experimental studies a quantitative estimate of the possible importance that BC could have in the atmosphere if a process were discovered to make BC particles to nucleate ice. Currently, the most recently reported upper limits values of n_s for BC particles are in the range where BC would not substantially contribute to atmospheric INP concentrations. Given the

complex nature of BC aerosols, we cannot neglect that some atmospheric processes might make BC particles to nucleate ice with higher efficiencies in certain occasions, which could potentially explain the discrepancies between the old and new laboratory estimates.

Recommendations for future studies:

f. Understanding the reasons for the discrepancy between the earlier laboratory measurements [*DeMott*, 1990; *Diehl and Mitra*, 1998] and the new estimates of BC n_s [*Schill et al.*, 2016; *Ullrich et al.*, 2017] is crucial to determine what caused BC particles to nucleate ice so efficiently in previous studies. If any experiment could show that any atmospherically relevant process can make BC particles to nucleate ice under mixed-phase cloud conditions, our estimates could provide a quick check of its possible atmospheric relevance. However, a more detailed modelling study will be needed afterwards to properly quantify its potential atmospheric importance.

g. Measurements of the INP efficiency of other aerosols particles emitted by human activities such as lead or agricultural dust will help quantify and resolve the question of whether if there is any anthropogenic influence on the atmospheric INP concentration.

3. **The importance of simulating correctly the low concentrations of INP found in the Southern Ocean has been studied. By modelling extratropical cyclones, I found that using INP representations based on the aerosol composition of the region, the radiative properties of the cyclones are in much better agreement with satellite observations.**

   a. Different representations of INP were tested in a high-resolution cloud-resolving model with a double moment representation of several hydrometeors. When using INP representations that account for the concentrations of ice-nucleating particles found in terrestrial environments [*Meyers et al.*, 1992; *DeMott et al.*, 2010], cloud

reflectance is closer to the values that the global model produces. Lower INP concentrations obtained from the global aerosol model (Chapter 1) significantly improve the magnitude and frequency distribution of cloud radiances.

b. The main change in cloud reflected SW radiation happens on the low-level stratocumulus and cumulus clouds that appear in the cold sector of the cyclones. These clouds have been identified in previous studies as the main contributors to the Southern Ocean radiative bias [*Bodas-Salcedo et al.*, 2016]. The frontal cloud of the cyclone, which is not as biased in models as the low-level cloud decks, is not affected by the changes in the INP concentration.

c. A large fraction of the Southern Ocean model shortwave radiative bias could be caused by the fact that cloud microphysical processes in global climate models are essentially tuned to match the properties of clouds in environments with much larger concentrations of INP than remote marine environments. By not accounting for the regional INP differences, ice formation is essentially too efficient in climate models compared with the reality in these remote regions. This efficient ice formation depletes large fractions of the condensed liquid water and hence reduces the reflection of solar radiation.

d. The liquid water content of the clouds in the cold sector of cyclones decreases linearly with the logarithm of the INP concentration. A similar relation is found in terms of the radiative properties of these clouds. This relation holds up to INP concentrations of about 1 L^{-1}. At this point the liquid content is so strongly depleted that the cloud reflectivity decreases sharply with further increases in INP.

e. Temporal variations in INP over the Southern Ocean could modulate the reflected solar radiation of similar cloud systems by between 24 and 60 W/m^2. Globally, as the variations on the INP concentration are much larger, the modulation of radiative properties could be much higher.

f. Adjusting the glaciation temperature of clouds in a global model to increase the liquid content of the clouds will likely create broadly uniform changes in different regions and might lead to unphysical

relation between different cloud parameters [*McCoy et al.*, 2016]. Then, to account for the important variations created by temporally and spatially variable concentrations of INP, cloud glaciation should be linked to realistic aerosol concentrations.

Recommendations for future studies:

a. The limitations of this study come largely from the computational cost of running high-resolution simulations with a complex cloud microphysical scheme. These computational limitations make simulating SO clouds on a convective-resolving scale too expensive unless the domain is reduced to just a small part of a cyclone and the simulation limited to a few days. A possible way to overcome this problem would be to study how much the resolution could be decreased without significantly affecting the model results. A decrease of resolution will allow for much longer simulations, which are necessary to get a more representative view of the long-term effect of improving the representation of INP. However, other uncertainties such as the sub-grid partition between ice and liquid in mixed-phase clouds could potentially increase.

b. The Southern Ocean is a region were INP are critical to represent the right cloud properties, however, different cloud systems in other regions might not be affected so strongly by the representation of INP. Hence, the impact of ice-nucleating particles on different cloud systems across the globe with different dynamical conditions should be studied in future.

c. Observational, experimental and modelling studies to improve our fundamental understanding of secondary ice multiplication processes are crucial to improve the way they are simulated and determine its potential importance for cloud glaciation.

d. I have shown that different concentrations of INP can have a critical effect in the radiative properties of clouds when linked to a high-resolution cloud resolving model with double moment representation of ice particles. However, many global models partition cloud liquid and ice in a such a way that it is effectively dependant just on temperature all across the globe [*McCoy et al.*, 2015, 2016]. Hence, we suggest that future work improving the microphysics of global models to make them able to link cloud glaciation to the aerosol composition is a necessary step towards our understanding of the role of INP in the climate system.

e. The species used in this study (marine organics and K-feldspar) are aerosols emitted by natural processes. However, the emissions of these components in past epochs were substantially different to present day emissions. Studies looking at the past and future atmospheric loading of these aerosols will help estimating whether they can play a role in modulating climate through affecting the number of ice-nucleation events in mixed-phase clouds [*Carslaw et al.*, 2017; *Sagoo and Storelvmo*, 2017].

References:

Atkinson, J. D., B. J. Murray, M. T. Woodhouse, T. F. Whale, K. J. Baustian, K. S. Carslaw, S. Dobbie, D. O'Sullivan, and T. L. Malkin (2013), The importance of feldspar for ice nucleation by mineral dust in mixed-phase clouds., *Nature*, *498*(7454), 355–8, doi:10.1038/nature12278.

Augustin-Bauditz, S., H. Wex, S. Kanter, M. Ebert, D. Niedermeier, F. Stolz, a. Prager, and F. Stratmann (2014), The immersion mode ice nucleation behavior of mineral dusts: A comparison of different pure and surface modified dusts, *Geophys. Res. Lett.*, *41*(20), 7375–7382, doi:10.1002/2014GL061317.

Baustian, K. J., D. J. Cziczo, M. E. Wise, K. A. Pratt, G. Kulkarni, A. G. Hallar, and M. A. Tolbert (2012), Importance of aerosol composition, mixing state, and morphology for heterogeneous ice nucleation: A combined field and laboratory approach, *J. Geophys. Res. Atmos.*, *117*(D6), n/a-n/a, doi:10.1029/2011JD016784.

Bodas-Salcedo, A., P. G. Hill, K. Furtado, K. D. Williams, P. R. Field, J. C. Manners, P. Hyder, and S. Kato (2016), Large contribution of supercooled liquid clouds to the solar radiation budget of the Southern Ocean, *J. Clim.*, *29*(11), 4213–4228, doi:10.1175/JCLI-D-15-0564.1.

Carslaw, K. S., H. Gordon, D. S. Hamilton, J. S. Johnson, L. A. Regayre, M. Yoshioka, and K. J. Pringle (2017), Aerosols in the Pre-industrial Atmosphere, *Curr. Clim. Chang. Reports*, *3*(1), 1–15, doi:10.1007/s40641-017-0061-2.

Cziczo, D. J. et al. (2009), Inadvertent climate modification due to anthropogenic lead, *Nat. Geosci.*, *2*(5), 333–336, doi:10.1038/ngeo499.

DeMott, P. J. (1990), An Exploratory Study of Ice Nucleation by Soot Aerosols, *J. Appl. Meteorol.*, *29*, 1072–1079, doi:10.1175/1520-0450(1990)029<1072:AESOIN>2.0.CO;2.

DeMott, P. J., a J. Prenni, X. Liu, S. M. Kreidenweis, M. D. Petters, C. H. Twohy, M. S. Richardson, T. Eidhammer, and D. C. Rogers (2010), Predicting global atmospheric ice nuclei distributions and their impacts on climate., *Proc. Natl. Acad. Sci. U. S. A.*, *107*(25), 11217–11222, doi:10.1073/pnas.0910818107.

Diehl, K., and S. K. Mitra (1998), A laboratory study of the effects of a kerosene-burner exhaust on ice nucleation and the evaporation rate of ice crystals, *Atmos. Environ.*, *32*(18), 3145–3151, doi:10.1016/S1352-2310(97)00467-6.

Hoose, C., J. E. Kristjánsson, J.-P. Chen, and A. Hazra (2010), A Classical-Theory-Based Parameterization of Heterogeneous Ice Nucleation by Mineral Dust, Soot, and Biological Particles in a Global Climate Model, *J. Atmos. Sci.*, *67*(8), 2483–2503, doi:10.1175/2010JAS3425.1.

Kamphus, M., M. Ettner-Mahl, T. Klimach, F. Drewnick, L. Keller, D. J. Cziczo, S.

Mertes, S. Borrmann, and J. Curtius (2010), Chemical composition of ambient aerosol, ice residues and cloud droplet residues in mixed-phase clouds: Single particle analysis during the cloud and aerosol characterization experiment (CLACE 6), *Atmos. Chem. Phys.*, *10*(16), 8077–8095, doi:10.5194/acp-10-8077-2010.

Kupiszewski, P. et al. (2016), Ice residual properties in mixed-phase clouds at the high-alpine Jungfraujoch site, *J. Geophys. Res. Atmos.*, *121*(20), 12,343-12,362, doi:10.1002/2016JD024894.

McCoy, D. T., D. L. Hartmann, M. D. Zelinka, P. Ceppi, and D. P. Grosvenor (2015), Mixed-phase cloud physics and Southern Ocean cloud feedback in climate models, *J. Geophys. Res. Atmos.*, *120*, 9539–9554, doi:10.1002/2015JD023603.Received.

McCoy, D. T., I. Tan, D. L. Hartmann, M. D. Zelinka, and T. Storelvmo (2016), On the relationships among cloud cover, mixed-phase partitioning, and planetary albedo in GCMs, *J. Adv. Model. Earth Syst.*, *8*(2), 650–668, doi:10.1002/2015MS000589.

Meyers, M. P., P. J. DeMott, and W. R. Cotton (1992), New Primary Ice-Nucleation Parameterizations in an Explicit Cloud Model, *J. Appl. Meteorol.*, *31*(7), 708–721, doi:10.1175/1520-0450(1992)031<0708:NPINPI>2.0.CO;2.

Niedermeier, D., S. Augustin-bauditz, S. Hartmann, H. Wex, and F. Stratmann (2015), Can we define an asymptotic value for the ice active surface site density for heterogeneous ice nucleation ?, *J. Geophys. Res. Atmos.*, *120*(May), 5036–5046, doi:10.1002/2014JD022814.The.

Niemand, M. et al. (2012), A Particle-Surface-Area-Based Parameterization of Immersion Freezing on Desert Dust Particles, *J. Atmos. Sci.*, *69*(10), 3077–3092, doi:10.1175/JAS-D-11-0249.1.

O'Sullivan, D., B. J. Murray, J. Ross, and M. E. Webb (2016), The adsorption of fungal ice-nucleating proteins on mineral dusts: a terrestrial reservoir of atmospheric ice-nucleating particles, *Atmos. Chem. Phys. Discuss.*, (January), 1–22, doi:10.5194/acp-2015-1018.

Peckhaus, A., A. Kiselev, T. Hiron, M. Ebert, and T. Leisner (2016), A comparative study of K-rich and Na/Ca-rich feldspar ice-nucleating particles in a nanoliter droplet freezing assay, *Atmos. Chem. Phys.*, *16*(18), 11477–11496, doi:10.5194/acp-16-11477-2016.

Reddington, C. L. et al. (2017), THE GLOBAL AEROSOL SYNTHESIS AND SCIENCE PROJECT (GASSP): Measurements and modelling to reduce uncertainty, *Bull. Am. Meteorol. Soc.*, BAMS-D-15-00317.1, doi:10.1175/BAMS-D-15-00317.1.

Sagoo, N., and T. Storelvmo (2017), Testing the sensitivity of past climates to the indirect effects of dust, *Geophys. Res. Lett.*, *44*(11), 5807–5817, doi:10.1002/2017GL072584.

Schill, G. P. et al. (2016), Ice nucleating particle emissions from photochemically-aged diesel and biodiesel exhaust, *Geophys. Res. Lett.*, 1–8, doi:10.1002/2016GL069529.

Schmidt, S., J. Schneider, T. Klimach, S. Mertes, L. P. Schenk, P. Kupiszewski, J. Curtius, and S. Borrmann (2017), Online single particle analysis of ice particle residuals from mountain-top mixed-phase clouds using laboratory derived particle type assignment, *Atmos. Chem. Phys.*, *17*(1), 575–594, doi:10.5194/acp-17-575-2017.

Spracklen, D. V., and C. L. Heald (2014), The contribution of fungal spores and bacteria to regional and global aerosol number and ice nucleation immersion freezing rates, *Atmos. Chem. Phys.*, *14*(17), 9051–9059, doi:10.5194/acp-14-9051-2014.

Ullrich, R., C. Hoose, O. Möhler, M. Niemand, R. Wagner, K. Höhler, N. Hiranuma, H. Saathoff, and T. Leisner (2017), A New Ice Nucleation Active Site Parameterization for Desert Dust and Soot, *J. Atmos. Sci.*, *74*(3), 699–717, doi:10.1175/JAS-D-16-0074.1.

Wilson, T. W. et al. (2015), A marine biogenic source of atmospheric ice-nucleating particles, *Nature*, *525*(7568), 234–238, doi:10.1038/nature14986.

Appendices and supporting information

Appendix A: Marine organic emissions

In order to represent the distribution of submicron marine organics aerosols, first we simulate the distribution of sea- salt aerosols (SS) with GLOMAP mode for the year 2001. Then we look at the correlation between the monthly mean emission flux of sea-salt particles in the accumulation mode (100nm<r <1 μm) and the monthly mean surface concentration of submicron sea salt in the grid boxes corresponding to Mace Head and Amsterdam Island. We then take the grid boxes that score a correlation R >0.9 and assume that, as a first order approach, the emissions of these grid boxes will drive the concentrations of submicron sea spray in their corresponding stations (Fig. A1). Once these grid boxes are identified for every station, we calculate the organic mass fraction (OMF) in surface air (lowest model layer) at both stations with modelled concentrations of sea spray and measured concentrations of water insoluble organic matter (WIOM) following Eq. A1.

$$OMF = \frac{[WIOM]}{[SS_{mass}] + [WIOM]} \qquad (A1)$$

The WIOM in Mace Head data is obtained from *Rinaldi et al.* [2013] by averaging measurements corresponding to a few days (from 5 to 14 days) in every month. For Amsterdam island, WIOM is derived from *Sciare et al.* [2009] using a factor of 1.9 to convert from water insoluble organic carbon to WIOM [*Burrows et al.*, 2013]. The chlorophyll a maps correspond to monthly mean values obtained from GLOBCOLOUR [*Maritorena and Siegel*, 2005], which made use of data from three different satellites to merge their chlorophyll a maps and produce a final product with an enhanced global coverage.

In order to develop a parameterization of the organic mass

fraction to be used in both hemispheres, we use the monthly mean values of the chlorophyll a content in the grid boxes that were previously related to each station, together with the monthly mean reanalysis (ECMWF) wind speed at 10m over the surface (U10M) of these grid boxes and relate these two variables to the organic

mass fraction previously calculated (Fig. A2a). We then fit the OMF to a two-dimensional equation with the wind speed and chlorophyll a content as variables (Fig. A2b). This gives us a parameterization of the OMF emitted with submicron sea spray that can fit our model. In order to avoid unrealistic OMF values due to extrapolation, we limit the maximum value of our OMF to 0.85. The mass flux of marine organic material can then be from

the sea-salt flux following Eq. A5:

$$Flux_{total} = Flux_{SS} + Flux_{WIOM} \qquad (A2)$$

$$Flux_{WIOM} = OMF \cdot Flux_{total} \qquad (A3)$$

$$Flux_{total} = \frac{Flux_{WIOM}}{OMF} \qquad (A4)$$

$$Flux_{WIOM} = \frac{Flux_{SS} \cdot OMF}{1 - OMF} \qquad (A5)$$

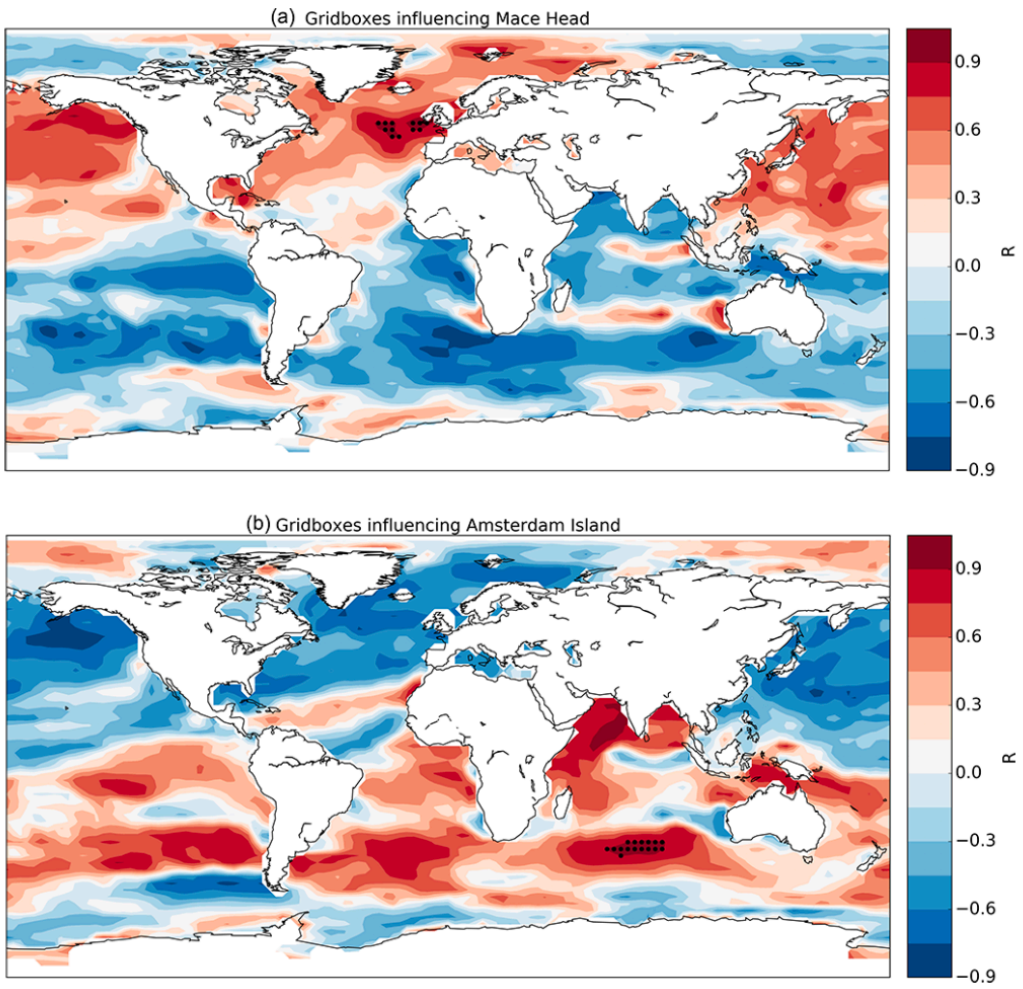

Figure A1. Linear correlation values between the monthly emission of submicron sea spray and their monthly concentrations in (a) Mace Head, (b) Amsterdam Island. The dots represent the grid boxes related to every station because they have a value R >0.9.

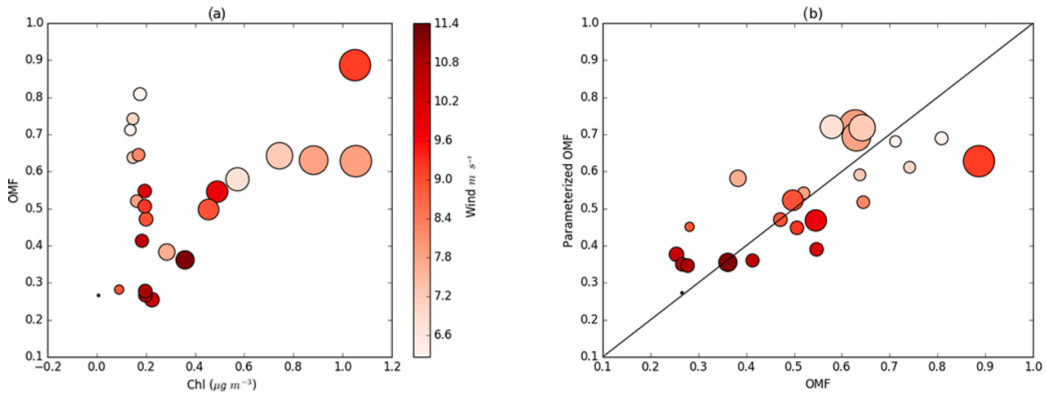

Figure A2. (a) OMF compared as a function of chlorophyll a content and surface wind speed for the monthly mean values in both stations. The size of the points represents the mean chlorophyll a content of the grid boxes related previously to every station (Fig. A1), the colour of the points is related to the wind speed of those grid boxes. Panel (b) shows the performance of the parameterization for reproducing the OMF calculated with the simulated concentration of submicron sea salt and the observed values of WIOM. The parameterization for the OMF is $OMF = A \times [CHL(mg\ m^{-3})] + B \times [U10M(m\ s^{-1})]^c + D$ with $A = 0.241, B = -7.503, C = 0.075, D = 9.274$.

References:

Burrows, S. M., C. Hoose, U. Pöschl, and M. G. Lawrence (2013), Ice nuclei in marine air: biogenic particles or dust?, *Atmos. Chem. Phys.*, *13*(1), 245–267, doi:10.5194/acp-13-245-2013.

Maritorena, S., and D. a. Siegel (2005), Consistent merging of satellite ocean color data sets using a bio-optical model, *Remote Sens. Environ.*, *94*(4), 429–440, doi:10.1016/j.rse.2004.08.014.

Rinaldi, M. et al. (2013), Is chlorophyll- a the best surrogate for organic matter enrichment in submicron primary marine aerosol?, *J. Geophys. Res. Atmos.*, *118*(10), 4964–4973, doi:10.1002/jgrd.50417.

Sciare, J., O. Favez, R. Sarda-Estève, K. Oikonomou, H. Cachier, and V. Kazan (2009), Long-term observations of carbonaceous aerosols in the Austral Ocean atmosphere: Evidence of a biogenic marine organic source, *J. Geophys. Res.*, *114*(D15), D15302, doi:10.1029/2009JD011998.

Appendix B: Calculation of INP concentrations

Assuming that the active sites from which ice nucleation can occur under the singular description are randomly distributed in the aerosol population, the probability of one particle having a certain number of active sites (k) can be represented by the Poisson distribution of Eq. B1.

$$f(k,\lambda) = \frac{e^{-\lambda}\lambda^{k}}{k!} \quad (B1)$$

Here, f is the probability of having k active sites in a particle and λ represents the expected value of active sites per particle at a certain temperature (T). We can calculate the probability of a particle immersed in a water droplet to freeze it (P) as the sum of the probabilities of having 1 or more active sites in Eq. B2:

$$P = \sum_{k=1}^{\infty} f(k,\lambda) \quad (B2)$$

As the sum from k =0 to k =∞ of Eq. B1 has to be equal to 1, we can also represent this sum as Eq. B3:

$$P = \sum_{k=0}^{\infty} f(k,\lambda) - f(0,\lambda) = 1 - e^{-\lambda} \quad (B3)$$

If we have a distribution of particles of the same size and same density of active sites, this probability P will be the same for all of them, and so the fraction of supercooled water droplets that will freeze known as fraction frozen (ff), will therefore be:

$$ff = 1 - e^{-\lambda} \quad (B4)$$

We can then calculate the INP concentration as:

$$[INP] = ff \cdot [N] \quad (B5)$$

where [N] represents the concentration of a certain type

of aerosol. For the case in which we have a density of active sites distributed across the surface area of a particle depending on temperature n_s(T), we can calculate λ for a particle of radius r as:

$$\lambda(r,T) = 4\pi r^2 \cdot n_s(T) \quad (B6)$$

Hence:

$$ff(r,T) = 1 - e^{-n_s(T)\cdot 4\pi r^2} \quad (B7)$$

In GLOMAP mode, the size distribution of aerosols is represented in log-normal modes, and their probability density function (PDF) is given by:

$$PDF(r) = \frac{1}{r\ln(\sigma)\sqrt{2\pi}} e^{-\frac{(\ln(r)-\ln(r_m))^2}{2\ln(\sigma)^2}} \quad (B8)$$

where r_m is the mean radius of the mode and σ the standard deviation of the mode. The INP concentration is therefore the integral across all

the possible values of r for every mode, and it will change for every temperature:

$$[INP]_{mode}(T) = [N]\int_0^{\infty}\left(1 - e^{-4\pi r^2 n_s(T)}\right)\frac{1}{r\ln(\sigma)\sqrt{2\pi}} e^{-\frac{(\ln(r)-\ln(r_m))^2}{2\ln(\sigma)^2}} dr \quad (B9)$$

In our case, we consider that just the soluble modes can

activate into water droplets, so the total INP concentration is the sum of the concentrations for every soluble mode. In the special case of having a value of λ small (λ<0.1),

we can approximate the value of the fraction frozen (ff) using a first-order Taylor series centred in 0:

$$ff = ff_{\lambda=0} + \frac{1}{1}\frac{\partial ff}{\partial \lambda}\bigg|_{\lambda=0}\cdot\lambda + \cdots \quad (B10)$$

$$ff_{\lambda=0} = 1 - e^0 = 0 \quad (B11)$$

$$\frac{\partial ff}{\partial \lambda}\bigg|_{\lambda=0} = \left[-e^{-\lambda}\cdot(-1)\right]_{\lambda=0}\cdot\lambda = 1\cdot\lambda \quad (B12)$$

$$ff \approx \lambda \quad (B13)$$

In other words, if the number of active sites is small compared with the number of particles, we can approximate the number of particles having one or more actives sites, to the number of active sites. And the INP concentration can be calculated as follows:

$$[INP](T) \approx \lambda(T)\cdot[N] \quad (B14)$$

Appendix C: INP data set

The data set used in this study is a compilation of published and unpublished data provided by different groups contributing to the BACCHUS data set of INPs (http://www. bacchus-env.eu/in/index.php). Table C1 shows a summary of the data sets. We note that a study from Bigg [1996] reported INP concentrations in the high Arctic. We could not include it in our database as the exact locations could not be obtained. However, we note that the range of concentrations reported by Bigg [1996] (from 13 to 2.9m^{-3} at −15ºC) are close to our simulated values using feldspar and marine organics (from 7.4 to 0.1m^{-3}) during the months of the campaign (August to October). The data sets obtained through the BACCHUS project database are labelled "BACCHUS" in Table C1. The data sets corresponding to long-term measurements in a single location were resized to account for a single data point at every temperature. This is done in order to avoid statistical overweighting of a single location or campaign.

Campaign	Location	Marine or Terrestrial	Technique	Data points	Reference
Bigg73	Australia	Terrestrial	Filter	24	[*Bigg*, 1973]
CLEX	East Canada	Terrestrial	CFDC	60	[*DeMott et al.*, 2010]
Yin	China	Terrestrial	Filter	21	[*Yin et al.*, 2012]
ICE-L Ambient	Central USA	Terrestrial	CFDC	31	[*DeMott et al.*, 2010]
Conen_JFJ	Jungfraujoch	Terrestrial	Filter	6	BACCHUS [*Conen et al.*, 2015]
DeMott2016	Marine locations	Marine	Filter	44	[*DeMott et al.,2016*]
Mason2016 terrestrial	Terrestrial locations	Terrestrial	Filter	15	[*Mason et al.*, 2016]
KAD_South_Pole	South Pole	Terrestrial	Filter	8	BACCHUS [*Ardon-Dryer et al.*, 2011]
ICE-L CVI	Central USA	Terrestrial	CFDC	27	[*DeMott et al.*, 2010]
Rosisnky	Gulf of Mexico	Marine	Filter	5	[*Rosinski et al.*, 1988]
Bigg1973	Southern Ocean	Marine	Filter	102	[*Bigg*, 1973]
Conen_chaumont	Chaumont	Terrestrial	Filter	7	BACCHUS [*Conen et al.*, 2015]
AMAZE-08	Amazon rainforest	Terrestrial	CFDC	63	[*DeMott et al.*, 2010]
INSPECT-I	Central USA	Terrestrial	CFDC	13	[*DeMott et al.*, 2010]
Mason2016 Marine	Marine Locations	Marine	Filter	6	[*Mason et al.*, 2016]
KAD_Israel	Jerusalem	Terrestrial	Filter	16	BACCHUS [*Ardon-Dryer and Levin, 2014*]
INSPECT-II	Central USA	Terrestrial	CFDC	11	[*DeMott et al.*, 2010]

Table C1. Table of the data sets used for this study (Chapter 2)

References:

Ardon-Dryer, K., and Z. Levin (2014), Ground-based measurements of immersion freezing in the eastern Mediterranean, *Atmos. Chem. Phys.*, *14*(10), 5217–5231, doi:10.5194/acp-14-5217-2014.

Ardon-Dryer, K., Z. Levin, and R. P. Lawson (2011), Characteristics of immersion freezing nuclei at the South Pole station in Antarctica, *Atmos. Chem. Phys.*, *11*(8), 4015–4024, doi:10.5194/acp-11-4015-2011.

Bigg, E. K. (1973), Ice Nucleus Concentrations in Remote Areas, *J. Atmos. Sci.*, *30*(6), 1153–1157, doi:10.1175/1520-0469(1973)030<1153:INCIRA>2.0.CO;2.

Conen, F., S. Rodríguez, C. Hüglin, S. Henne, E. Herrmann, N. Bukowiecki, and C. Alewell (2015), Atmospheric ice nuclei at the high-altitude observatory Jungfraujoch, Switzerland, *Tellus B*, *67*(1), 1–10, doi:10.3402/tellusb.v67.25014.

DeMott, P. J., a J. Prenni, X. Liu, S. M. Kreidenweis, M. D. Petters, C. H. Twohy, M. S. Richardson, T. Eidhammer, and D. C. Rogers (2010), Predicting global atmospheric ice nuclei distributions and their impacts on climate., *Proc. Natl. Acad. Sci. U. S. A.*, *107*(25), 11217–11222, doi:10.1073/pnas.0910818107.

DeMott, P. J. et al. (2016), Sea spray aerosol as a unique source of ice nucleating particles, *Proc. Natl. Acad. Sci.*, *113*(21), 5797–5803, doi:10.1073/pnas.1514034112.

Mason, R. H. et al. (2016), Size-resolved measurements of ice-nucleating particles at six locations in North America and one in Europe, *Atmos. Chem. Phys.*, *16*(3), 1637–1651, doi:10.5194/acp-16-1637-2016.

Rosinski, J., P. L. Haagenson, C. T. Nagamoto, B. Quintana, F. Parungo, and S. D. Hoyt (1988), Ice-forming nuclei in air masses over the Gulf of Mexico, *J. Aerosol Sci.*, *19*(5), 539–551, doi:10.1016/0021-8502(88)90206-6.

Yin, J., D. Wang, and G. Zhai (2012), An evaluation of ice nuclei characteristics from the long-term measurement data over North China, *Asia-Pacific J. Atmos. Sci.*, *48*(2), 197–204, doi:10.1007/s13143-012-0020-8.

Supplementary information for Chapter 3 "Is black carbon an unimportant ice-nucleating particle in mixed-phase clouds?"

Soot generation and freezing experiments:

Eugenol and *n*-decane soots were generated using a diffusion burner method. The eugenol (99 %, Alfa Aesar, UK) and *n*-decane (99 %, Alfa Aesar) were placed into a metal container. A braided cotton wick, in contact with the fuel, was used to hold the flame. The length of exposed wick above the container was 5 mm. The burner was placed into a glass chimney and a 10 $Lmin^{-1}$ flow of compressed air, passed through a HEPA filter, provided a source of oxygen. Once the wick was lit, the resulting soot was collected at the top of the funnel on glass microscope slides, which were removed and replaced with fresh slides every 30 seconds until the experiment was terminated.

A drop freezing assay method was used to study the ice nucleation abilities of the soot produced using the Nucleation by Immersed Particles Instrument (μL-NIPI). The method has been described previously [*Whale et al.*, 2014]. The soot particles were suspended in MilliQ ultra-pure water (18.2 MΩ.cm resistivity). To effectively disperse the soot, the suspensions were sonicated for 1-5 minutes, before being stirred with a teflon lined stirrer bar to maintain the suspension. Arrays of 1μL droplets from each soot suspension were pipetted onto hydrophobic glass slides (siliconised glass slides, Hampton Research) that were placed on an EF600 Stirling engine cryo-cooler (Grant Asymptote). The stage was cooled at a constant ramp rate of 1 $°Cmin^{-1}$, and freezing events and their corresponding temperatures were recorded using optical methods.

The soot suspension particle size distribution was measured using laser diffraction (Malvern Mastersizer 2000E). This technique is sensitive to particles with a grain size between 0.1 and 1000 μm. The suspensions were sonicated for 5 minutes before measurements. Figure S1 shows the results of laser diffraction analysis for suspensions of *n*-decane and eugenol soots of different concentrations. No significant difference in particle size distribution was observed for soot concentrations of 10^{-2} and 10^{-3} wt. %, with ≥80 % of the surface area measured associated with grain sizes below 1 μm. For soot concentrations of 10^{-1} wt. %, over 50 % of the surface area was associated with grain sizes larger than 1μm. Nucleation

significantly above the instrument baseline was not observed for any experiments. When parameterized, the results at higher concentrations will yield lower values of $n_s(T)$. Therefore, it is desirable to parameterize our upper limit using the highest possible concentration, since the maximum values of $n_s(T)$ that the soot may have can be better constrained. Since the highest concentration measurements (10^{-1} wt. %) are affected significantly by particle aggregation, the NEW-UPL parameterization was calculated using the data at 10^{-3} wt. %, which is an order of magnitude lower than the concentration at which aggregation becomes less significant. This means we are confident that no aggregation was happening in any of the samples, yet the concentration used allows enough resolution for the GLOMAP analysis, as demonstrated in Figure 4a.

GLOMAP modelling and evaluation:

We use the global tropospheric model of aerosol processes (GLOMAP) [*Mann et al.*, 2010] to simulate global BC INP distribution. The model traces aerosol mass and number in 7 lognormal modes. All particles within a mode are assumed internally mixed. The model was run at 2.8° x 2.8° resolution with 31 vertical levels. The simulation was done for the year 2001 using meteorological fields diagnosed from the European Center of Medium Weather Forecast (ECMWF). Anthropogenic BC emissions come from the inventory of *Bond*, [2004] and biomass burning emisions from [*Van der Werf et al.*, 2003]. Black Carbon particles are emitted into the Aitken insoluble mode, and assumed internally mixed with co-emitted organic carbon. BC particles are aged into the soluble modes via the condensation of SO2 and organics whereafter they are subject to nucleation scavenging via activation in clouds.

The spatial distribution of BC mass concentration and an evaluation of the simulated BC concentrations with several aircraft campaigns using Single Particle Soot Photometer (SP2) from the GASSP database (*Reddington et al.*, [2017]) are shown in figure S2. For references for the individual datasets see Table S1.

The evaluation was done by interpolating every campaign datapoint on latitude, longitude, and height with the modelled monthly mean values. The modelled values were filtered to sizes within 90nm to 500nm to make the values comparable with the SP2 observational range. The model produces values within a factor of three from the observations for half of the analysed campaings and withing an order of magnitude from for 14 out of 16 campaigns

(87.5%) (Fig 2). A larger variability is observed in the observed values than in the modelled values which is expected as we are comparing modelled values with a much lower temporal and spatial variability than the observations [*Schutgens et al.*, 2016, 2017].

BC $[INP]_T$ were calculated offline using mode particle number and BC surface area following the method shown in *Vergara-Temprado et al.*, [2017]. The method integrates numerically the lognormal size distribution assumed in GLOMAP-mode with the fraction of frozen aerosol particles at each size. The final number is obtained by adding the values from every BC containing mode. We find that the Aitken mode contributes to more than 70% of the total BC INP concentration. Using internal or external mixing assumptions among the aerosol components for calculating BC INP does not change significantly the concentrations.

The modelling of feldspar INP builds on the modelling reported by *Vergara-Temprado et al.*, [2017] which is based on a two-species base representation of INP using k-feldspar and marine organic aerosols. The INP parameterization for K-feldspar is based on the study of *Atkinson et al.*, [2013] and the marine organic parameterization on *Wilson et al.*, [2015]

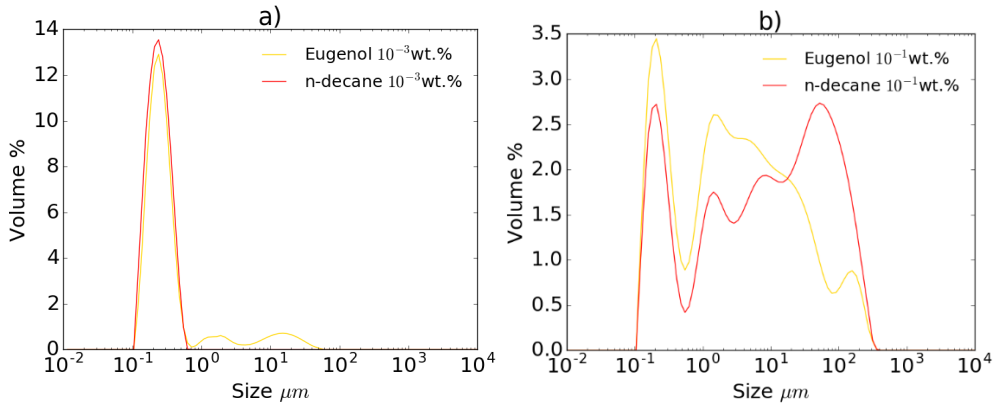

Figure S1. Plots of particle size distributions obtained for eugenol and n-decane soot suspension, at (a) 10^{-3} wt. % and (b) 10^{-1} wt. %

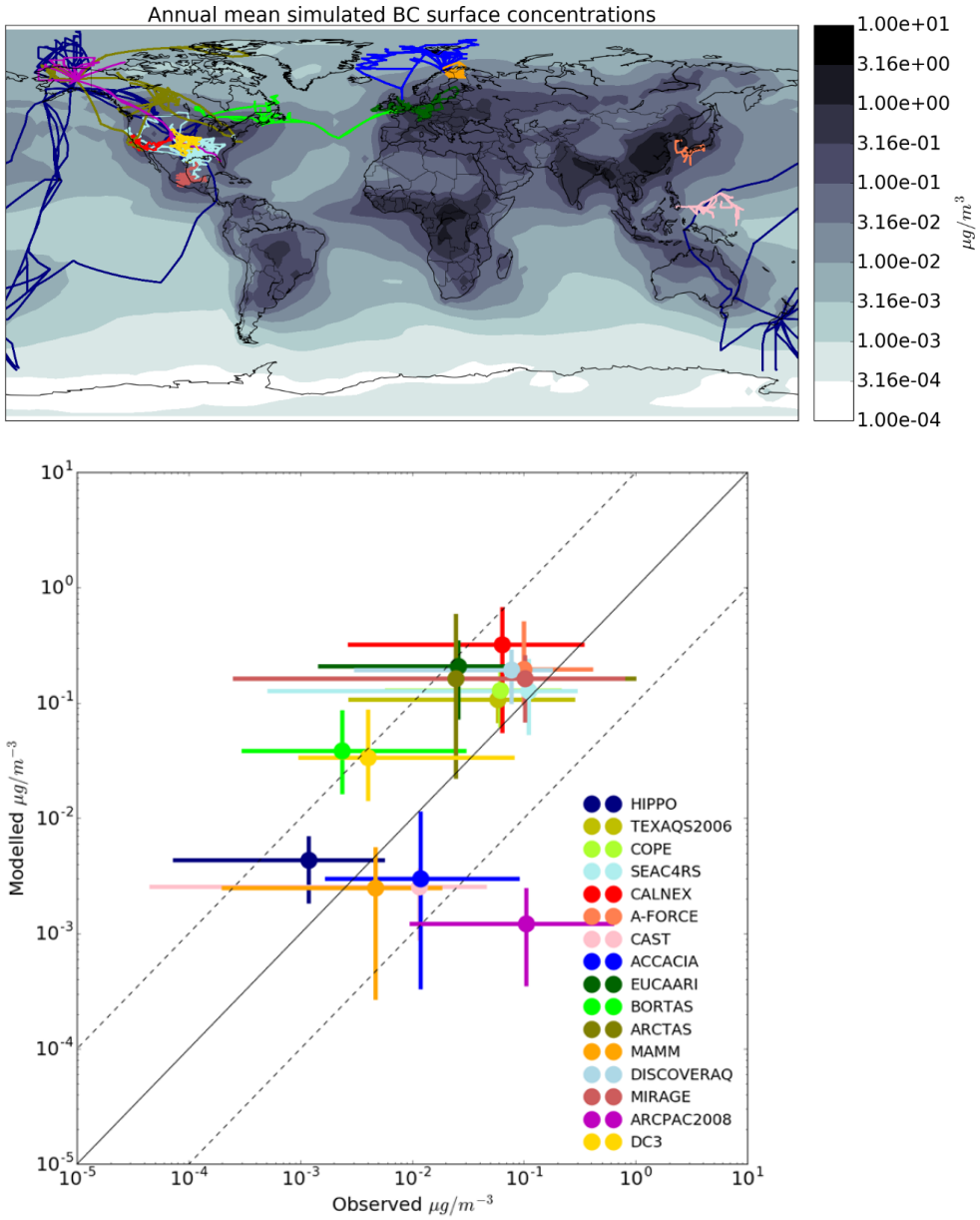

Figure S2. (Top) Annual mean surface concentration of BC mass. (Bottom) Evaluation of BC mass concentrations with several aircraft campaigns (Table S1). The campaign locations are plotted in the map following the legend in the top figure. The variability error bars represent the 95% interval of observed and modelled concentrations. The variability in the model data is lower as the comparison was done with monthly mean values for the year 2001, so it cannot capture all the temporal variability of the aircraft observations.

Project/Campaign	**Reference**
ACCACIA	[*Liu et al.*, 2015]
A-FORCE	[*Oshima et al.*, 2012]
ARCPAC-2008	[*Spackman et al.*, 2010]
ARCTAS	[*Matsui et al.*, 2011]
BORTAS	[*Taylor et al.*, 2014]
CALNEX	[*Metcalf et al.*, 2012]
CAST	[*Harris et al.*, 2017]
COPE	[*Leon et al.*, 2016]
DC3	[*Barth et al.*, 2015]
DISCOVER-AQ	[*Ryerson et al.*, 2013]
EUCAARI-LONGREX	[*McMeeking et al.*, 2010, 2011]
HIPPO	[*Schwarz et al.*, 2010]
MAMM	[*O'Shea et al.*, 2014]
MIRAGE	[*Subramanian et al.*, 2010]
SEAC4RS	[*Perring et al.*, 2017]
TEXAQS- 2006	[*Schwarz et al.*, 2008]

Table S1. Information on the Single Particle Soot Photometer (SP2) datasets obtained from the GASSP database (*Reddington et al.*, [2017]]) and used for model evaluation (Section S2).

References:

Atkinson, J. D., B. J. Murray, M. T. Woodhouse, T. F. Whale, K. J. Baustian, K. S. Carslaw, S. Dobbie, D. O'Sullivan, and T. L. Malkin (2013), The importance of feldspar for ice nucleation by mineral dust in mixed-phase clouds., *Nature*, *498*(7454), 355–8, doi:10.1038/nature12278.

Barth, M. C. et al. (2015), The deep convective clouds and chemistry (DC3) field campaign, *Bull. Am. Meteorol. Soc.*, *96*(8), 1281–1310, doi:10.1175/BAMS-D-13-00290.1.

Bond, T. C. (2004), A technology-based global inventory of black and organic carbon emissions from combustion, *J. Geophys. Res.*, *109*(D14), D14203, doi:10.1029/2003JD003697.

Harris, N. R. P. et al. (2017), Coordinated airborne studies in the tropics (CAST), *Bull. Am. Meteorol. Soc.*, *98*(1), 145–162, doi:10.1175/BAMS-D-14-00290.1.

Leon, D. C. et al. (2016), The Convective Precipitation Experiment (COPE): Investigating the origins of heavy precipitation in the southwestern United Kingdom, *Bull. Am. Meteorol. Soc.*, *97*(6), 1003–1020, doi:10.1175/BAMS-D-14-00157.1.

Liu, D. et al. (2015), The importance of Asia as a source of black carbon to the European Arctic during springtime 2013, *Atmos. Chem. Phys.*, *15*(20), 11537–11555, doi:10.5194/acp-15-11537-2015.

Mann, G. W., K. S. Carslaw, D. V. Spracklen, D. a. Ridley, P. T. Manktelow, M. P. Chipperfield, S. J. Pickering, and C. E. Johnson (2010), Description and evaluation of GLOMAP-mode: a modal global aerosol microphysics model for the UKCA composition-climate model, *Geosci. Model Dev.*, *3*(2), 519–551, doi:10.5194/gmd-3-519-2010.

Matsui, H. et al. (2011), Seasonal variation of the transport of black carbon aerosol from the Asian continent to the Arctic during the ARCTAS aircraft campaign, *J. Geophys. Res. Atmos.*, *116*(5), 1–19, doi:10.1029/2010JD015067.

McMeeking, G. R. et al. (2010), Black carbon measurements in the boundary layer over western and northern Europe, *Atmos. Chem. Phys.*, *10*(19), 9393–9414, doi:10.5194/acp-10-9393-2010.

McMeeking, G. R., W. T. Morgan, M. Flynn, E. J. Highwood, K. Turnbull, J. Haywood, and H. Coe (2011), Black carbon aerosol mixing state, organic aerosols and aerosol optical properties over the United Kingdom, *Atmos. Chem. Phys.*, *11*(17), 9037–9052, doi:10.5194/acp-11-9037-2011.

Metcalf, A. R., J. S. Craven, J. J. Ensberg, J. Brioude, W. Angevine, A. Sorooshian, H. T. Duong, H. H. Jonsson, R. C. Flagan, and J. H. Seinfeld (2012), Black carbon aerosol over the Los Angeles Basin during CalNex, *J. Geophys. Res. Atmos.*, *117*(8), 1–24, doi:10.1029/2011JD017255.

O'Shea, S. J. et al. (2014), Methane and carbon dioxide fluxes and their regional scalability for the European Arctic wetlands during the MAMM project in summer 2012, *Atmos. Chem. Phys.*, *14*(23), 13159–13174, doi:10.5194/acp-14-13159-2014.

Oshima, N. et al. (2012), Wet removal of black carbon in Asian outflow: Aerosol Radiative Forcing in East Asia (A-FORCE) aircraft campaign, *J. Geophys. Res. Atmos.*, *117*(3), 1–24, doi:10.1029/2011JD016552.

Perring, A. E. et al. (2017), In situ measurements of water uptake by black carbon-containing aerosol in wildfire plumes, *J. Geophys. Res. Atmos.*, *122*(2), 1086–1097, doi:10.1002/2016JD025688.

Reddington, C. L. et al. (2017), THE GLOBAL AEROSOL SYNTHESIS AND SCIENCE PROJECT (GASSP): Measurements and modelling to reduce uncertainty, *Bull. Am. Meteorol. Soc.*, BAMS-D-15-00317.1, doi:10.1175/BAMS-D-15-00317.1.

Ryerson, T. B. et al. (2013), The 2010 California Research at the Nexus of Air Quality and Climate Change (CalNex) field study, *J. Geophys. Res. Atmos.*, *118*(11), 5830–5866, doi:10.1002/jgrd.50331.

Schutgens, N., S. Tsyro, E. Gryspeerdt, D. Goto, N. Weigum, M. Schulz, and P. Stier (2017), On the spatio-temporal representativeness of observations, *Atmos. Chem. Phys.*, *17*(16), 9761–9780, doi:10.5194/acp-17-9761-2017.

Schutgens, N. A. J., E. Gryspeerdt, N. Weigum, S. Tsyro, D. Goto, M. Schulz, and P. Stier (2016), Will a perfect model agree with perfect observations? The impact of spatial sampling, *Atmos. Chem. Phys.*, *16*(10), 6335–6353, doi:10.5194/acp-16-6335-2016.

Schwarz, J. P. et al. (2008), Measurement of the mixing state, mass, and optical size of individual black carbon particles in urban and biomass burning emissions, *Geophys. Res. Lett.*, *35*(13), 1–5, doi:10.1029/2008GL033968.

Schwarz, J. P., J. R. Spackman, R. S. Gao, L. A. Watts, P. Stier, M. Schulz, S. M. Davis, S. C. Wofsy, and D. W. Fahey (2010), Global-scale black carbon profiles observed in the remote atmosphere and compared to models, *Geophys. Res. Lett.*, *37*(18), 1–5, doi:10.1029/2010GL044372.

Spackman, J. R., R. S. Gao, W. D. Neff, J. P. Schwarz, L. A. Watts, D. W. Fahey, J. S. Holloway, T. B. Ryerson, J. Peischl, and C. A. Brock (2010), Aircraft observations of enhancement and depletion of black carbon mass in the springtime Arctic, *Atmos. Chem. Phys.*, *10*(19), 9667–9680, doi:10.5194/acp-10-9667-2010.

Subramanian, R. et al. (2010), Black carbon over Mexico: the effect of atmospheric transport on mixing state, mass absorption cross-section, and BC/CO ratios, *Atmos. Chem. Phys.*, *10*(1), 219–237, doi:10.5194/acp-10-219-2010.

Taylor, J. W. et al. (2014), Size-dependent wet removal of black carbon in Canadian biomass burning plumes, *Atmos. Chem. Phys.*, *14*(24), 13755–13771, doi:10.5194/acp-14-13755-2014.

Vergara-Temprado, J. et al. (2017), Contribution of feldspar and marine organic aerosols to global ice nucleating particle concentrations, *Atmos. Chem. Phys.*, *17*(5), 3637–3658, doi:10.5194/acp-17-3637-2017.

Van der Werf, G. R., J. T. Randerson, G. J. Collatz, and L. Giglio (2003), Carbon emissions from fires in tropical and subtropical ecosystems, *Glob. Chang. Biol.*, *9*(4), 547–562,

doi:10.1046/j.1365-2486.2003.00604.x.

Whale, T. F., B. J. Murray, D. O'Sullivan, N. S. Umo, K. J. Baustian, J. D. Atkinson, and G. J. Morris (2014), A technique for quantifying heterogeneous ice nucleation in microlitre supercooled water droplets, *Atmos. Meas. Tech. Discuss.*, *7*(9), 9509–9536, doi:10.5194/amtd-7-9509-2014.

Wilson, T. W. et al. (2015), A marine biogenic source of atmospheric ice-nucleating particles, *Nature*, *525*(7568), 234–238, doi:10.1038/nature14986.

Supporting information for Chapter 4: "Strong control of Southern Ocean cloud reflectivity by ice-nucleating particles"

Model description

The Unified Model (UM) (version 10.3)[*Walters et al.*, 2017] is used in its global setup (GA6, N512 resolution) to provide the initial and boundary conditions for the high resolution regional simulations. We use two different high-resolution nests: the coarser domain (Fig 2 a-d) is composed of 600x600 grid-boxes with a grid-spacing of 0.07^{o} (rotated grid) and the higher resolution nest (Fig. 2e-h, Fig. 3 and Fig. 4) is composed of 500x500 grid-boxes with a spacing of 0.02^{o}. Both domains have a vertical resolution of 70 height levels quadratically spaced up to 40 km (116 meters grid-box height at 1km). We perform the simulations for a total of 18 h, so we can perform a satellite evaluation with the A-train satellites in all our simulations. To avoid influences from boundary effects, we eliminate the closest 100 grid boxes to the boundaries in all the 0.02^{o} resolution simulations before analysing them.

Cloud microphysical processes are simulated by using CASIM (Cloud AeroSol Interaction Microphysics)[*Shipway and Hill*, 2012; *Grosvenor et al.*, 2016; *Miltenberger et al.*, 2017]. It represents cloud droplets, rain, ice crystals, snow and graupel and uses a double moment scheme that predicts both number and mass of each of the hydrometeor types. The hydrometeor size distributions are represented by gamma function with a fixed width.

An aerosol vertical profile obtained from a GLOMAP simulation [*Mann et al.*, 2010] is used in the model for the initial and boundary conditions. The profile is calculated from the mean values of the summer season in a South Atlantic transect (40-70^{o}S, 20^{o}W). It is composed of three soluble modes (Aitken, accumulation and coarse modes) and two insoluble modes (accumulation and coarse) that each follow a lognormal distribution. The two insoluble modes are used to represent the dust concentrations simulated by GLOMAP that are necessary to calculate INP when

using the DM15 parameterization. Aerosol particles are subject to horizontal and vertical advection, however they are not modified by the actions of cloud-feedbacks, so their distribution is similar to the initial profile across the entire domain. We use the *Abdul-Razzak and Ghan*, [2000] activation scheme to calculate the number of activated cloud droplets, which depend on the aerosol distribution and the cloud updraft. The model produces reasonable values of cloud droplet number concentrations when compared against satellite observations (see below).

Autoconversion of cloud droplets to rain and droplet accretion follows *Khairoutdinov and Kogan*, [2000] and self-collection of rain is parameterized based on *Beheng*, [1994]. The mass-fall speed relation for graupel follows *Locatelli and Hobbs*, [1974] and the graupel density is set at 250 kg m^{-3} [*Miltenberger et al.*, 2017]. The mass-fall speed and mass-diameter relations used for all the hydrometeors are described in *Miltenberger et al.*, [2017] The primary production of ice is defined by the parameterizations described in the main text (Figure 1). The Hallet-Mossop secondary ice production process is represented by producing 350 ice splinters per 1 mg of rimed mass on snow or graupel at a temperature of -5°C and a linearly decreasing rate to zero at -2.5 and -7.5°C. Freezing of rain drops follows *Bigg*, [1953]. Switching on and off the Hallet-Mossop process and rain droplet freezing did not play a substantial role in the properties of our studied clouds. Other processes affecting the transfer rates between hydrometers include vapour deposition, evaporation, sublimation, collision-coalescence and sedimentation.

In figure 4 we calculated the distribution of INP concentrations at cloud temperature to estimate the concentration of INPs affecting the clouds. We do this by filtering out the gridboxes with a total water mass mixing ratio less than 10^{-6} (residual water amount)[*Furtado and Field*, 2017]. We then calculate the distribution of INPs using the different parameterizations in the various simulations combined with the temperature of the gridboxes (in-cloud INP). These values represent the INP concentration affecting the different cloudy grid-boxes. From the distribution of INP

values calculated, we then obtain the median and the 66 and 95% intervals of the distribution shown in figure 4.

Satellite data and model evaluation

The model has been evaluated with several satellite products from the A-Train constellation. The simulated values (output every hour) were interpolated to the time when the A-Train passes through the model domains.

The radiative properties (outgoing shortwave and longwave radiation) were obtained from the NASA Clouds and the Earth's Radiant Energy System (CERES) [*Kratz et al.*, 2014] satellite instrument. Data from the Moderate Resolution Imaging Spectroradiometer (MODIS Collection 6, Level 2 data) [*Platnick, S., Ackerman, S., King*, 2015] mounted on the Aqua satellite was used to compare against cloud top temperatures and cloud-top phase. Observed cloud liquid water path (LWP) was obtained from the Advanced Microwave Scanning Radiometer 2 (AMSR2) [*Wentz, F.J., T. Meissner, C. Gentemann, K.A. Hilburn*, 2014]. For simulated case C2, due to the small scale of the cumulus clouds composing the cloud system, a comparison with MODIS cloud liquid water path was used instead of AMSR2 as it provides a higher resolution product being able to resolve the scale of the clouds formed. We note that the observed subdomain mean LWP using the microwave retrieval (AMRS2) for this cloud is 28% lower than the MODIS estimate (0.068 mm for AMSR2 and 0.094 mm with MODIS).

The distribution of cloud-top temperatures (CTT) for the three studied clouds are shown in Extended data figure 1 (top row). Overall the model creates clouds with similar CTT, although for C2 it seems to miss some warm clouds above 265K. Changing the INP parameterization does not change CTT substantially, although the M92 parameterization (high-INP) tends to produce higher temperature cloud tops as the higher nucleation events deplete the top (colder) part of the cloud.

The distribution of LWP has a similar behaviour as the distributions of reflected SW. The models with low INP representations produce distributions much closer to the satellite observations than the global model or the high INP representation (M92), which produce too few grid boxes with more than 0.1 mm LWP.

The simulated longwave outgoing flux is very close to the satellite observations (Extended data figure 2) for all the cases studied, including the global model. Modifying the INP parameterization makes a very small change on the LW radiative properties compared with the change observed in SW (Figure 2).

Cloud-top phase from the model was calculated as follows. First, we filter all the grid boxes with water (ice or liquid) mass mixing ratios less than 10^{-6} to exclude grid boxes with residually small amounts of water. Second, we obtain the cloud top height for water and ice clouds. If the top of the ice cloud is in a grid-box above the top of the liquid cloud we consider that column as having an ice top and conversely, we consider columns with a higher liquid cloud top as being liquid-topped. We consider as mixed-phase/uncertain cloud top phase the columns where the liquid and ice cloud top is in the same grid-box. The derived cloud top phase is then compared against the MODIS optical and infrared cloud-top products (Extended data figure 3). The global model and the M92 simulations produce too-little liquid phase cloud when compared with the satellite products. The comparison improves greatly when the other INP parameterizations are used, producing liquid cloud fractions that are much closer (or in between) the two retrieved estimates.

Satellite CDNC are derived from MODIS Level-2 Collection 6 swath data using 1 km (at nadir) resolution pixel-level values of cloud liquid effective radius, cloud optical depth and cloud top temperature data using the method described in Grosvenor and Wood, [2014], although with some differences related to the use of Collection 6 rather than Collection 5 data. Namely, in Collection 6 pixel level retrieval confidence QA flags are no longer used and also here we only examine pixel level data so the restrictions applied when aggregating to lower resolution are not necessary. Pixels were filtered to include only liquid water pixels that were

diagnosed as “confident cloudy” and as not being affected by any thin cirrus on top, nor shadowing by the MODIS algorithm. Only pixels that had an optical depth larger than 5 are included since biases are likely in thinner clouds [*Zhang and Platnick*, 2011; *Sourdeval et al.*, 2016]. Furthermore, pixels were required to have a cloud top height (derived from the 5 km MODIS product) between 0.5 and 3.2km; the lower limit is imposed to remove pixels that are either low level fog, or where the height retrieval is erroneous, and the upper limit restricts the analysis to low altitude clouds that are most likely to meet the assumptions made for the derivation of CDNC. The maximum solar zenith angle for the swath used in this analysis was 59^{o} so biases due to high solar zenith angles are unlikely since these have been shown to begin for angles larger than 65-70^{o} [*Grosvenor and Wood*, 2014].

Domain-mean CDNC values in cloudy columns with low-level liquid containing clouds for the different simulations and the satellite derived values are shown in Extended data figure 4. The mean simulated values are close to the satellite values for the first and second clouds (C1, C2). The simulations of C3 produce values that are relatively lower than the satellite values. To test the importance of this bias, we repeated one of the simulations (C3_M92) with a higher aerosol concentration (with around 100 cm^{-3} in the accumulation mode as opposed to around 35 cm^{-3} used previously). In this simulation, CDNC is slightly above the satellite derived observations, however, the radiative properties of the cloud do not change substantially (Extended data figure 5).

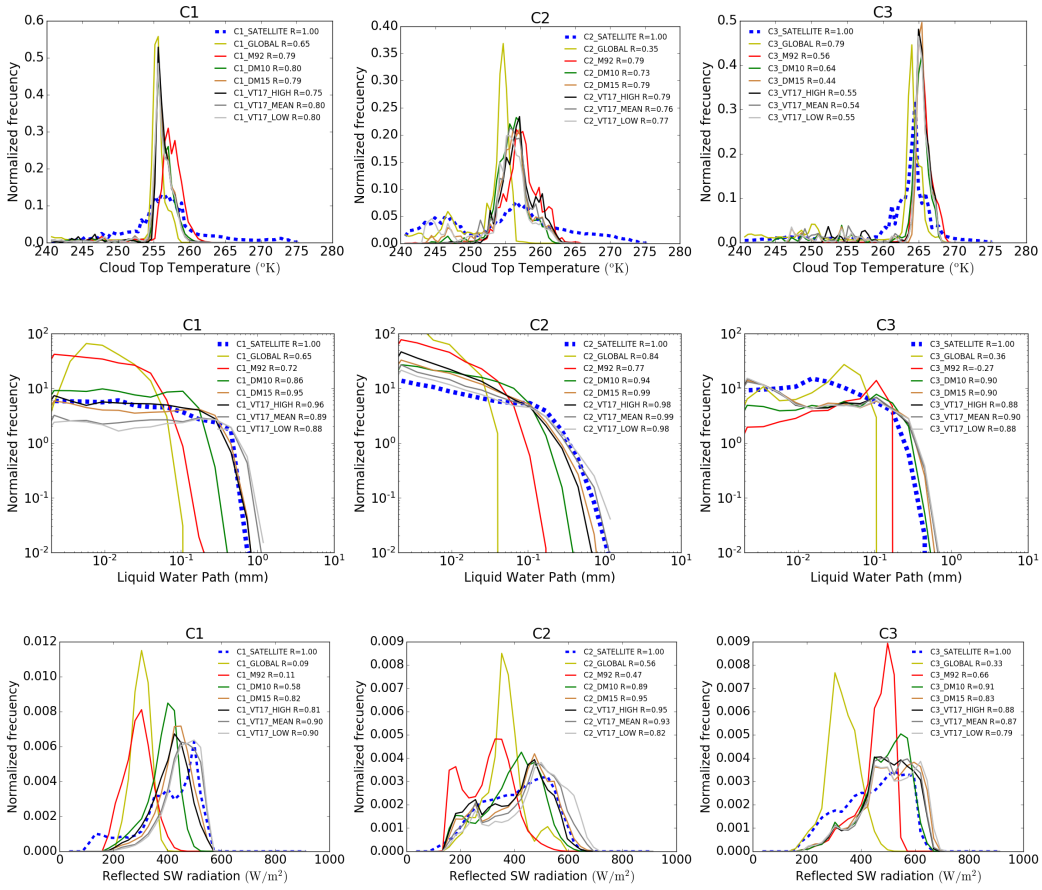

Extended data figure 1 Frequency distributions. (Top row) Distribution of frequencies of cloud-top temperatures for the three studied cloud systems derived from MODIS-retrieved cloud-top temperature and the model simulations with the different INP parameterizations. (Middle row) Same but for LWP retrieved with AMSR2 (MODIS for C2). (Bottom row) Same but for SW retrieved with CERES. The R coefficients refer to the correlation between the satellite PDF and the modelled values.

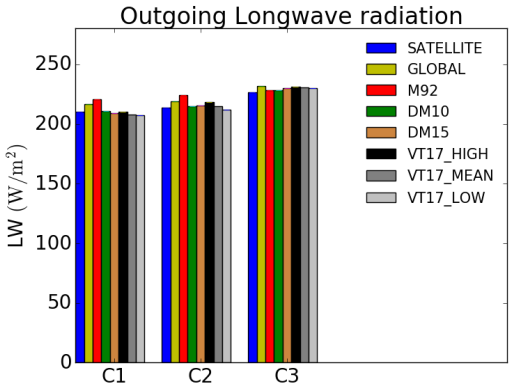

Extended data figure 2 Barplot of sub-domain averaged outgoing longwave radiation. Similar to Figure 2a but for LW instead of SW.

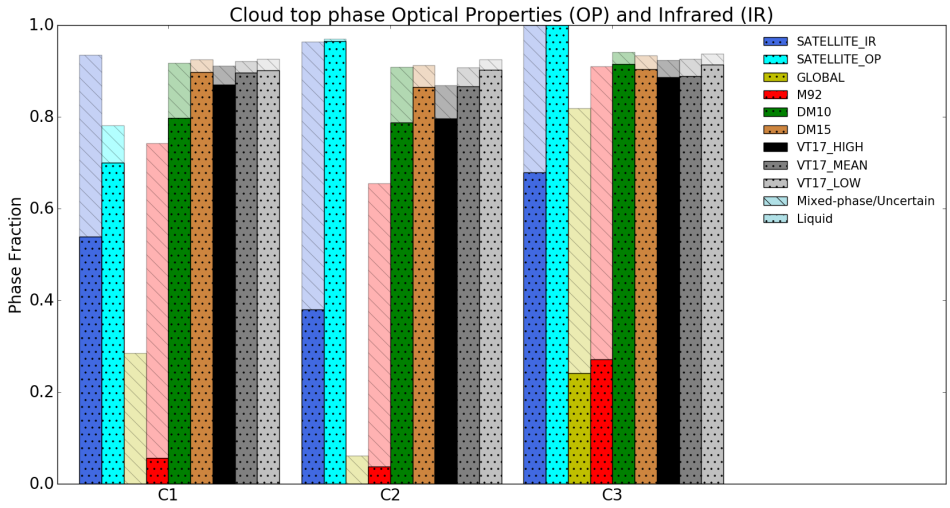

Extended data figure 3 Cloud-top phase comparison. Runs for the clouds studied with the different INP representations. The satellite columns correspond to the MODIS infrared (IR) and optical (OP) cloud top phase product.

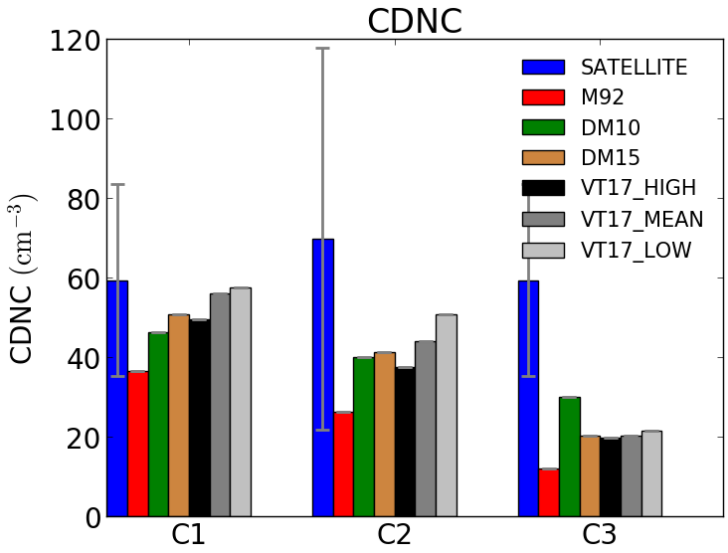

Extended data figure 4 Satellite-derived cloud droplet number concentrations (CDNC) and domain mean simulated CDNC. The errorbars represent 2 standard deviation of the distribution of satellite calculated CDNC.

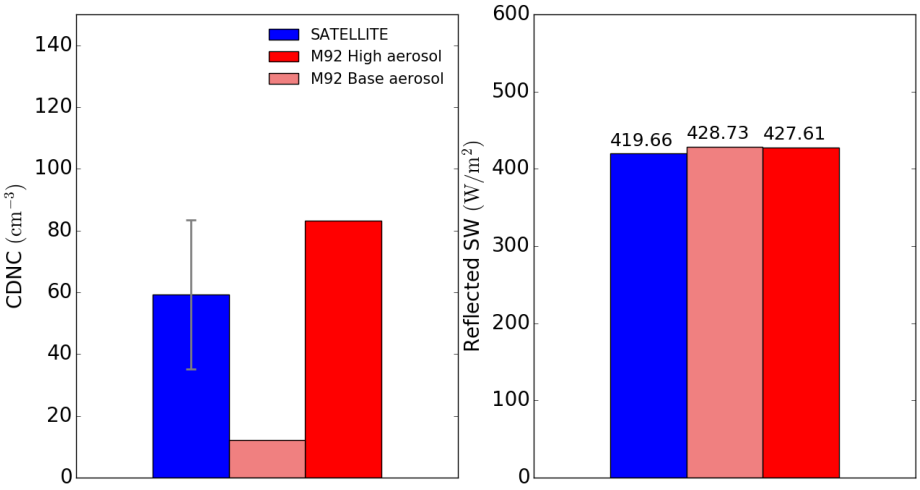

Extended data figure 5 CDNC sensitivity test. Domain-mean cloud droplet number concentration (left) and reflected short wave radiation (right) for the simulations using M92 with a high aerosol loading and the standard aerosol profile from GLOMAP used in all the other simulations. The satellite observations are shown for comparison.

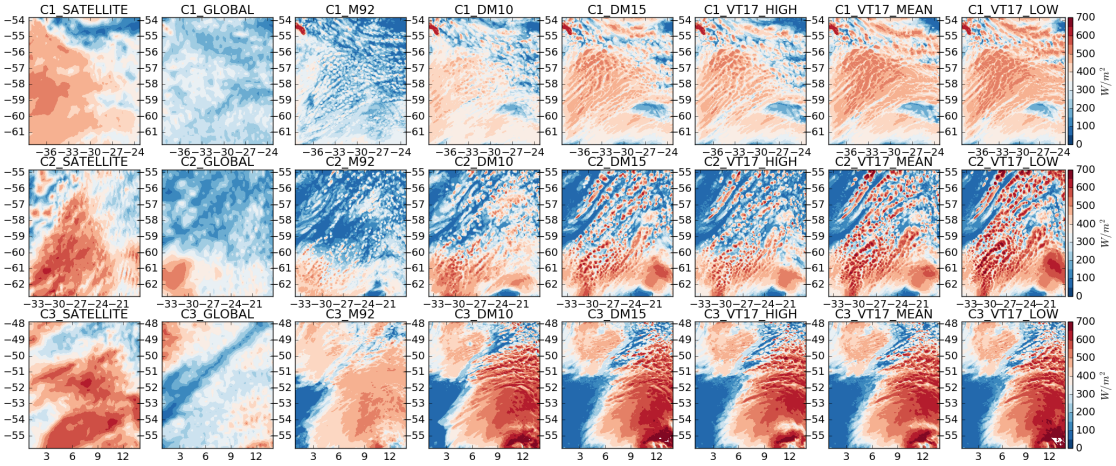

Extended data Figure S6 Sub-domain reflected SW radiation for all the 0.02º resolution simulations. Each line corresponds to the each of the different cloud studied (C1, C2 and C3). The first column corresponds to the satellite observations and the following columns correspond to the global model and the 0.02º resolution simulations with the different INP parameterizations tested (following the naming previously defined in the main text)

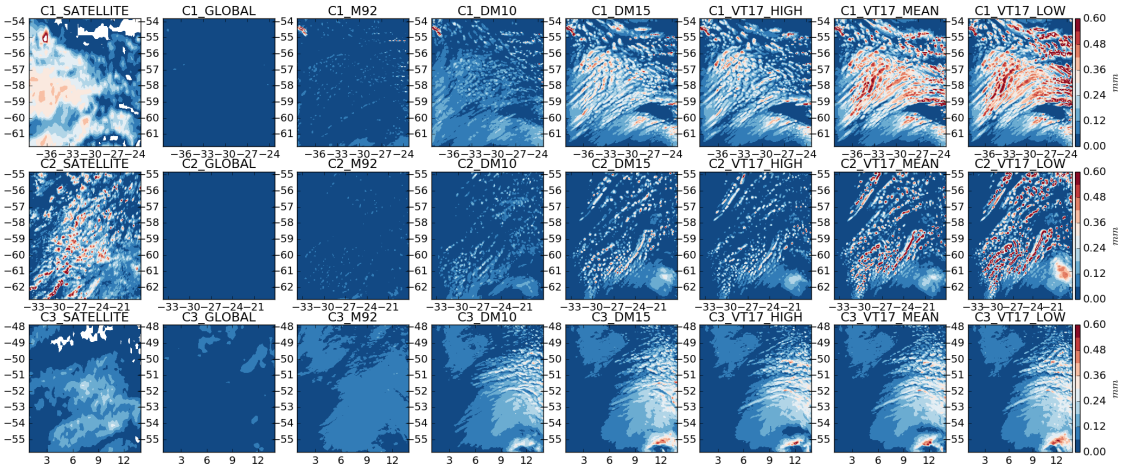

Extended data Figure S7 Sub-domain LWP for all the 0.02º resolution simulations. Same as Figure S6 but for LWP

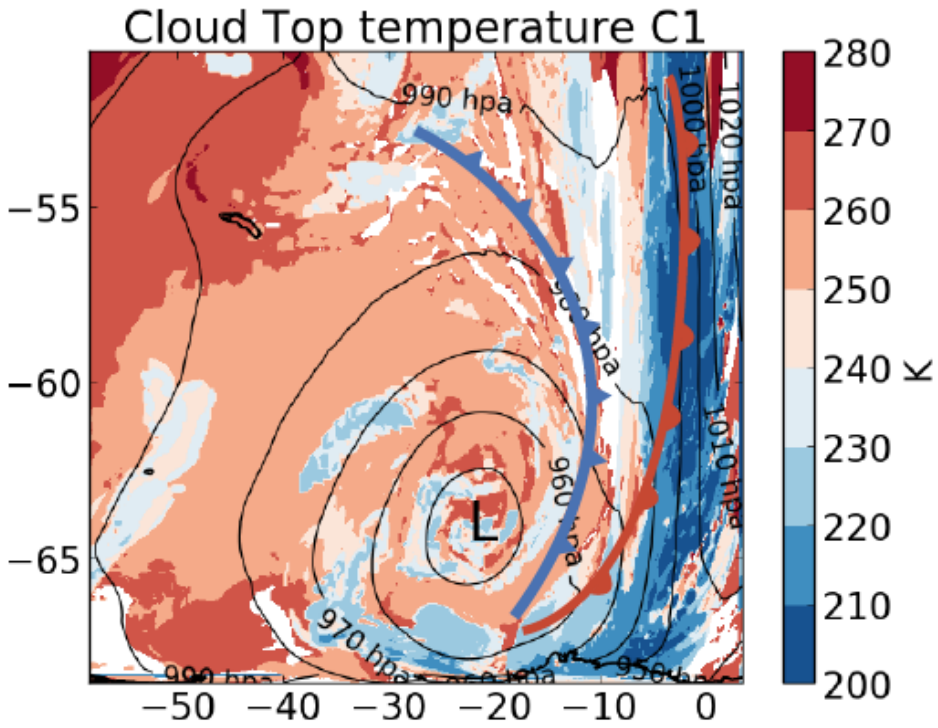

Extended data Figure S8 Cloud top temperatures for one the 7km resolution simulations of the whole cyclone composite. The black contourlines correspond to the surface pressure in hpa. The cold and warm fronts are depicted with blue and red lines.

Cloud	Centre of domain	Date	Time A-train passes
C1	58°S, 30°W	1st March 2015	16:30 UTC
C2	59°S, 25°W	10th January 2015	16:40 UTC
C3	52°S, 8°E	9th December 2014	13:25 UTC

Extended data Table 1 Time and location of the simulated clouds systems.

References:

Abdul-Razzak, H., and S. J. Ghan (2000), A parameterization of aerosol activation: 2. Multiple aerosol types, *J. Geophys. Res. Atmos.*, *105*(D5), 6837–6844, doi:10.1029/1999JD901161.

Beheng, K. D. (1994), A parameterization of warm cloud microphysical conversion processes, *Atmos. Res.*, *33*(1–4), 193–206, doi:10.1016/0169-8095(94)90020-5.

Bigg, E. K. (1953), The formation of atmospheric ice crystals by the freezing of droplets, *Q. J. R. Meteorol. Soc.*, *79*(342), 510–519, doi:10.1002/qj.49707934207.

Furtado, K., and P. Field (2017), The role of ice-microphysics parametrizations in determining the prevalence of supercooled liquid water in high-resolution simulations of a Southern Ocean midlatitude cyclone, *J. Atmos. Sci.*, JAS-D-16-0165.1, doi:10.1175/JAS-D-16-0165.1.

Grosvenor, D. P., and R. Wood (2014), The effect of solar zenith angle on MODIS cloud optical and microphysical retrievals within marine liquid water clouds, *Atmos. Chem. Phys.*, *14*(14), 7291–7321, doi:10.5194/acp-14-7291-2014.

Grosvenor, D. P., P. R. Field, A. A. Hill, and B. J. Shipway (2016), The relative importance of macrophysical and cloud albedo changes for aerosol induced radiative effects in stratocumulus, *Atmos. Chem. Phys. Discuss.*, (November), 1–48, doi:10.5194/acp-2016-1017.

Khairoutdinov, M., and Y. Kogan (2000), A New Cloud Physics Parameterization in a Large-Eddy Simulation Model of Marine Stratocumulus, *Mon. Weather Rev.*, *128*(1), 229–243, doi:10.1175/1520-0493(2000)128<0229:ANCPPI>2.0.CO;2.

Kratz, D. P., P. W. Stackhouse, S. K. Gupta, A. C. Wilber, P. Sawaengphokhai, and G. R. McGarragh (2014), The fast longwave and shortwave flux (FLASHFlux) data product: Single-scanner footprint fluxes, *J. Appl. Meteorol. Climatol.*, *53*(4), 1059–1079, doi:10.1175/JAMC-D-13-061.1.

Locatelli, J. D., and P. V Hobbs (1974), Fall speeds and masses of solid precipitation particles, *J. Geophys. Res.*, *79*(15), 2185–2197, doi:10.1029/JC079i015p02185.

Mann, G. W., K. S. Carslaw, D. V. Spracklen, D. a. Ridley, P. T. Manktelow, M. P. Chipperfield, S. J. Pickering, and C. E. Johnson (2010), Description and evaluation of GLOMAP-mode: a modal global aerosol microphysics model for the UKCA composition-climate model, *Geosci. Model Dev.*, *3*(2), 519–551, doi:10.5194/gmd-3-519-2010.

Miltenberger, A. K., P. R. Field, A. A. Hill, P. Rosenberg, B. J. Shipway, J. M. Wilkinson, R. Scovell, and A. M. Blyth (2017), Aerosol-cloud interactions in

mixed-phase convective clouds. Part 1: Aerosol perturbations, *Atmos. Chem. Phys. Discuss.*, (September), 1–45, doi:10.5194/acp-2017-788.

Platnick, S., Ackerman, S., King, M. (2015), MODIS Atmosphere L2 Cloud Product (06_L2). NASA MODIS Adaptive Processing System, Goddard Space Flight Center, USA, , doi:http://dx.doi.org/10.5067/MODIS/MOD06_L2.006.

Shipway, B. J., and A. A. Hill (2012), Diagnosis of systematic differences between multiple parametrizations of warm rain microphysics using a kinematic framework, *Q. J. R. Meteorol. Soc.*, *138*(669), 2196–2211, doi:10.1002/qj.1913.

Sourdeval, O., L. C.-Labonnote, A. J. Baran, J. Mülmenstädt, and G. Brogniez (2016), A methodology for simultaneous retrieval of ice and liquid water cloud properties. Part 2: Near-global retrievals and evaluation against A-Train products, *Q. J. R. Meteorol. Soc.*, *142*(701), 3063–3081, doi:10.1002/qj.2889.

Walters, D. et al. (2017), The Met Office Unified Model Global Atmosphere 6.0/6.1 and JULES Global Land 6.0/6.1 configurations, *Geosci. Model Dev.*, *10*(4), 1487–1520, doi:10.5194/gmd-10-1487-2017.

Wentz, F.J., T. Meissner, C. Gentemann, K.A. Hilburn, J. S. (2014), Wentz, F.J., T. Meissner, C. Gentemann, K.A. Hilburn, J. Scott, 2014: Remote Sensing Systems GCOM-W1 AMSR2 Daily Environmental Suite on 0.25 deg grid, Version 7.2. Remote Sensing Systems, Santa Rosa, CA. Available online at www.remss.com/missions/amsr.,

Zhang, Z., and S. Platnick (2011), An assessment of differences between cloud effective particle radius retrievals for marine water clouds from three MODIS spectral bands, *J. Geophys. Res. Atmos.*, *116*(20), 1–19, doi:10.1029/2011JD016216.